

**RECTENNA DESIGN  
FOR  
WIRELESS POWER TRANSMISSION**

By

MOHD IQBAL HAQIM BIN MAHAT

FINAL PROJECT REPORT II

Submitted to the Electrical & Electronics Engineering Programme  
in Partial Fulfillment of the Requirements  
for the Degree  
Bachelor of Engineering (Hons)  
(Electrical & Electronics Engineering)

Universiti Teknologi Petronas  
Bandar Seri Iskandar  
31750 Tronoh  
Perak Darul Ridzuan

© Copyright 2008

by

Mohd Iqbal Haqim Bin Mahat, 2008

# CERTIFICATION OF APPROVAL

## RECTENNA DESIGN FOR WIRELESS POWER TRANSMISSION

by

Mohd Iqbal Haqim Bin Mahat

A project dissertation submitted to the  
Electrical & Electronics Engineering Programme  
Universiti Teknologi PETRONAS  
in partial fulfilment of the requirement for the  
Bachelor of Engineering (Hons)  
(Electrical & Electronics Engineering)

Approved:



**DR ABDALLAH BELAL ADAM**  
Senior Lecturer  
Electrical & Electronics Engineering Programme  
New Academic Block 23-3-25  
Universiti Teknologi PETRONAS  
31750 Tronoh  
Perak Darul Ridzuan, MALAYSIA.

Dr. Abdallah Belal Adam

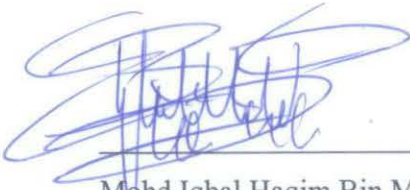
Project Supervisor

UNIVERSITI TEKNOLOGI PETRONAS  
TRONOH, PERAK

Jun 2008

## **CERTIFICATION OF ORIGINALITY**

This is to certify that I am responsible for the work submitted in this project, that the original work is my own except as specified in the references and acknowledgements, and that the original work contained herein have not been undertaken or done by unspecified sources or persons.



---

Mohd Iqbal Haqim Bin Mahat

## ABSTRACT

The solar energy received by the solar cells satellite in space produced electricity. Then the electricity will be converted into microwave signal. The microwave signal will be transmitted by the satellite's transmitter, wirelessly and received by the rectifying antenna or known as 'rectenna' on the Earth. Rectenna acts as microwave receiver and a converter of microwave signal into DC power. This system is known as Wireless Power Transmission system (WPT). The frequency for the rectenna element is 2.45 GHz. Nevertheless, the simulations and analysis concentrate only on power rectangular microstrip patch antenna (RMPA) and Schottky diode using Microwave Office 2004 simulation. In reality the achieved of the transmitted power is merely at 0.9% bandwidth. Thus, to improve it to more than 0.9% of bandwidth, a research on dielectric substrate is required. The design of the rectenna is also crucial so that the 0.9% of bandwidth or more can be achieved. By using this simulator, the performances of these two elements can be obtained. Based on the results, the PTFE/Glass mix dielectric substrate offered better performance than the other dielectric substrate, producing 1.84% of antenna bandwidth. For the Schottky diode, the total power that has been successfully analyzed is at 1769923.5 mW. The diode conversion efficiency has been evaluated as 44.375%. This project covers chapter 1, for introduction, chapter 2 for literature review, chapter 3 for methodology, chapter 4 for results and discussions and chapter 5 for conclusion and recommendation. Overall, the simulations have been successful, thus the objectives of the project are achieved.

## **ACKNOWLEDGEMENTS**

Thank first and foremost to Allah for blessing me with talent and strength in accomplishing this project. Then I would like to thanks Dr. Abdallah Belal Adam for his supervision, advices and helps during the course of this project. Also warmly thanks for my father, my mother and my little sister, whom I appreciate more than word can express and for their love concern, support, inspiration and confidence in me. For all my colleagues for their patience, criticism, support and beautiful friendship and a special thank for anyone who always has been there with love and inspiration. Last but certainly not least, thank to those who was involved directly or indirectly throughout course of this project. Thank you.

## TABLE OF CONTENTS

LIST OF TABLES .....	ix
LIST OF FIGURES .....	x
LIST OF ABBREVIATIONS .....	xiii
CHAPTER 1 INTRODUCTION .....	1
1.1 Background of Study.....	1
1.2 Problem Statement .....	4
1.3 Objective .....	5
1.4 Scope .....	5
CHAPTER 2 LITERATURE REVIEW .....	6
2.1 Introduction .....	6
2.2 Microstrip Structure .....	7
2.2.1 Substrate .....	7
2.2.2 Metallization .....	8
2.3 Antenna Feeds .....	8
2.3.1 Directly Coupled.....	8
<b>2.3.1.1 Microstrip Line Feed.....</b>	<b>9</b>
<b>2.3.1.2 Coaxial Feed.....</b>	<b>10</b>
2.3.2 Electromagnetically Coupled.....	11
2.3.3 Aperture Coupled.....	11
2.4 Models .....	12
2.4.1 Transmission Line Model .....	12
2.4.2 The Cavity Model .....	13
2.5 Microstrip Patch Antenna.....	15
2.5.1 Rectangular Microstrip Patch Antenna.....	15
2.5.2 Other Patch Shapes .....	17
2.6 Shottky Diode.....	18
2.6.1 Introduction.....	18
2.6.2 Schottky – Mott and Bardeen Theory.....	19
2.6.3 Characteristic .....	22
2.6.4 Rectifying Diode: Derivation of Closed Form Equation for Conversion Efficiency .....	25

2.6.5 Summary ..... 27

CHAPTER 3 METHODOLOGY ..... 28

3.1 Procedure Identification ..... 28

3.2 Tools Required ..... 30

3.3 Introduction on Simulation..... 30

3.4 Simulation on Rectangular Microstrip Patch Antenna..... 30

3.5 Nonlinear Simulation of Schottky Diode ..... 35

3.6 Summary ..... 36

CHAPTER 4 RESULTS AND DISCUSSION ..... 37

4.1 The Power Rectangular Microstrip Antenna Results ..... 37

4.2 Schottky Diode Results ..... 63

CHAPTER 5 CONCLUSION AND RECOMMENDATION..... 70

5.1 Conclusion..... 70

5.2 Recommendation..... 71

REFERENCES..... 72

APPENDICES ..... 75

Appendix A List of dielectric substrate..... 76

Appendix B Table of common dielectric materials and conductor types  
..... 77

Appendix C ..... 78

Appendix D USER MANUAL ..... 82

Appendix E GANTT CHARTS ..... 91

## LIST OF TABLES

Table 1 Properties of dielectric substrates .....	33
Table 2 Calculated parameters for rectangular microstrip patch antenna.....	34
Table 3 Circular Polarization and E field pattern, results .....	38
Table 4 Total Radiated Power.....	39
Table 5 Voltage Standing Wave Ratio (VSWR) and Reflection Coefficient .....	40
Table 6 Voltage, current and total power of diode values .....	63
Table 7 Diode harmonics components.....	64
Table 8 List of some dielectric substrate with the electric constant and loss tangent.	76
Table 9 Table of common dielectric materials (This table is obtained from Microwave Office 2004).....	77
Table 10 Table of common conductor types and its conductivities (This table is obtained from Microwave Office 2000).....	77
Table 11 Evaluation of the Selected Properties of GaAs, Ge, InP and Si.....	78
Table 12 Gantt Chart for FYP I July 2007 .....	91
Table 13 Gantt Chart for FYP II January 2008.....	92

## LIST OF FIGURES

Figure 1 Component of Wireless Power Transmission .....	3
Figure 2 Basic structure of rectenna.....	4
Figure 3 Cross-section of microstrip geometry.....	7
Figure 4 Patch antenna with microstrip line feed.....	10
Figure 5 Microstrip feed with inset.....	10
Figure 6 Patch antenna with coaxial feed. ....	10
Figure 7 Example of aperture-coupled feed.....	11
Figure 8 Rectangular patch antenna with radiating field. ....	13
Figure 9 Transmission line model.....	13
Figure 10 Cavity Model .....	15
Figure 11 The half-wavelength rectangular microstrip patch antenna.....	17
Figure 12 Electron energy band diagrams. ....	19
Figure 13 Electron energy band diagram .....	22
Figure 14 Schottky contact.....	23
Figure 15 Equivalent circuit of Schottky diode. ....	25
Figure 16 Rectangular patch .....	32
Figure 17 Enclosure of the antenna with Polyster/Resin dielectric substrate .....	33
Figure 18 Equivalent circuit of Schottky diode .....	35
Figure 19 The antenna with Polyster/Resin dielectric substrate current distributions	41
Figure 20 The antenna with Polyster/Resin laminated with GML 1000 dielectric substrate current distributions.....	42
Figure 21 The antenna with PTFE/Glass mix dielectric substrate current distributions .....	43
Figure 22 The antenna with Polyster/Resin dielectric substrate circular polarization	44
Figure 23 The antenna with Polyster/Resin laminated with GML 1000 dielectric substrate circular polarization.....	45
Figure 24 The antenna with PTFE/Glass mix dielectric substrate circular polarization .....	46
Figure 25 The antenna with Polyster/Resin dielectric substrate E_PHI and E_THETA .....	47
Figure 26 The antenna with Polyster/Resin laminated with GML 1000 dielectric substrate E_PHI and E_THETA .....	48

Figure 27 The antenna with PTFE/Glass mix dielectric substrate E_PHI and E_THETA.....	49
Figure 28 The antenna with Polyster/Resin dielectric substrate total radiated power	50
Figure 29 The antenna with Polyster/Resin laminated with GML 1000 dielectric substrate total radiated power .....	51
Figure 30 The antenna with PTFE/Glass mix dielectric substrate total radiated power .....	52
Figure 31 The antenna with Polyster/Resin dielectric substrate (single point simulation) Voltage Standing Wave Ratio (VSWR).....	53
Figure 32 The antenna with Polyster/Resin laminated with GML 1000 dielectric substrate (single point simulation) Voltage Standing Wave Ratio (VSWR).....	53
Figure 33 The antenna with PTFE/Glass mix dielectric substrate (single point simulation) Voltage Standing Wave Ratio (VSWR).....	54
Figure 34 The antenna with Polyster/Resin dielectric substrate (simulation between 2.4 GHz and 2.5 GHz) Voltage Standing Wave Ratio (VSWR) .....	54
Figure 35 The antenna with Polyster/Resin laminated with GML 1000 dielectric substrate (simulation between 2.4 GHz and 2.5 GHz) Voltage Standing Wave Ratio (VSWR).....	55
Figure 36 The antenna with PTFE/Glass mix dielectric substrate (simulation between 2.4 GHz and 2.5 GHz) Voltage Standing Wave Ratio (VSWR) .....	56
Figure 37 The antenna with Polyster/Resin dielectric substrate (single point simulation) Reflection Coefficient.....	57
Figure 38 The antenna with Polyster/Resin laminated with GML 1000 dielectric substrate (single point simulation) Reflection Coefficient .....	58
Figure 39 The antenna with PTFE/Glass mix dielectric substrate (single point simulation) Reflection Coefficient.....	59
Figure 40 The antenna with Polyster/Resin dielectric substrate (simulation between 2.4 GHz and 2.5 GHz) Reflection Coefficient.....	60
Figure 41 The antenna with Polyster/Resin laminated with GML 1000 dielectric substrate (simulation between 2.4 GHz and 2.5 GHz) Reflection Coefficient....	61
Figure 42 The antenna with PTFE/Glass mix dielectric substrate (simulation between 2.4 GHz and 2.5 GHz) Reflection Coefficient.....	62
Figure 43 Voltage versus Time graph.....	64
Figure 44 Current versus Time graph .....	65
Figure 45 Total Power versus Frequency graph .....	66
Figure 46 Harmonics Component of Voltage graph.....	67
Figure 47 Harmonics Component of Current graph .....	68
Figure 48 Harmonics Component of Power graph .....	69

Figure 49 Enclosure information with polyster/resin as a substrate ..... 84

Figure 50 Division cell size and x and y dimension ..... 84

Figure 51 Dielectric layers information with polyster/resin as a dielectric substrate. 85

Figure 52 Boundaries information ..... 85

Figure 53 Rectangular patch ..... 86

Figure 54 The position of Via Port ..... 87

Figure 55 Type of graphs ..... 88

Figure 56 Add measurements for the graph..... 88

Figure 57 Circuit of Schottky diode..... 89

Figure 58 Dialog box to edit the parameter of Schottky diode ..... 90

## LIST OF ABBREVIATIONS

$\tan \delta$	:	Loss tangent
$Z_A$	:	Antenna input impedance
$Z_0$	:	Characteristic impedance
$Z_0'$	:	Characteristic impedance of the matching section
$\Delta X_p$	:	Probe distance from patch edge
$L$	:	Length of patch
$W$	:	Width of patch
$\lambda_0$	:	Free space wavelength
$\lambda_d$	:	Wavelength in dielectric
$t$	:	Dielectric thickness
$\epsilon_e$	:	Effective dielectric constant
$\epsilon_r$	:	Dielectric constant (permittivity)
$\epsilon_0$	:	Free space permittivity
$Q_{rad}$	:	Radiation admittance
$\Delta L$	:	Effective length
$\beta$	:	Bandwidth
$\phi_m$	:	Work function of metal
$\phi_s$	:	Work function of semiconductor
$X_s$	:	Electron affinity
$E_F$	:	Fermi level
$E_c$	:	Conduction band edge
$E_v$	:	Valence band edge
$V_i$	:	Contact potential different or built potential
$q$	:	Electronic charge
$qV_i$ or $\phi_B$	:	Potential barrier
$\phi_n$	:	Penetration of Fermi level
$\phi_0$	:	Neutral level
$w$	:	Depletion layer width
$N_D$	:	Donor density

$V_D$	:	Diffusion or metal – semiconductor potential
$V$	:	Applied voltage
$A$	:	Area
$A^*$	:	Richardson constant
$I_s$	:	Saturation current
$T$	:	Absolute temperature
$R_s$	:	Series resistance
$\mu_e$	:	Electron mobility in the depletion layer
$\rho$	:	Resistivity of depletion layer
$\rho_s$	:	Substrate resistivity
$d$	:	Active junction diameter
$V_0$	:	Output DC voltage
$V_I$	:	Peak voltage of incident microwave
$V_d$	:	Diode junction voltage
$V_{d0}$	:	DC component
$V_{d1}$	:	Fundamental frequency component
$V_{d,DC}$	:	Average value of $V_d$
$\theta_{off}$	:	Phase angle when diode is turned off
$V_f$	:	Forward voltage drop
$C_j$	:	Junction capacitance
$P_{DC}$	:	DC power
$P_{loss}$	:	Loss power

# CHAPTER 1

## INTRODUCTION

### 1.1 Background of Study

Over 100 years ago, the concept of Wireless Power Transmission (WPT) began with ideas and demonstration by Tesla [9]. Although Tesla was unsuccessful at implementing his Wireless Power Transmission System (WPTS) for commercial use; he did transmit power from his oscillators that operated up to 100MV at 150 kHz [9].

The modern era of wireless power transmission began in the 1950's and the United State of America has been historical leader in done the experiments and demonstrations of WPTS [9], [10]. William C. Brown championed the first development of high power microwave tubes for aircraft application in the late 1950's. Brown constructed and flew a series of electrically powered helicopter designed to demonstrate the feasibility of microwave powered and microwave guided aircraft.

The first practically designed of rectenna is in early 1960's for 2.45 GHz [8]. Since that time the efficiency of rectenna increased to over 85% from 38% [6], [8]. In 1964, Brown demonstrates a beam-powered helicopter, which received all of its propulsive power via a 2.45 GHz microwave beam [10]. Next, in 1967, Brown again demonstrated a beam positioned helicopter which used a microwave beam to provide all of the information necessary to control the roll, pitch and yaw of a small helicopter [10].

The first demonstration of a complete WPTS was demonstrated on 22 May 1963 at Spencer Laboratory, Massachusetts. In this demonstration DC power was converted into 400W with assumed efficiency of 50% at 2.45 GHz [10].

This technology then continued when Dr. Peter E. Glaser patented the concept of solar power satellite (SPS) in 1968. The electricity is transmitted to collectors on the ground in the form of radio frequency (microwave) and used to provide base load electrical power [1], [10].

The highest conversion efficiency ever recorded is achieved by Brown in 1977 [11]. Brown used GaAs – Pt Schottky barrier and aluminum bar dipole and transmission lines to achieve 90.6% conversion efficiency at an input microwave power level of 8W [11].

From late 1990 – 1991, Rockwell International and David Sarnoff Laboratory in Princeton, N.J. operated a microwave-powered rover at 5.86 GHz. 3 kW power was transmitted and 500 DC was received to operate the test device [10].

From 1994 to 1995, the ground-to-ground WPT experiment was carried out in Yamasaki, Japan by a joint team from the Radio Atmospheric Science Center of Kyoto University, Kobe University and Kansai Electric Power Company [3].

Beside, there are many demonstrations and experiments on WPT have been done all over the world. A growing community of researchers in WPT is emerging with variety of ground, air and space demonstration system.

Wireless Power Transmission System (WPT) is the system that converts power energy into microwave on space and reconvert microwave signal into DC (direct current) by means of reception antenna [1]. Studies on WPT are divided into microwave transmission, reception and radio frequency (RF) – DC conversion. This study proposed to measure the important efficiency in system design and investigate the fundamental system to realize this WPT. Moreover, this technology has higher efficiency than solar energy and do not affects the weather [2].

Viewed from existing concept of the Wireless Power Transmission, the design parameter of the transmission system has already been established so the entire

characteristic of transmission efficiency could be evaluate through this capacity analysis of rectenna (rectifying antenna), converted microwave energy into DC voltage [1]. Figure 1 shows the components of Wireless Power Transmission with unit of cell measurement system [1].

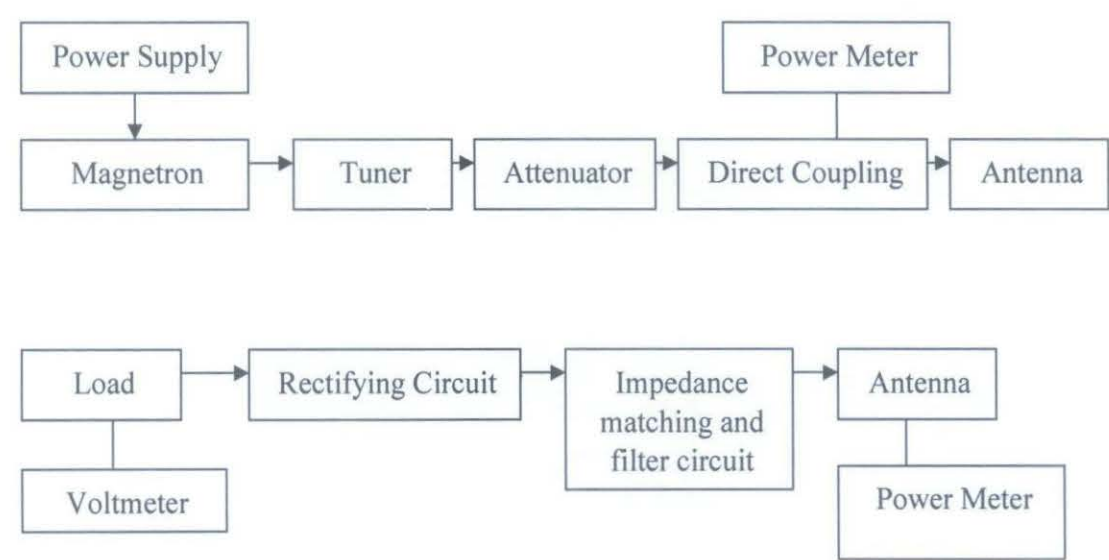


Figure 1    Component of Wireless Power Transmission

The word ‘rectenna’ is firstly used by Brown and means rectifying antenna (rectifier + antenna) [3], [4]. In other words, rectenna is a microwave receiver and a converter of microwaves power into DC useful power [3], [5], [6]. Rectenna basically consists of reception antenna, impedance matching circuits, filter circuits and rectifying circuits [1], [7]. However, in this project the concentration only made on simulations of rectangular microstrip patch antenna as a power reception antenna and Schottky diode as a rectifying circuit.

Rectifying antenna (rectenna) is one of the main components in WPT system [4], [8]. Rectenna functions as a receiver of the signal transmitted and converted the microwave incident power into DC voltage. The basic structure of rectenna is shown in Figure 2 [1].

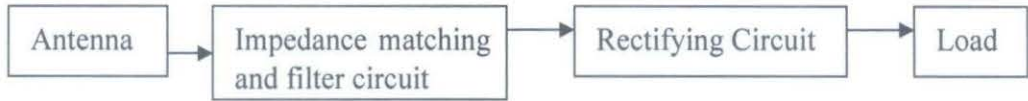


Figure 2 Basic structure of rectenna

Microstrip rectenna is selected as reception antenna due to lightweight, easy to manufacture and small sized [1], [2]. While, Shottky diode is chosen as a rectifying circuit based on having a great forward current, reverse withstands voltage and low power consumption of the diode itself [2].

Consideration should be taken in the frequency used in microwave signal and atmospheric attenuation when done the simulations. 2.45 GHz frequency is selected because of its low atmospheric attenuation and is located at the center of ISM (Industrial, Medical, and Scientific) band [1]. Also this frequency is the proper frequency for ground to ground, ground to space and space to ground transmission applications [4].

## 1.2 Problem Statement

Experimental works that related to WPT system have the difficulty to achieve more that 0.9% of bandwidth for power transmission. This happened because of design limitations of the rectenna. The rectenna also depends heavily on the type of dielectric substrate materials. Before this, the types of dielectric substrate materials were not the best types to be used. They contributed lower percentage of bandwidth to transmit power that is less than 0.9%.

The previous designs of rectifying circuit for experimental works that will reconvert microwave to DC power provide lower power input/output efficiency, barely to reach more that 20% efficiency since cable is the best medium to transmit power.

### 1.3 Objective

The main objective of this project is to achieve the targeted bandwidth of 0.9% or better, through the followings:

- To design and choose the best dielectric substrate for rectangular microstrip patch antenna as a reception antenna in Wireless Power Transmission.
- To design and choose the best Schottky diode designs as a rectifying circuit in Wireless Power Transmission.
- To use Microwave Office 2004 for simulations.
- To get results from the simulations.

### 1.4 Scope

This part of this project (FYP II) will focus on the concept of rectangular microstrip patch antenna (RMPA) and the Schottky diode, without any implementation on WPTS yet. This part of the project involves understanding of RMPA and Schottky diode; what are they, how they work, and their essential components. The project will consists of the EM (Electromagnetic) Simulation for RMPA and nonlinear analysis for Schottky diode from Microwave Office 2004.

## CHAPTER 2

### LITERATURE REVIEW

#### 2.1 Introduction

The most common form of printed antenna is the microstrip antenna patch elements and array of patches. Printed antennas are constructed using printed circuit fabrication techniques such that a portion of the metallization layer is responsible for radiation [12]. Printed antenna are popular with antenna engineers because it is easy to handle with and this can be configured to specialized geometries and because of their low cost when produced in large quantities.

Microstrip device in its simple form is a layered structure with 2 parallel conductors separated by a thin dielectric substrates and the lower conductor acting as a ground plane. Microstrips are printed circuit for very high frequency electronics and microwaves [13]. When a microwave radiating or receiving element is form on top of dielectric substrate with a complete ground plate, it is a microstrip antenna or a patch antenna depending on the shape of the pattern of the active element on the substrate. In principle, microstrip antennas are thin planar configuration that are lightweight, low cost, easy to manufacture and can be made conformal with the surfaces of vehicles, missiles etc [14].

The antenna assembly is physically simple and flat. The upper surface of the dielectric substrate supports the printed conducting strip which is suitably contoured while the entire lower surface of the substrate is backed by the conducting ground plate [14]. Many types of microstrip antenna have been evolved which are variants of the basic sandwich structure but the underlying concept is the same; that is printed radiating element is electrically driven with respect to ground plane. This definition

admits a wide range of dielectric substrate thickness and permittivity and of course the special case when the strip and ground are separated only by an air space. This then is what the term microstrip antenna generally understands [14].

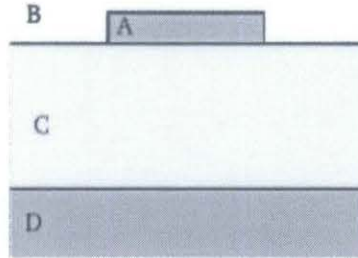


Figure 3 Cross-section of microstrip geometry.

In Figure 3, conductor (A) is separated from ground plane (D) by dielectric substrate (C). Upper dielectric (B) is typically air.

## 2.2 Microstrip Structure

Basically, microstrip structure consists of a thin plate of low – loss insulating material, the substrate, covered with metal completely on one side, the ground plane and partly on the other, where the circuit or antenna patterns are printed [13].

### 2.2.1 Substrate

It is referring to a single body of material in which circuit elements are fabricated [15]. A thick substrate of low relative permittivity is a better choice when a substrate is chosen for a microstrip patch antenna [16]. Low value of permittivity produces more loosely bound fields, which enhance radiation efficiency. A low cost substrate with tight dielectric tolerance ( $<\pm 2\%$ ), low thickness tolerance ( $<\pm 5\%$  and low dissipation factor ( $\tan\delta < 0.005$ ) is required [16]. List of substrates with it dielectric constant and loss tangent can be referred from Appendix A and Appendix B. The substrate basically fulfills 2 functions [13].

1. Function as mechanical support that ensures that implanted components are properly positioned and mechanically stable.
2. It behaves as an integral part of connecting transmission lines and deposited circuit component: its permittivity and thickness determine the electrical characteristic of the antenna.

### **2.2.2 Metallization**

Most commercially available microstrip substrates are metallized on both faces. The photolithographic process realizes the circuit pattern. A mask of the circuit to be realized is drawn at a suitable scale, cut and then reduced and placed on top of a photoresistive layer, which was previously deposited on top of the microstrip [13]. The structure is then exposed to ultraviolet radiation, which reaches the photosensitive layer through mask opening. The exposed parts are removed by photographic development, and the metal is etched away from the exposed area [13].

## **2.3 Antenna Feeds**

Techniques for feeding the microstrip antenna can be classified into three group: directly coupled, electromagnetically coupled and aperture coupled. Details about this feeding technique will be explained throughout this section.

### **2.3.1 Directly Coupled**

It is the most popular and the oldest method. But, this method provides only one degree of freedom to adjust impedance. This method has a narrow bandwidth, which can only increased by increasing the substrate thickness. The examples of direct feeds are microstrip feed line and coaxial feeds.

### 2.3.1.1 Microstrip Line Feed

For the microstrip feed is planar, permitting the patch and feed to be printed on a single metallization layer. It means that, microstrip patch and microstrip line feed are undoubtedly combined on the same substrate. Figure 4 [13] shows the example on microstrip line feed. This structure cannot be optimized as an antenna. Because of the feed line does not radiate too much at the discontinuities, some compromise between the two must be made [13].

It is not often convenient to change the patch width to control impedance. But, a quarter-wave matching section of microstrip transmission line can be used to transform the impedance edge – fed patch, that is, with a section of transmission line is a quarter – wavelength long based on the wavelength in the transmission line, the antenna input impedance  $Z_A$  can be matched to a transmission line of characteristic impedance  $Z_0$  (often  $50 \Omega$ ) [12].

$$Z_0 = \sqrt{Z_A Z_0} \quad (2.1)$$

The characteristic impedance of microstrip line decreases as the strip width increases.

The inset feed is another type of microstrip feed line as shown in Figure 5 [13]. This type of feed is easily etched as well as providing adjustable input impedance and being planar. But, changing the input impedance by a large amount required high permittivity substrate demand significant inset depth, which will affect cross polarization and radiation pattern shape.

However, because of the feed line does not radiate too much at the discontinuities, some compromise and consideration between the microstrip line and microstrip patch must be made [14]. The spurious radiation increase the side – lobe level and the cross polarization and downgrading the antenna performance. Bandwidth is reduced as the considerable reactive power is accumulate below the patch [14].

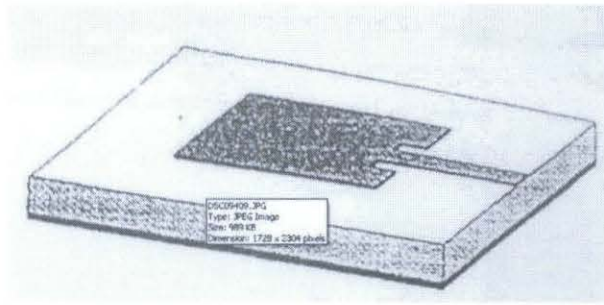


Figure 4 Patch antenna with microstrip line feed.

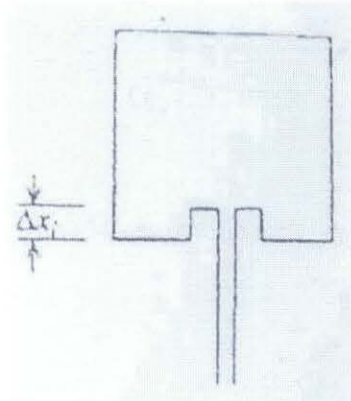


Figure 5 Microstrip feed with inset.

### 2.3.1.2 Coaxial Feed

Theoretical developments nearly always considered coaxial feeds located perpendicularly to the patch antenna (Figure 6 [13]). Impedance can be adjusted by proper placement of the probe feed by using this method. The input resistance is reduced by factor [12]  $\cos^2(\pi\Delta X_P / L)$  if the probe distance from the patch edge  $\Delta X_P$  is increased. When the substrate is thin, the intrinsic of the coaxial feed is small and can be neglected. Instead of thick substrate, is become significant, in which case the feed of adjacent element can also couple to one another.

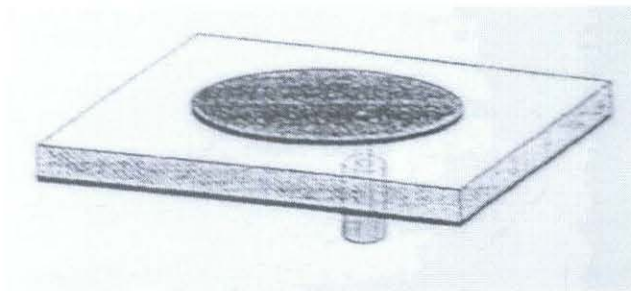


Figure 6 Patch antenna with coaxial feed.

Practically, coaxial feeds are difficult to realize. Holes have to be drilled through the substrate, an operation that tries to avoid. The conductor must be introduced through the holes and soldered to the patch. This operation needs careful handling and mechanical control of the connection, which always difficult to be done.

### 2.3.2 *Electromagnetically Coupled*

It is also known as proximity, non - contacting or gap feeds. Feeds do not contact the patch and have at least two design parameters. The advantage of this method is by being less sensitive to etching error. The gap capacitance partially cancels the probe inductance and permitting thicker substrates. The microstrip feed with a gap is entirely planar and easy to etch. The gap distance may become small in high permittivity design.

### 2.3.3 *Aperture Coupled*

This method becomes famous from time to time. By placing the patch and the feed at a different level as shown if Figure 7, some amount of decoupling between antenna and feed is obtained [12], [13]. Usually, the upper substrate has low dielectric permittivity to promote radiation. To enhance binding of the field to the feed lines, the lower substrates containing the feed has the higher dielectric constant [12]. It leads to increase bandwidth of the antenna. The central ground plane acts to isolate the feed system from patches is its other advantage.

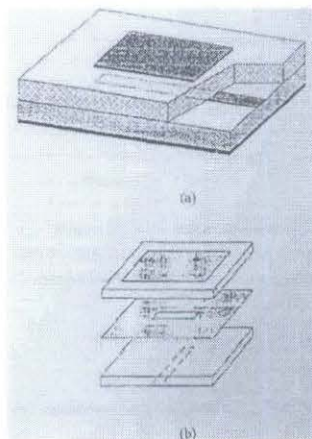


Figure 7 Example of aperture-coupled feed.

In Figure 7, (a) patch antenna of buried feed (b) aperture coupled feed.

## 2.4 Models

Transmission line model and cavity model are the examples of the simple models on microstrip antenna analysis. These simple models only provide the first order approximation of the radiation pattern of the antenna and do not take the surface waves into account. Later in this section, the descriptions about these models are included.

### 2.4.1 Transmission Line Model

The simplest analytical model is transmission line model. The advantage of this model is that the feed point impedance can easily be computed [17]. The rectangular patch antenna acts as a half – wave resonant transmission line with the end gap producing the radiating field as shown in Figure 8 [17]. Then, two vertical radiating apertures under the open – ended edges of the upper conductor (Figure 9) [13] replaced the rectangular patch antenna. A transmission line, half – wavelength long connected the two apertures.

This model present that, the ends are terminated with radiation susceptance and conductance and the effective dielectric was used is constant. The effective dielectric constant is given by:

$$\epsilon_e = \frac{1}{2}(\epsilon_r + 1) \frac{\epsilon_r - 1}{2\sqrt{1 + 12t/W}} \quad (2.2)$$

The radiation admittance implies a radiation  $Q$ , which is:

$$Q_{rad} = \frac{\sqrt{\epsilon_e \lambda_0}}{4t} - \frac{\epsilon_e \Delta L}{t} \quad (2.3)$$

Where  $\Delta L$  is the change in effective length produced by field fringing [17]:

$$\frac{\Delta L}{t} = 0.412 \frac{(\epsilon_e + 0.300)(W/t + 0.262)}{(\epsilon_e - 0.258)(W/t + 0.813)} \quad (2.4)$$

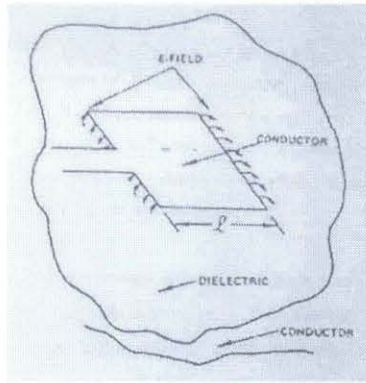


Figure 8 Rectangular patch antenna with radiating field.

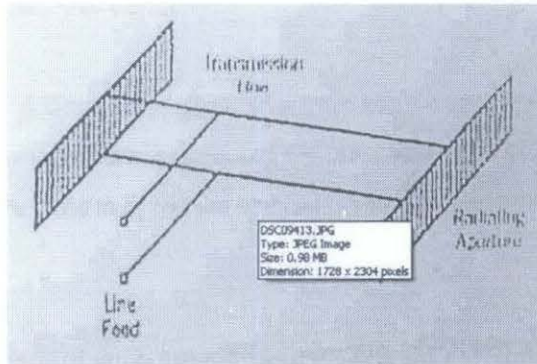


Figure 9 Transmission line model.

The transmission line model was later improved to take into account substrate and conductor losses, coupling between the two apertures and reactive effects. This approach was also extended to consider radiation from circular or annular patches.

#### 2.4.2 The Cavity Model

The cavity model (Figure 10) is particularly popular and first developed by Lo and colleagues [17], and by Carver and colleagues. The advantages [18] of this model are it is being simple, providing physical insight and design information for rectangular, circular, annular and triangular patches can be obtained with relative ease.

This model represents that the field between patch and the ground plane as a series of rectangular (or circular) cavity modes. This means, the upper patch and the section of the ground plane located below it joined by magnetic wall under the edge

of the patch, which will form a dielectric resonator. The magnetic currents flowing on the cavity sidewalls radiate at a resonant frequencies of the cavity, which is assumed to be surrounded by free space [13].

Treat the region between the patch and the ground plane, as a resonant leaky cavity is the basic idea of the cavity model. The radiation fields then can be calculated if the fields in the cavity excited by the probe can be obtained and the equivalent sources can be put in the exit region of the cavity. An effective loss tangent can be produced to account for conductor loss, dielectric loss and radiation loss. This effective loss tangent is used to calculate the input impedances and impedances bandwidth and the resonant frequencies of the rectenna are determined by the resonant frequency of the cavity.

There is some assumption, which renders the calculation for the simple cavity model. Assumed that the thickness of the substrate is smaller than the wavelength, so that the electric field only has the vertical ( $z$ ) component. From this, it follows that [18]:

1. The field in cavity is transverse magnetic (TM);
2. The cavity is bounded by magnetic wall on the sides;
3. Surface wave excitation is negligible;
4. The current is coaxial probe is independent of  $z$ .

However there are some limitations in using the cavity model. This model cannot handle design involving parasitic elements and cannot analyze microstrip antennas with superstrates. The cavity model results will become inaccurate when the thickness substrate exceed until 2% of free space wavelength [18]. So, more accurate analyses on microstrip antenna are using full wave models.

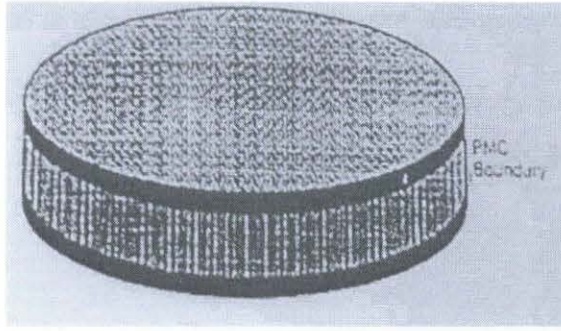


Figure 10 Cavity Model

## 2.5 Microstrip Patch Antenna

If the upper conductor of the microstrip device is a patch, that is appreciable fraction of the wavelength in extent, the device becomes a microstrip antenna. The patch antenna belongs to the class of resonant antennas and its resonant behavior is responsible for the main challenge in microstrip antenna designing – achieving adequate bandwidth. Conventional patch design yields a few percentages of bandwidth [12].

Patches are firstly invented by Deschamps (1953) [17], probably based on the earlier partial sleeves (shorter quarter – wave patch). There're many shape of patches but most commonly and most popular are rectangular and circular. Patches may have electromagnetically coupled portions.

### 2.5.1 Rectangular Microstrip Patch Antenna

Rectangular patch is commonly used in microstrip antenna and usually being fed from a microstrip transmission line as shown in Figure 11 [12]. The substrate thickness  $t$  is much less than a wavelength (usually on the order of  $0.01 \lambda_0$ ) [19]. The selected of  $t$  is based on the bandwidth over which the antenna must operate. Operation of the rectangular patch is usually near resonance in order to obtain real value input impedance. The most popular rectangular patch is half – wave patch.

The pattern of the half – wave rectangular patch antenna is rather broad with a maximum direction normal to the plane of the antenna. The far field components of this microstrip patch antenna given as [12]:

$$E_{\theta} = E_0 \cos \phi f(\theta, \phi) \quad (2.5)$$

$$E_{\phi} = -E_0 \cos \theta \sin \phi f(\theta, \phi) \quad (2.6)$$

where

$$f(\theta, \phi) = \frac{\sin \left[ \frac{\beta W}{2} \sin \theta \sin \phi \right]}{\frac{\beta W}{2} \sin \theta \sin \phi} \cos \left( \frac{\beta L}{2} \sin \theta \sin \phi \right) \quad (2.7)$$

Another rectangular patch antenna encountered in practice is a quarter – wave element that has  $L \approx \lambda_d / 4$  and is formed by placing shorting bins from the patch to the ground plane at  $x = 0$ . The current peak is then in the same position as a half wave patch.

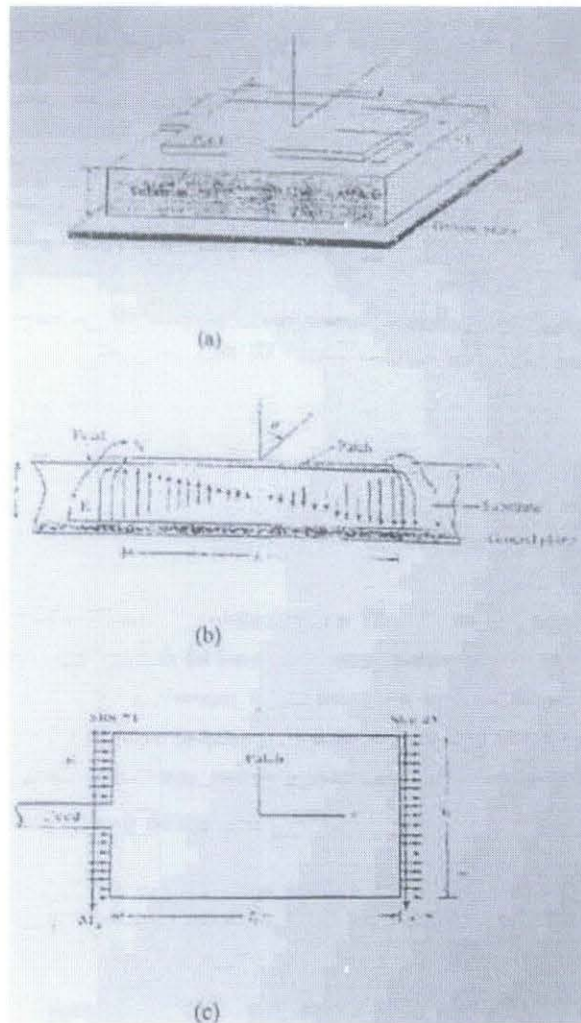


Figure 11 The half-wavelength rectangular microstrip patch antenna.

In Figure 11,  $L \approx 0.49\lambda_d$  (a) geometry for analyzing the edge-fed microstrip patch antenna (b) side view showing the electric fields (c) top view showing fringing electric fields that are responsible for radiation. The equivalent magnetic surface M, currents are also shown.

### 2.5.2 Other Patch Shapes

Other popular patch shape is circular shape which creating circular polarization. Circular polarization can be achieved by feeding the corner of the rectangular patch, by using two feeds at  $90^\circ$  with a  $90^\circ$  hybrid connected to the feed line. A simpler but narrow – band version replaces the hybrid by a power divider, with an extra  $\lambda/4$  line length in one feed.

However, over which the circular polarization occurs is significantly reduced from the intrinsic patch bandwidth. The circular patch also can be modified to be an elliptical shape.

## **2.6 Schottky Diode**

### **2.6.1 Introduction**

Due to its advantages as stated on previous section [9], Schottky diode is selected as a rectifying circuit. To rectify or to convert the microwave power that has been received to the DC power, this diode incorporates with the antenna. Typically diode is loaded onto the single patch antenna to improve the impedance behavior of the radiating element [20].

Schottky diodes are metal – semiconductor rectifying junction. Schottky diode is formed by depositing a variety of metals of n –type or p –type semiconductor materials by chemical deposition (electroplating), evaporation or sputtering. The theory about rectifying metal – semiconductor junction is founded in 1930's by Walter Schottky [21]. In early 1960s, Schottky diodes [21] were introduced for similar applications. The most popular and commonly used materials in this diode are n – type silicon and n – type gallium arsenide (GaAs). For frequency up to 40 GHz the Silicon Schottky diode is still available, but for the higher frequency applications GaAs is used [22] (see Appendix 2A for semiconductor material comparison).

A Silicon Schottky diode is used for rectifying circuit in Wireless Power Transmission System in C – band frequency [9]. The rectenna incorporates with this diode to convert the received microwave power signal to direct current (DC) useful power. The selection of Schottky diode is depending on having great forward current and reverse withstand voltage among other commercial diodes.

### 2.6.2 Schottky – Mott and Bardeen Theory

Schottky – Mott theory [23], [24] is the earliest model of Schottky diode, which explains about the barrier height. Barrier is resulted from the difference in the work functions of the two substances. Figure 12 [24], the energy band diagram is illustrated the process of the barrier formation. Figure 12 (a) shows that the electron energy band diagram of the metal work function  $\phi_m$  and the n – type semiconductor of work function  $\phi_s$ , the amount of energy required to raise the electron from Fermi level to the vacuum level is the work function of metal. The work function  $\phi_s$  of the semiconductor is defined similarly and is a variable quantity because the Fermi level in semiconductor is varies due to doping. An important surface parameter, which does not depend on doping, is the electron affinity  $\chi_s$ , defined as the energy difference of an electron between the vacuum level and the lower edge of the conduction band. These three work functions normally are expressed in electron volts (eV).

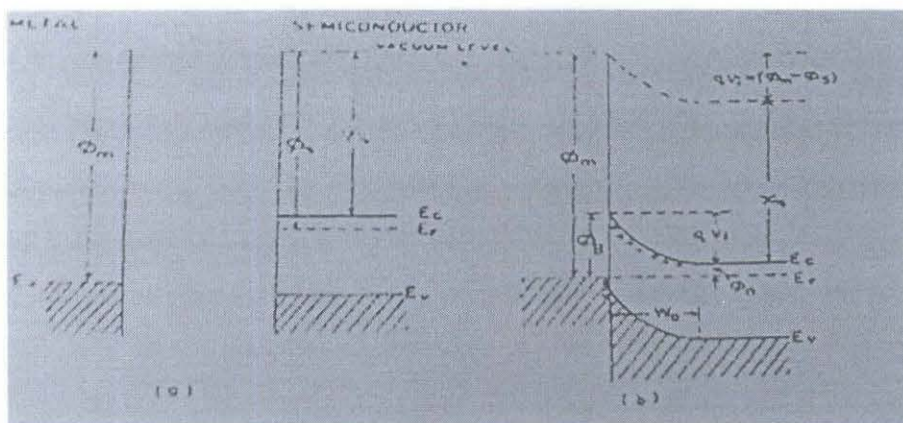


Figure 12 Electron energy band diagrams.

Figure 12 shows electron energy band diagrams of metal contact to n – type semiconductor with  $\phi_m > \phi_s$  (a) neutral materials separated from each other (b) thermal equilibrium situation after the contact has been made.

While Figure 12 (b) is presented the energy band diagram after the contact is made and equilibrium has been reached. When the two substances are brought into intimate contact electrons from the conduction band of the semiconductor, which has the higher energy than the metal electrons, flow into the metal until the Fermi level on

the two sides are brought into coincidence. When the electron move out of the semiconductor region, the boundary decreases. Since the separation between the conduction band edge  $E_c$  and Fermi level  $E_F$  increase with decreasing electron concentration and in thermal equilibrium  $E_F$  remains constant throughout, the conduction band edge  $E_c$  bends up as shown in Figure 12 (b).

The valence band edge  $E_v$  will move up parallel to the conduction band edge  $E_c$  since the band gap of the semiconductor not change by making contact with the metal. The vacuum level also will follow the same variation as  $E_c$ . All of this is because the electron affinity of the semiconductor is assumed to remain unchanged even after the metal contact is made. The important point to determine the barrier height is that the vacuum level must remain the continuous across the transition region. The difference between the two vacuum levels is the amount of band bending, which can be expressed as [23], [24]:

$$qV_i = (\phi_m - \chi_s) \quad (2.8)$$

$V_i$  is known as contact potential different or the built in potential of the junction and  $q$  is the electronic charge. The function of  $qV_i$  obviously is the potential barrier. However the barrier looking from the metal towards the semiconductor is different and is given by [23], [24]:

$$\phi_B = (\phi_m - \chi_s) \quad (2.9)$$

Since

$$\phi_s = \chi_s + \phi_n \quad (2.10)$$

where

$$\phi_B = (qV_i + \phi_n) \quad (2.11)$$

and

$$\phi_n = (E_c - E_F) \quad (2.12)$$

$\phi_m$  is representing the penetration of the Fermi level in the band gap of the semiconductor. The exact shape of the potential barrier can be calculated from the charge distribution within the space charge layer. In most cases, the height  $\phi_B$  of the barrier is orders of magnitude larger than the thermal voltage, and the space charge region in semiconductor becomes high – resistivity depletion region devoid of mobile carriers.

However, in practical, the theory above does not appear to apply. The equation (2.9) shows that the barrier height is strongly depends on the  $\phi_m$  is observed only in predominantly ionic semiconductor but actually in many covalent semiconductors the barrier height is a less sensitive function of  $\phi_m$ , and in some cases it is almost independent of  $\phi_m$ . The modification about the first theory has been made by Bardeen [23], [24]. As a result the barrier height is given by [24]:

$$\phi_B = (E_g - \phi_0) \quad (2.13)$$

Where,  $\phi_0$  is a neutral level (see Figure 13 [39]). In this case the barrier height is said to be pinned by surface state. The example of the covalent semiconductor is Si (silicon), Ge (germanium) and GaAs (gallium arsenide). This equation is called as a Bardeen limit.

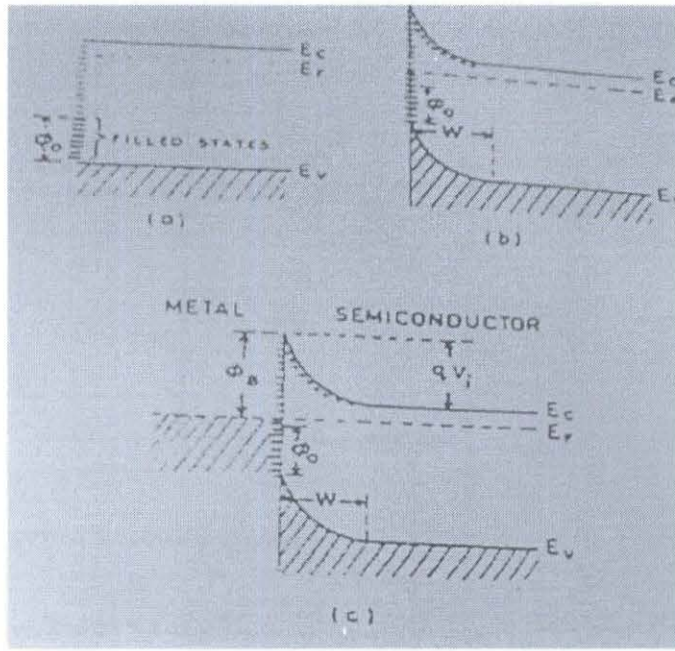


Figure 13 Electron energy band diagram

In Figure 13, electron energy band diagram of n – type semiconductor with surface states. The diagram shows, (a) flat band at the surface (b) surface in thermal equilibrium with the bulk (c) semiconductor with contact in metal.

### 2.6.3 Characteristic

Figure 14 [25] shows the structure and band diagram of the Schottky diode. Normally, electron potential energy is differenced between the metal and the conduction band of about 0.7 eV. Therefore, when the metal is joined to an n – type semiconductor, electrons will diffuse from the semiconductor into the metal where the energy is lower. This difference is called the barrier potential  $\phi_B$ , which is expressed in volt. This barrier height or potential is an important parameter in determined the local oscillator power necessary to bias the diode into its nonlinear region [21].

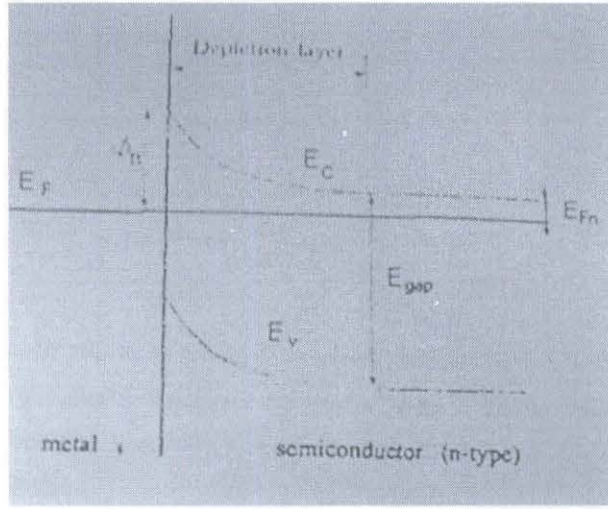


Figure 14 Schottky contact.

From Figure 14, the depletion region layer is formed. The depletion layer width,  $w$  is equal to [25]:

$$w = \left[ \frac{2\epsilon}{qN_D} (V_D - V) \right]^{\frac{1}{2}} \quad (2.13)$$

with

$$V_D = \phi_B - E_F \quad (2.14)$$

The donor density,  $N_D$ , is in n – layer and  $V_D$  is the diffusion or metal – semiconductor potential. While,  $V$  is applied voltage and  $\epsilon$  is permittivity of the dielectric. Equation (2.13) is derived with the assumption that Schottky diode is as a p – n junction with an infinitely p doping.

The current – voltage (CV) characteristic of the ideal Schottky diode is given by an expression [21], [25] – [27], in its most simple form,

$$I = I_s \left( \exp \frac{qV_d}{nkT} - 1 \right) \quad (2.15)$$

where,

$$I_s = AA^* T^2 \exp \left( - \frac{q\phi_B}{kT} \right) \quad (2.16)$$

the saturation current is  $I_s$ ,  $T$  is the absolute temperature,  $k$  is the Boltzmann's constant,  $n$  is the ideality factor,  $A$  is the area,  $A^*$  is the Richardson constant (the calculated value of  $A^*$  at 300 K is shown at Appendix 2B) and  $V_d$  is voltage across the diode junction.

The junction capacitance is given simply by the one – sided abrupt junction analysis. Device capacitance is given by the following relation [21], [28]:

$$C = A \left[ \frac{q \epsilon N_D}{2(V_D - V)} \right]^{\frac{1}{2}} \quad (2.17)$$

It is desirable to have capacitance reactance of the junction large with respect to the diode small signal conductance, in order to achieve high conversion efficiency.

To explain device series resistance and individual contribution thereto, several models of Schottky diodes have been proposed. The series resistance  $R_s$  is voltage and frequency dependent. While, for resistance in the epitaxial layer and the semi conducting substrates also depends on the junction geometry and to the lesser extent, on the applied voltage. Due to the Figure 15 [21],  $R_s = R_{s1} + R_{s2}$  where  $R_{s1}$  is [24]:

$$R_{s1} = \frac{\rho}{A} = \frac{2w}{(q\mu_n N_D)A} \quad (2.18)$$

and,

$$R_{s2} = \frac{\rho}{2d} = 2\rho_s \left( \frac{A}{\pi} \right)^{\frac{1}{2}} \quad (2.18)$$

with,

$$d = 2 \left( \frac{A}{\pi} \right)^{\frac{1}{2}} \quad (2.19)$$

the electron mobility is  $\mu_n$ ,  $\rho$  is the resistivity of the depletion layer,  $\rho_s$  is the substrate resistivity and  $d$  is the active junction diameter.

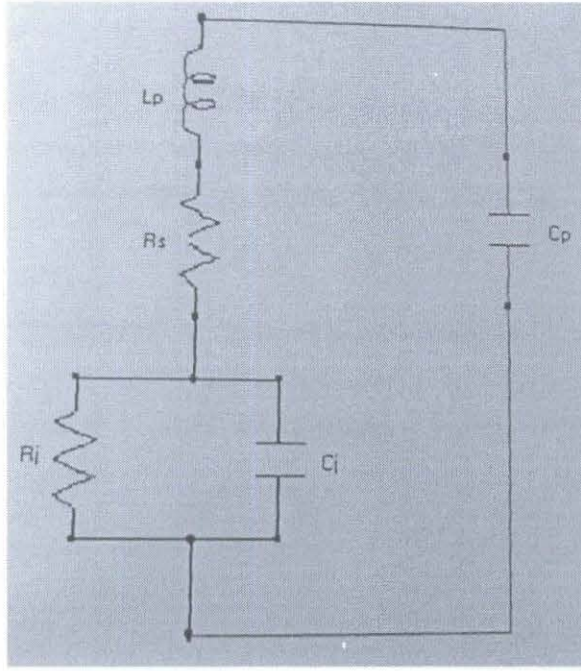


Figure 15 Equivalent circuit of Schottky diode.

#### 2.6.4 Rectifying Diode: Derivation of Closed Form Equation for Conversion Efficiency

The rectifying efficiency and the effective microwave impedance of the diode, theirs' closed form expressions are derived with the assumption that the current due to the junction capacitance is negligible when the diode is forward biased. This is based on the change of  $V_d$  is small during this period. Plus, the forward voltage drop across the intrinsic diode junction is constant during the forward biased period. After considering this assumptions, the voltage wave form  $V$  and  $V_d$  is stated as [4]:

$$V = -V_0 + V_1 \cos(\omega t) \quad (2.19)$$

$$V_d \begin{cases} -V_{d0} + V_{d1} \cos(\omega t - \phi) & \text{if diode is off} \\ V_f & \text{if diode is on} \end{cases} \quad (2.20)$$

$V_0$  is the output DC voltage and the voltage  $V_1$  is a peak voltage of an incident microwave.  $V_{d0}$  and  $V_{d1}$  are the DC and the fundamental frequency components of

diode junction voltage  $V_d$ . While  $V_f$  is the forward voltage drop of the diode.

By relating the other variables like  $V_i, V_{d0}, V_{d1}$  and  $\phi$  to the known variable i.e.  $V_0$  the efficiency and diode effective are computed. By applying Kirchoff's voltage law along the DC pass loop, the DC voltage is related to the DC component of  $V$  according to [4].

$$V_0 = \frac{V_{d.DC}}{1+r} \quad (2.21)$$

$r = R_s / R_L$  and  $R_L$  is the DC load resistance and  $V_{d.DC}$  is the average value of the waveform  $V_d$ , which is derived as [4]:

$$V_{d.DC} = V_{d0} \left( 1 - \frac{\mathcal{G}_{off}}{\pi} \right) + \frac{V_{d1}}{\pi} \sin \mathcal{G}_{off} - V_f \frac{\mathcal{G}_{off}}{\pi} \quad (2.22)$$

$\mathcal{G}_{off}$  is the phase angle when the diode is turned off and can be computed using [4]:

$$\cos \mathcal{G}_{off} = \frac{V_f + V_{d0}}{V_{d1}} \quad (2.23)$$

The other equation of current with the function of  $R_s$  can be derived as follows [4] when the diode is turn off:

$$R_s = \frac{d(C_j V_d)}{dt} = V - V_d \quad (2.24)$$

and  $C_j$  can be expended as:

$$C_j = C_0 + C_1 \cos(\omega t - \phi) + C_2 \cos(2\omega t - 2\phi) + \dots \quad (2.25)$$

While  $V_f$  is solved with I-V relation of the diode, which is [4]:

$$I_s \left( \exp \frac{eV_f}{nkT} \right) - 1 = \frac{-V_0 + V_1 - V_f}{R_s} \quad (2.26)$$

DC power and the power loss are expressed as below [4]:

$$P_{DC} = \frac{V_0^2}{R_L} \quad (2.27)$$

$$P_{loss} = LOSS_{on.Rs} + LOSS_{on.diode} + LOSS_{off.Rs} + LOSS_{off.diode} \quad (2.28)$$

where,

$$LOSS_{on.Rs} = \frac{1}{2\pi} \int_{-\vartheta_{off}}^{\vartheta_{off}} \frac{(V - V_f)^2}{R_s} d\vartheta \quad (2.29)$$

$$LOSS_{on.diode} = \frac{1}{2\pi} \int_{-\vartheta_{off}}^{\vartheta_{off}} \frac{(V - V_f)V_f}{R_s} d\vartheta \quad (2.30)$$

$$LOSS_{off.Rs} = \frac{1}{2\pi} \int_{\vartheta_{off}}^{2\pi - \vartheta_{off}} \frac{(V - V_d)^2}{R_s} d\vartheta \quad (2.31)$$

$$LOSS_{off.diode} = \frac{1}{2\pi} \int_{\vartheta_{off}}^{2\pi - \vartheta_{off}} \frac{(V - V_d)V_d}{R_s} d\vartheta \quad (2.31)$$

$$efficiency = \frac{P_{DC}}{P_{loss} + P_{DC}} \quad (2.32)$$

The efficiency of diode can be calculated by using equation (2.26) to (2.32). However, in this project no consideration and concentration on the efficiency of the diode has been made.

### 2.6.5 Summary

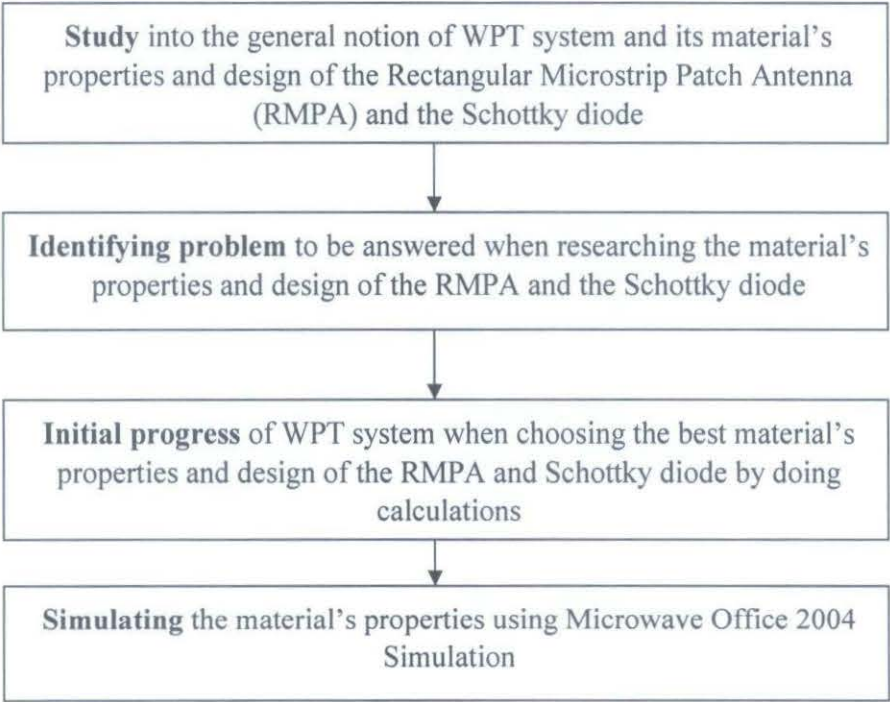
Barrier height or potential is an important parameter in analyze the Schottky diode, which must be considered in determined the local oscillator power necessary to bias the diode into its nonlinear region. Nowadays, the applications of this diode have been increased especially for the higher frequency.

## CHAPTER 3

### METHODOLOGY

#### 3.1 Procedure Identification

The procedures that were involved in the development of the Final Year Project 2 are as shown below:



### Study (Research)

The first procedure is to do research into the concept of Wireless Power Distribution (WPT) System and its properties. This is an essential part of the project, as the idea of WPT system is really new to the writer. The writer needs to understand what WPT system is to be able to complete the project. The outcome of the research can be found in the previous chapter. The initial research will take duration of two weeks, and still be done throughout the progress of the project.

### Identifying Problem

Next is identifying the problem to be answered in building WPT system, which is the material's properties and design of the Rectangular Microstrip Patch Antenna (RMPA) and the Schottky diode that will give the best efficiency of transmitting power. This is an important part of the project, where a simple yet credible problem needs to be identified to be able to demonstrate the concept of RMPA Schottky diode to others.

### Initial Progress

After identifying the problem, the material's properties and design of the RMPA and the Schottky diode were to be solved by doing calculation on it.

### Simulation

The final phase of this project is the simulation of the Microwave Office 2004 Simulation program. We will be able to see the effect of applying different selection methods, and also the effect of varying program parameters. The result to be observed is the variable values that can be change in the equations to complete the task. These results will be discussed later in Chapter 4.

### 3.2 Tools Required

The only tool required for this project is the Microwave Office 2004 Simulation software. This Microwave Office 2004 Simulation software will be used for programming and also simulation of the project. Other tools may be needed in this project (FYP II), so it will be confirmed later.

### 3.3 Introduction on Simulation

The rectangular microstrip patch antenna is the antenna that has been designed as a reception antenna. For rectifying circuit, Schottky diode is selected. For the electromagnetic simulation, linear and nonlinear analysis, the provided simulator is Microwave Office 2004. To simulate the performance of Schottky diode, concentration has been made on electromagnetic simulation for rectangular microstrip patch antenna and nonlinear analysis in this chapter. Appendix C is a guide in how to use the Microwave Office 2004.

### 3.4 Simulation on Rectangular Microstrip Patch Antenna

For Wireless Power Transmission (WPT), rectangular microstrip patch antenna act as a reception antenna in rectenna. The simulations have been done at single point frequency (2.45 GHz) and for the frequencies at range between 2.4 GHz and 2.5 GHz. By using the electromagnetic structure, the structure of the antenna can be accomplished. Rectangular microstrip patch antenna only has the ground plane at the bottom and the single rectangular patch on the top of the dielectric substrate. Three different types of dielectric substrates have been carried out in the simulation for comparison. Polyester/Resin, Polyester/Resin laminated with GML 1000 and PTFE/Glass mix are the substrates [16].

The shape of the patch antenna is rectangular (see Figure 16) with  $L$  is the length and  $W$  is the width. The effective length of the patch is extended by the fringing fields of patch antenna. Therefore, the length of a half-wave patch is slightly less than a half-wavelength in the dielectric substrate material. In favor of the length of a resonant half-wave patch, the approximate value is given by [12]:

$$L \approx 0.49\lambda_d \quad (4.1)$$

that is

$$\lambda_d = \frac{\lambda_0}{\sqrt{\epsilon_r}} \quad (4.2)$$

and

$$\lambda_0 = \frac{c}{f} \quad (4.3)$$

the velocity of light,  $c$ , that is  $3 \times 10^8 \text{ m/s}$ , and  $f$  is the project frequency (2.45GHz)

For the higher order modes not to be excited and to give proper radiation resistant at the input, the width of the patch,  $W$  must be less than the wavelength in the dielectric substrate. The rectangular patch's width,  $W$ , usually is taken about  $\lambda_0/2$  (free space wavelength divided by two). Substrate effects and slot width are neglected in this simple pattern expression. For the input impedance, an approximate expression is as presented below [12]:

$$W = \sqrt{\frac{90 \frac{\epsilon_r^2}{\epsilon_r - 1}}{Z_A}} L \quad (4.4)$$

therefore

$$Z_A = 90 \frac{\epsilon_r^2}{\epsilon_r - 1} \left( \frac{L}{W} \right)^2 \Omega \quad (4.5)$$

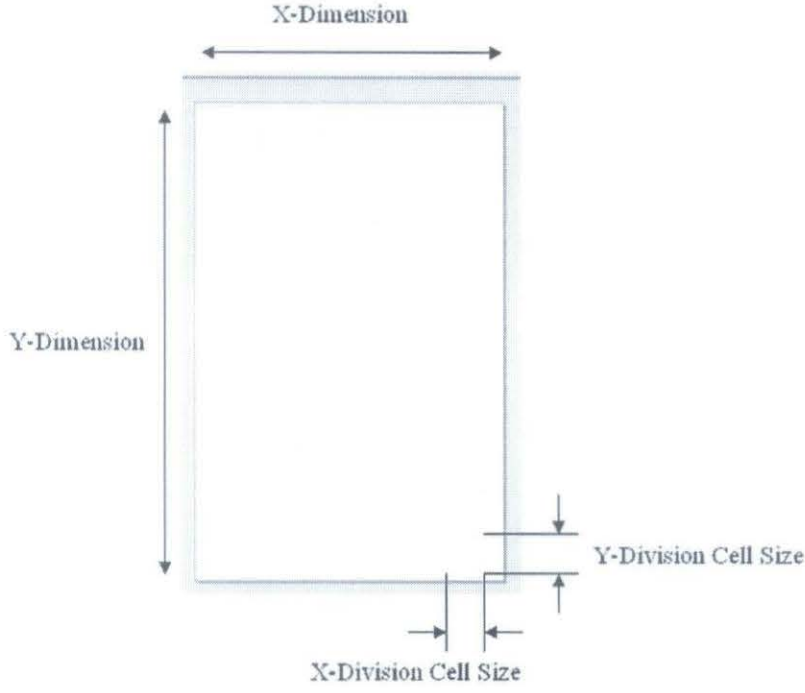


Figure 16 Rectangular patch

The  $x$  and  $y$  dimension must be calculated to simulate the rectangular microstrip patch antenna besides knowing the length and the width of the patch. The width and length of the enclosure are performed as these  $x$  and  $y$  dimensions as in Figure 17. By evaluating the width ( $W$ ) and ( $L$ ) of the rectangular patch, these parameters can be determined. The  $x$  dimension can be determined from these two values as [21]:

$$L + 2\left(\frac{\lambda_d}{8}\right) \quad (4.6)$$

and by using the equation below, the  $y$  dimension can be obtained as in:

$$W + 2\left(\frac{\lambda_d}{8}\right) \quad (4.7)$$

The properties of the dielectric substrates must be known for the enclosure of the antenna. The permittivity, the thickness and the loss tangent are in Table 1 are the properties of the substrates and please refer to Appendix A for more information.

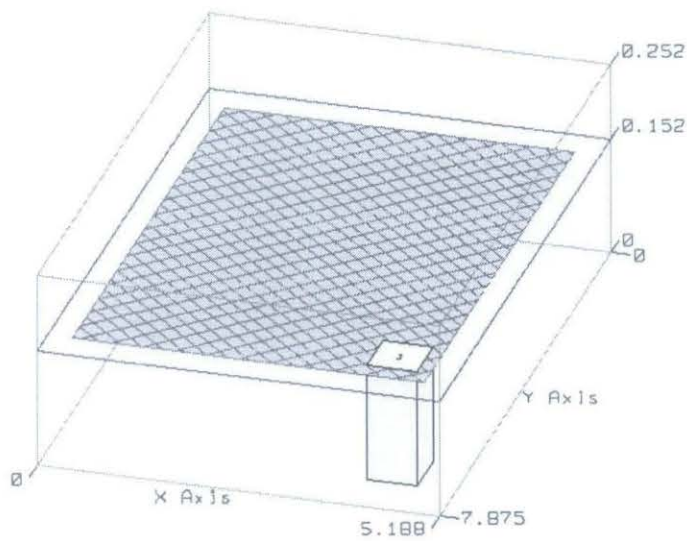


Figure 17 Enclosure of the antenna with Polyster/Resin dielectric substrate

Table 1 Properties of dielectric substrates

Dielectric	$\epsilon_r$	Thickness (cm)	Loss Tangent ( $\tan \delta$ )
Polyster/resin	$3.05 \pm 0.05$	$0.152 \pm 0.008$	0.003
Polyster/resin with GML 1000	$3.20 \pm 0.05$	$0.075 \pm 0.0005$	0.003
PTFE/glass mix	$2.33 \pm 0.02$	$0.157 \pm 0.0005$	0.0012

In Table 2, the tabulated values are the free space wavelength, wavelength in dielectric substrate, length of patch, width of patch,  $x$  dimension and  $y$  dimension Polyster/Resin, Polyster/Resin laminated with GML 1000 and PTFE/Glass mix dielectric substrates.

Table 2 Calculated parameters for rectangular microstrip patch antenna

Dielectric Substrate	$\lambda_0$ (cm)	$\lambda_d$ (cm)	$L$ (cm)	$W$ (cm)	$x$ dimension (cm)	$y$ dimension (cm)
Polyster/resin	12.245	7.011	3.435	6.1225	5.18775	7.87525
Polyster/resin with GML 1000	12.245	6.845	3.354	6.1225	5.06525	7.83375
PTFE/glass mix	12.245	8.022	3.931	6.1225	5.93650	8.128

The parameters of rectangular microstrip patch antenna which is designed by Microwave Office 2004 are  $x$  dimension and  $y$  dimension and properties of dielectric substrates by using electromagnetic (EM) simulation.

For rectangular microstrip patch feeding, coaxial feed/probe feed is chosen, which is used to guide electromagnetic energy from the source to the region of the patch. As shown in Figure 17, coaxial feed is located perpendicular to the patch antenna.

By increasing substrate thickness  $t$  and by lowering the  $\epsilon_r$ , the bandwidth and efficiency of a patch are increased. Bandwidth is often the ultimate limiting performance parameter and can be found from [12]:

$$B = 3.77 \left( \frac{\epsilon_r - 1}{\epsilon_r^2} \right) \left( \frac{W}{L} \right) \left( \frac{t}{\lambda_0} \right) \quad (4.8)$$

by means of

$$\frac{t}{\lambda_0} \leq 1 \quad (4.9)$$

In Chapter 4, the results and graphs of the simulation will be discussed briefly.

### 3.5 Nonlinear Simulation of Schottky Diode

By using the Microwave Office 2004 nonlinear analysis method, Schottky diode is analyzed. As in Figure 18, the diode is placed in series with the source. Si Schottky diode is used as a rectifier for 2.45 GHz in WPT. In analyzing the Schottky diode, these are the used parameters:

- a.  $C_{jo} = 3 \text{ pF}$  : zero bias junction capacitance
- b.  $R_s = 0.5 \Omega$  : series resistance
- c.  $B_v = 60 \text{ V}$  : breakdown voltage
- d.  $V_i = 0 \text{ V}$  : built in voltage
- e.  $I_s = 1 \times 10^{-11} \text{ A}$  : saturation current
- f.  $N = 1$  : ideality factor
- g.  $T = 27^\circ \text{ C}$  : temperature

240V is the source magnitude.

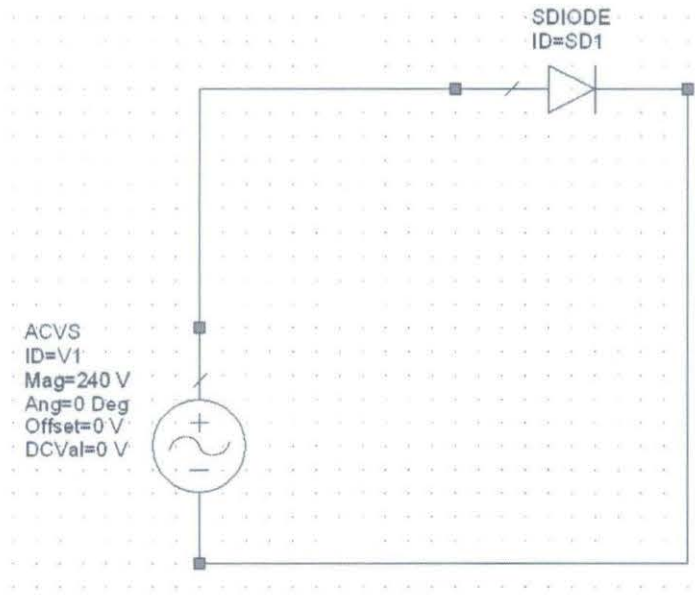


Figure 18 Equivalent circuit of Schottky diode

### 3.6 Summary

By using the Microwave Office 2004, all the simulations and analysis were done. The simulation of Schottky diode is done by using nonlinear simulation and the simulation of antenna is done by using EM simulation. The performances of rectangular microstrip patch antenna and Schottky diode are discussed later in Chapter 4.

## CHAPTER 4

### RESULTS AND DISCUSSION

#### 4.1 The Power Rectangular Microstrip Patch Antenna Results

The simulations have been done for three different substrates, which is Polyester/Resin, Polyester/Resin laminated with GML 1000 and PTFE/glass mix, as stated in Chapter 3. By using Microwave Office 2004 simulator, all the simulations have been done, using EM simulation method. The current distributions at the patch antenna are shown in Figure 19, Figure 20 and Figure 21. The currents are distributed on the top of the patch and flowing to the ground by coaxial feed.

The circular polarization of the antenna with Polyester/Resin dielectric substrate i.e. E\_LHCP and E\_RHCP is presented in Figure 22. The main reason of the simulation is to obtain the pattern of circular polarization and the total power radiated by the rectangular microstrip antenna. In the simulation, the angle,  $\phi$ , will be  $0^\circ$  and  $90^\circ$ . The antenna will give better performance if the maximum point of the polarization is located at the centre of graph that is  $0^\circ$ . E\_LHCP for  $\phi=0^\circ$  is  $8.112^\circ$ , while for  $\phi=90^\circ$  is at  $26.07^\circ$ , and, E\_RHCP is  $-7.765^\circ$  for  $\phi=0^\circ$  and  $18^\circ$  for  $90^\circ$ , as in Figure 22. Figure 23 is the circular polarization of antenna with Polyester/Resin laminated with GML 1000. The E\_LHCP for  $\phi=0^\circ$  is  $7.429^\circ$  and  $26.36^\circ$  for  $\phi=90^\circ$ . The E\_RHCP is at  $-8.429^\circ$  for  $\phi=0^\circ$  and  $3.611^\circ$  for  $\phi=90^\circ$ . Whereas, the E\_LHCP is at  $-0.199^\circ$  for  $\phi=0^\circ$  and  $13.67^\circ$  for  $\phi=90^\circ$  and the E\_RHCP is at  $-1.289^\circ$  for  $\phi=0^\circ$  and  $9.435^\circ$  for  $\phi=90^\circ$  as in Figure 24, for PTFE/Glass mix substrate.

In Table 3, the E\_PHI and E\_THETA pattern of the antenna are tabulated in this table. Moreover, the results of the circular polarization for these three substrates have been observed and also included in this table.

In Figure 25, for Polyster/Resin, the maximum E\_PHI pattern is at 20° and the E\_THETA pattern is at -1.742°. The E\_PHI is located at 12° and E\_THETA is at 0° for the Polyster/Resin laminated with GML 1000 substrate as in Figure 26. While PTFE/Glass mix dielectric substrate in Figure 27, the E\_PHI and E\_THETA are 11.74° and -1.103°

Table 3    Circular Polarization and E field pattern, results

Dielectric Substrate	E_LHCP (°)		E_RHCP (°)		E_PHI (°)	E_THETA (°)
	$\phi=0^\circ$	$\phi=90^\circ$	$\phi=0^\circ$	$\phi=90^\circ$		
Polyster/Resin	8.112	26.07	-7.765	18	20	-1.742
Polyster/Resin with GML 1000	7.429	26.36	-8.429	3.611	12	0
PTFE/Glass mix	-0.199	13.67	-1.289	9.435	11.74	-1.103

The better antenna occurs when the maximum total radiated power is located at the centre or at 0°, similar with the circular polarization. It means that, all the power that has been transmitted will be received by the reception antenna without loss or reflection when the total radiated power at 0°. The total power radiated is analyzed at 0° and 90° in this simulation. The maximum power radiated of the antenna with Polyster/Resin dielectric is 0° for  $\phi=0^\circ$  and 22.04° for  $\phi=90^\circ$  as in Figure 28. For the antenna with Polyster/Resin laminated with GML 1000 as in Figure 29, the maximum power radiated is at 0° for  $\phi=0^\circ$  and is at 11.89° for  $\phi=90^\circ$ . The total power radiated for the antenna using PTFE/Glass mix dielectric substrate as in Figure 30 is located at 0° for  $\phi=0^\circ$  and 12.06° for  $\phi=90^\circ$ . Table 4 is the results of the total radiated power of the antenna.

Table 4 Total Radiated Power

Dielectric Substrate	Total Radiated Power (°)	
	$\phi=0^\circ$	$\phi=90^\circ$
Polyster/Resin	0	22.04
Polyster/Resin with GML 1000	0	11.89
PTFE/Glass mix	0	12.06

Other than that, from the simulation, the voltage standing wave ratio (VSWR) also can be obtained. The VSWR that is representing the total reflection power must be ensured between 1 and 2, for a practical and optimum performance of the antenna. It means that, the bigger is the VSWR, the greater is the reflection power. The reflection coefficient must be small and the VSWR is below 2, to design the antenna without reflection and loss.

The VSWR is 2.317, 4.652 and 1.633 for the antenna with Polyster/Resin, Polyster/Resin laminated with GML 1000 and PTFE/Glass mix dielectric substrate as shown in Figure 31, 32 and 33. From the single point (2.45 GHz) simulation, these values are obtained.

Figure 34, 35 and 36 show the VSWR for simulation between 2.4 GHz and 2.5 GHz. It is not mean that frequency is better frequency operation, even though from these figures, there are other frequencies that give lower VSWR than the one with frequency 2.45 GHz. It happens as there are other factors that must be considered in selecting the frequency operation. The design is acceptable as long as VSWR is below than 2.

The higher is the magnitude of reflection coefficient, the higher is the value of VSWR. It showed that the value of VSWR is depends on the value of reflection coefficient. The reflection coefficient of Polyster/Resin, Polyster/Resin laminated with GML 1000 and PTFE/Glass mix for single point simulation (2.45 GHz) is presented in Figure 37, 38 and 39. While in Figure 40, 41 and 42 are the reflection coefficient of those three dielectric substrates for the simulation 2.4 GHz and 2.5 GHz. Table 5 is the tabulated results.

Table 5 Voltage Standing Wave Ratio (VSWR) and Reflection Coefficient

Dielectric Substrate	VSWR	$S_{1,1}$
Polyster/Resin	2.317	$0.577+j0.503$
Polyster/Resin with GML 1000	4.652	$0.217+j0.098$
PTFE/Glass mix	1.633	$0.681+j0.256$

Based on the estimation, the bandwidth covered by the antenna also has been calculated. For antenna with Polyster/Resin, the bandwidth is 1.838%, 0.906% for Polyster/Resin laminated with GML 1000 and lastly, antenna with PTFE/Glass mix is 1.84%.

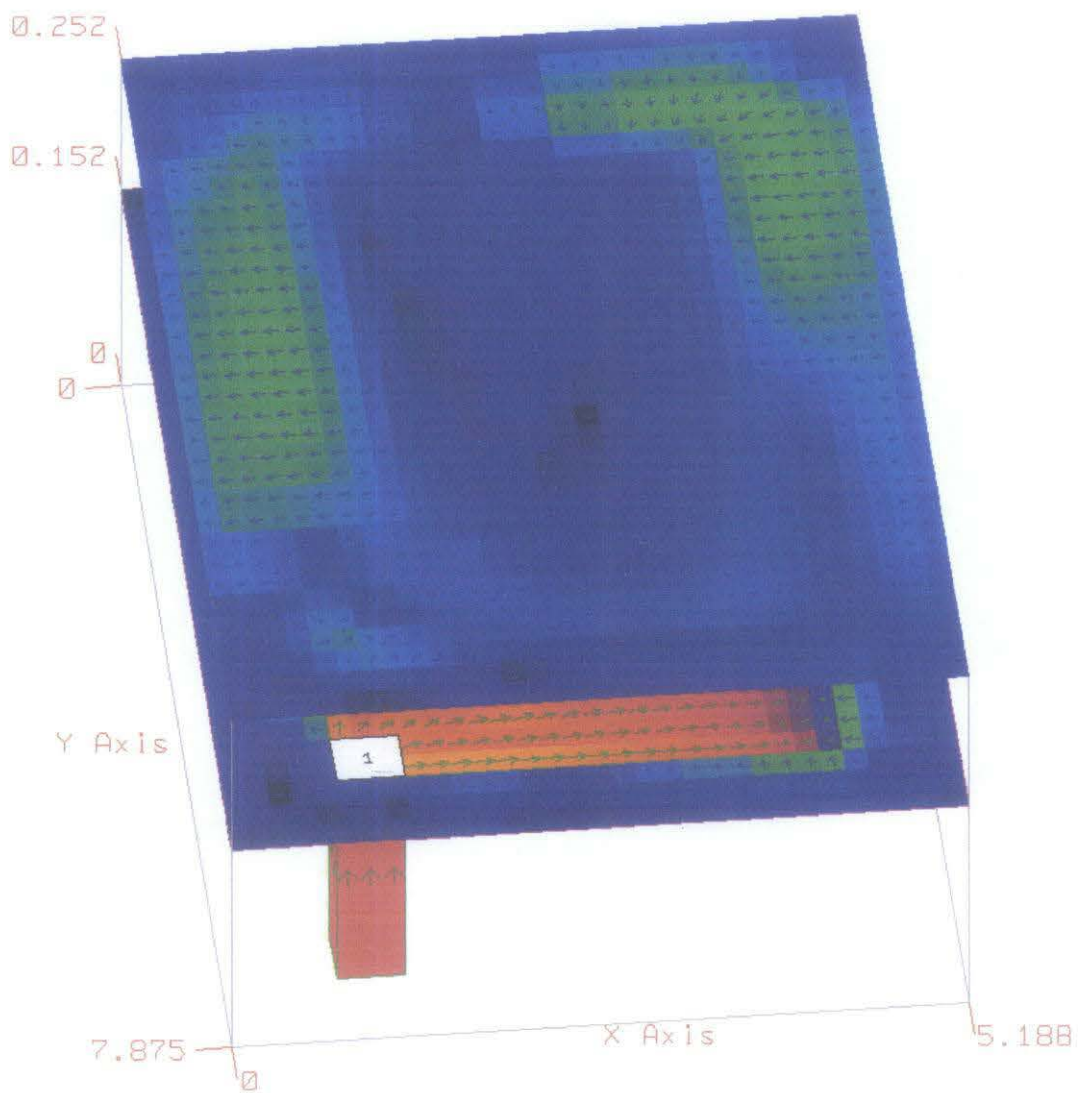


Figure 19 The antenna with Polyester/Resin dielectric substrate current distributions

The figure above shows the current distributions at the patch antenna. The currents are distributed on the top of the patch and flowing to the ground by coaxial feed. The current distribution found during the solution process can be viewed in either 2D or 3D structure. In this case, it will be viewed in 3D structure. The graphical display of the current distribution provides a visualization of the vector current distribution. Arrows indicate the direction of the current flow, while the color and also the arrow size indicate the magnitude. The lighter colors, yellow, represent the higher magnitude, while the darker colors, blue or black are used for the smaller magnitude.

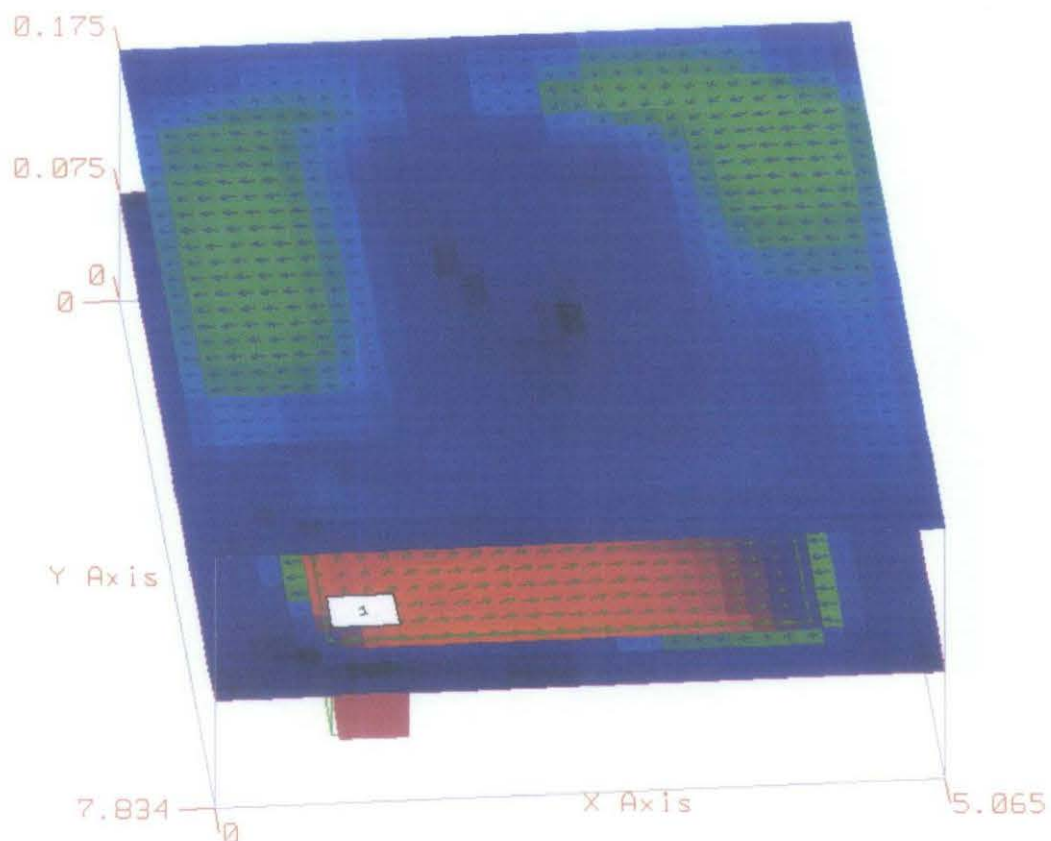


Figure 20 The antenna with Polyester/Resin laminated with GML 1000 dielectric substrate current distributions

This figure also shows the current distributions at the patch antenna. The different between the previous figure and this figure are the dimensions of the antenna, the thickness of the antenna and the dielectric characteristic of the antenna.

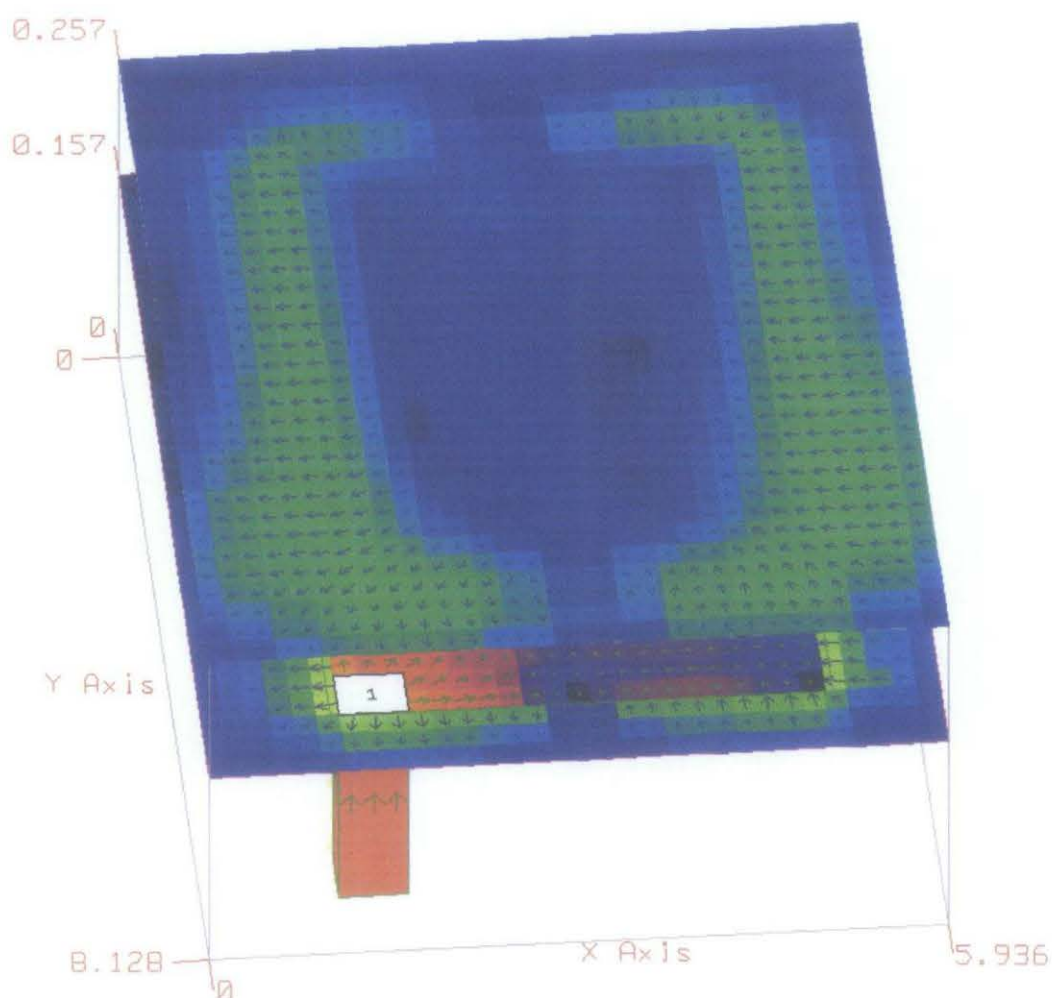


Figure 21 The antenna with PTFE/Glass mix dielectric substrate current distributions

This figure shows the current distributions at the patch antenna, quite similar from the two previous antennas. The dimensions of the antenna, the thickness of the antenna and the dielectric characteristic of the antenna are the differences between the two previous figures and this figure.

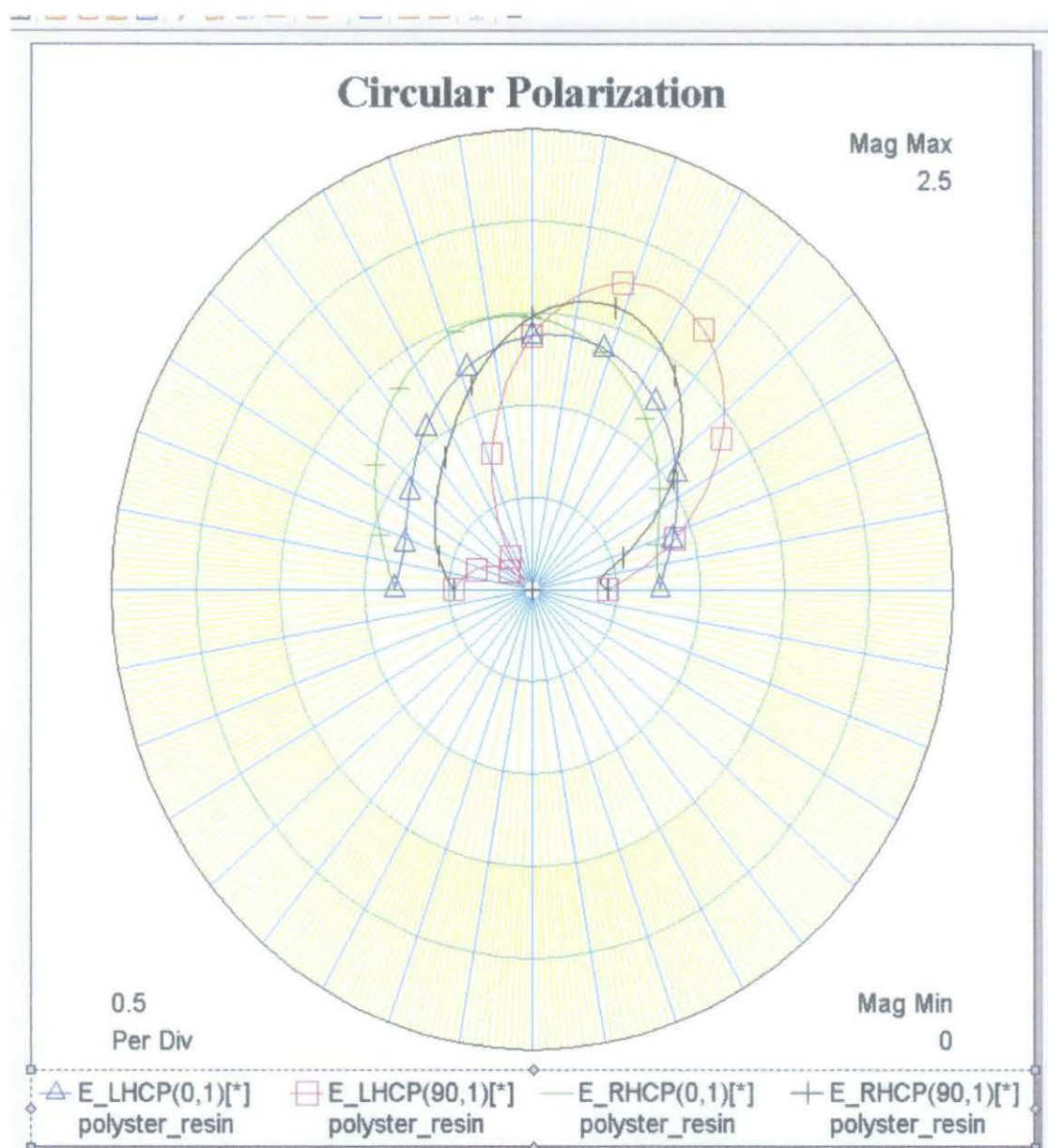


Figure 22 The antenna with Polyster/Resin dielectric substrate circular polarization

This figure shows the circular polarization of electromagnetic radiation is a polarization such that the tip of the electric field vector, at a fixed point in space, describes a circle as time progresses. The electric vector, at one point in time, describes a helix along the direction of wave propagation. The magnitude of the electric field vector is constant as it rotates. Circular polarization may be referred to as right hand circular polarization (RHCP) or left hand circular polarization (LHCP), depending on the direction in which the electric field vector rotates. E\_LHCP for  $\phi=0^\circ$  is  $8.112^\circ$ , while for  $\phi=90^\circ$  is at  $26.07^\circ$ , and, E\_RHCP is  $-7.765^\circ$  for  $\phi=0^\circ$  and  $18^\circ$  for  $90^\circ$ .

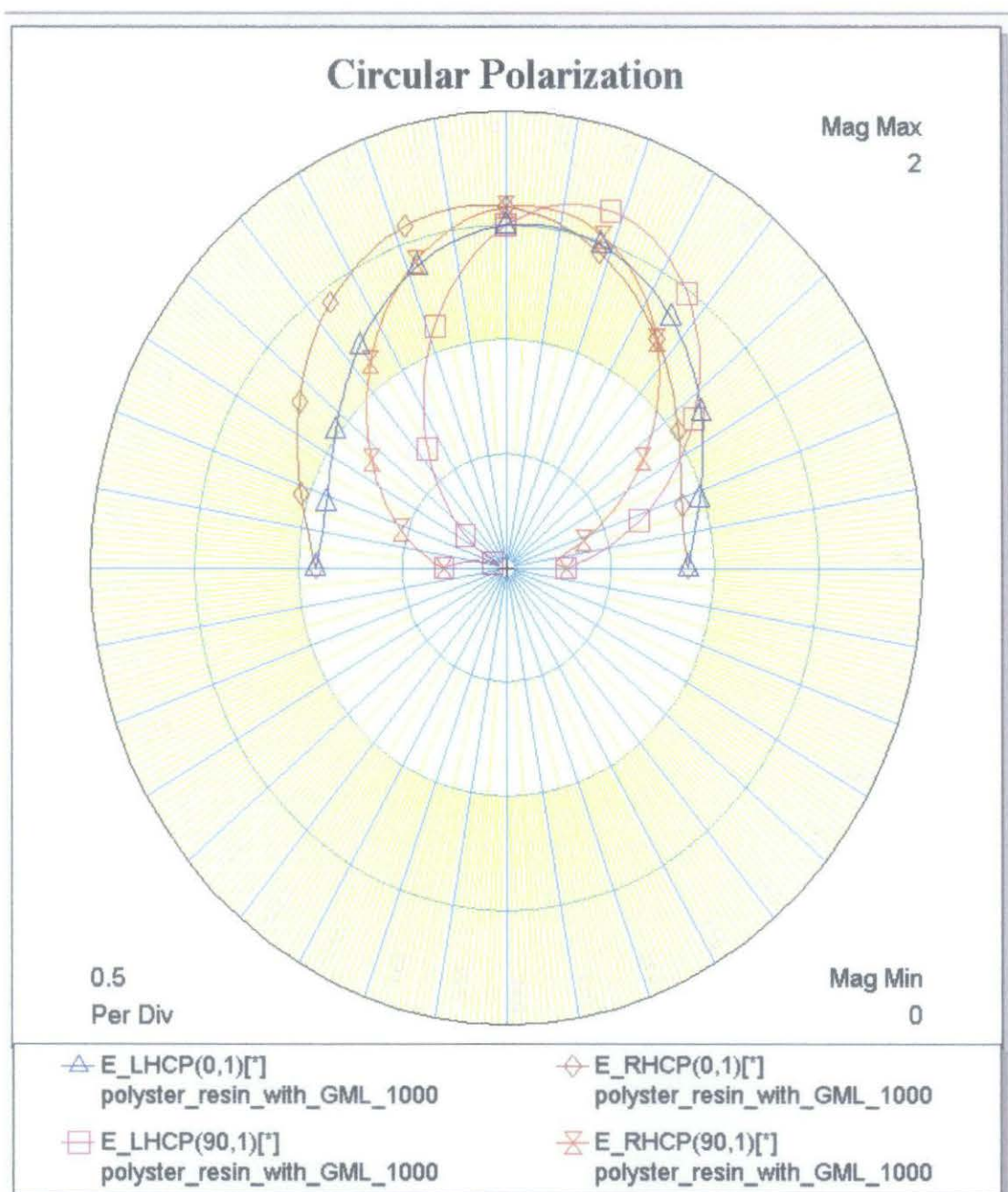


Figure 23 The antenna with Polyester/Resin laminated with GML 1000 dielectric substrate circular polarization

This figure also shows the circular polarization for the antenna with Polyester/Resin laminated with GML 1000 dielectric substrate. The  $E_{LHCP}$  for  $\phi=0^\circ$  is  $7.429^\circ$  and  $26.36^\circ$  for  $\phi=90^\circ$ . The  $E_{RHCP}$  is at  $-8.429^\circ$  for  $\phi=0^\circ$  and  $3.611^\circ$  for  $\phi=90^\circ$ .

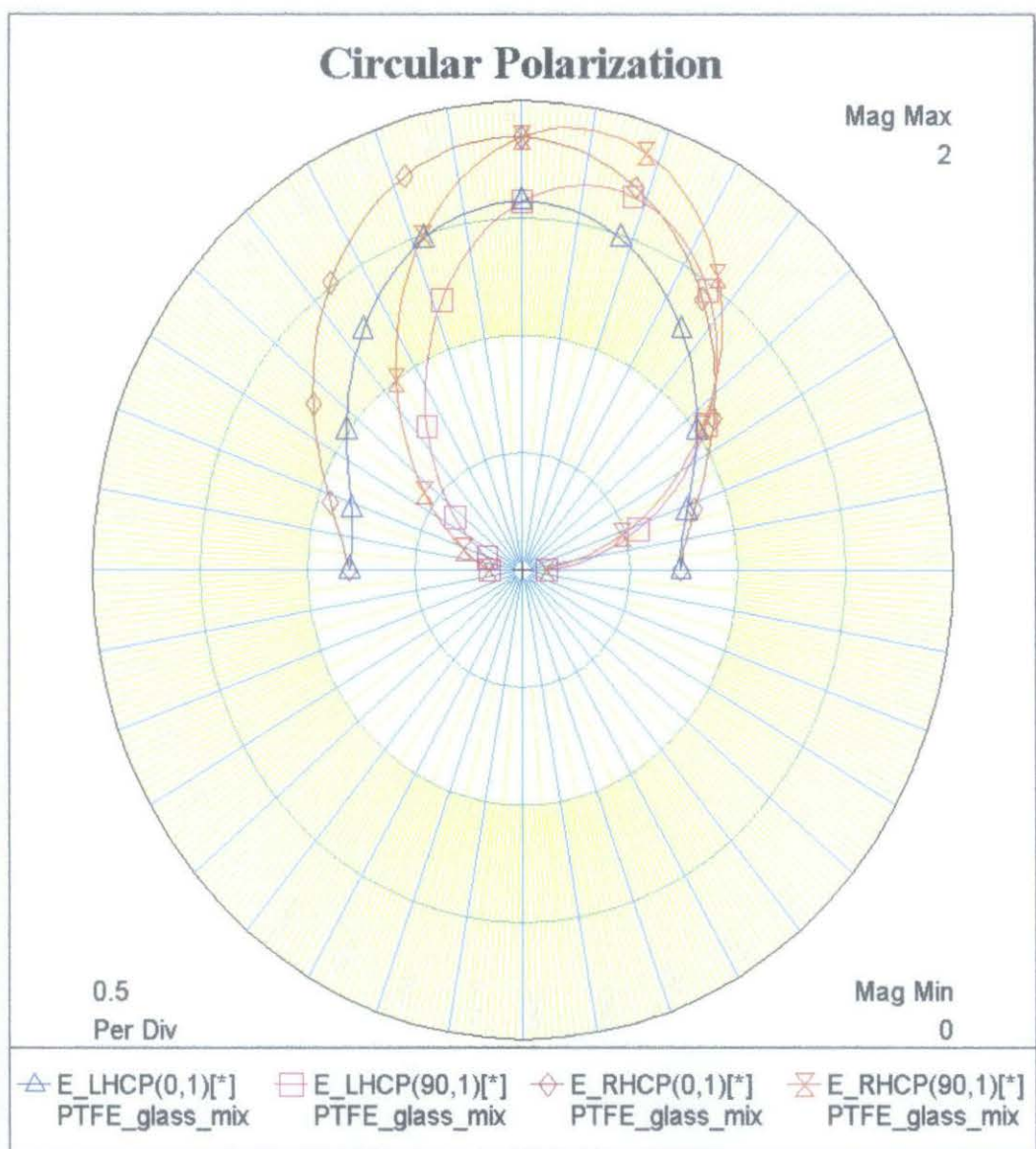


Figure 24 The antenna with PTFE/Glass mix dielectric substrate circular polarization

The  $E_{LHCP}$  is at  $-0.199^\circ$  for  $\phi=0^\circ$  and  $13.67^\circ$  for  $\phi=90^\circ$  and the  $E_{RHCP}$  is at  $-1.289^\circ$  for  $\phi=0^\circ$  and  $9.435^\circ$  for  $\phi=90^\circ$  as in figure above, for PTFE/Glass mix substrate.

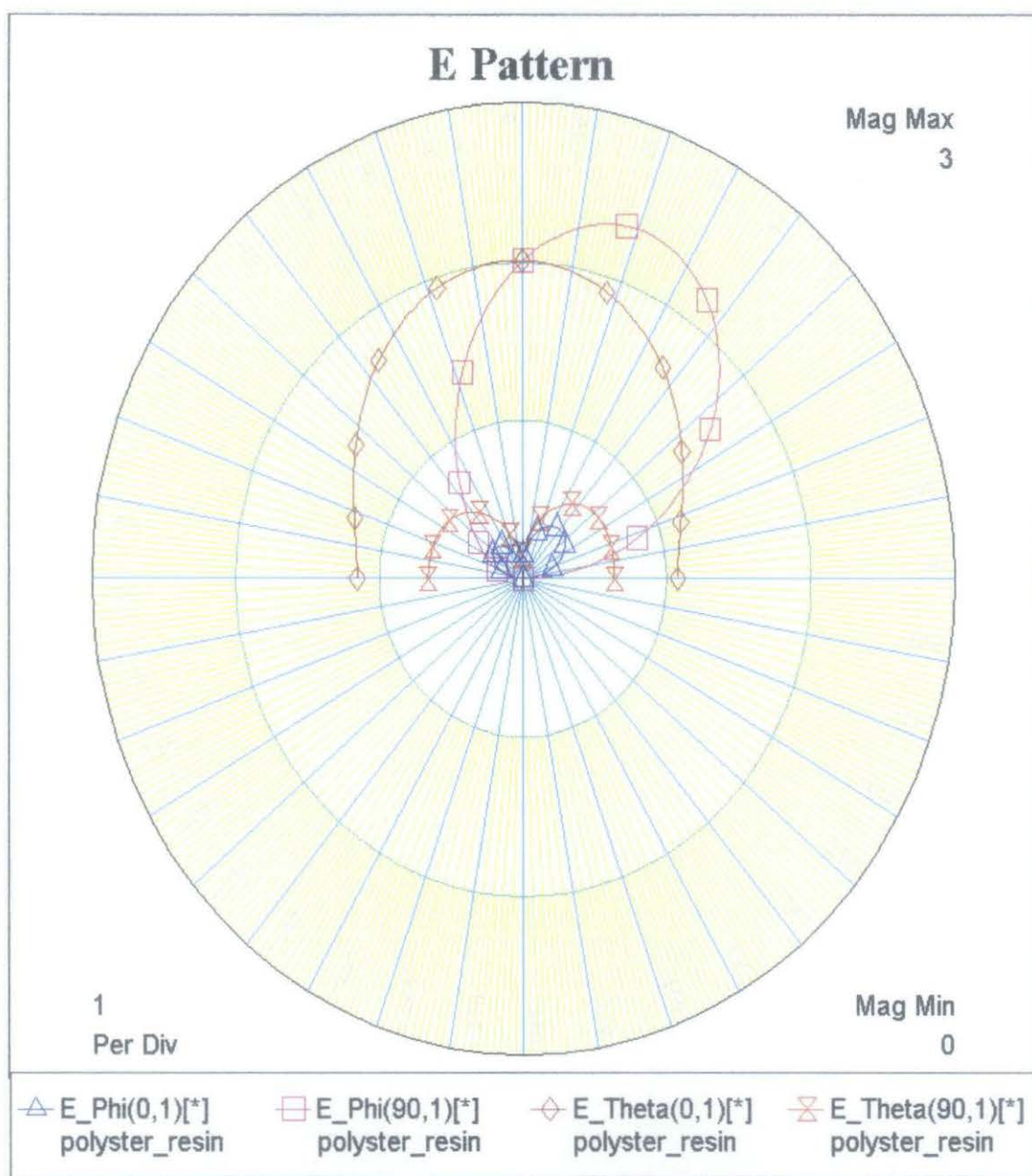


Figure 25 The antenna with Polyster/Resin dielectric substrate E\_PHI and E\_THETA

E-Phi or E-theta represents signals received or transmitted by the test antenna if it is linearly polarized with its E-field aligned with the unit vector  $d\phi$  or  $d\theta$  in the aforementioned antenna coordinate system. Importantly, the positive direction of  $d\phi$  or  $d\theta$  is in the increasing direction of  $\phi$  or  $\theta$ . The maximum E\_PHI pattern is at  $20^\circ$  and the E\_THETA pattern is at  $-1.742^\circ$ .

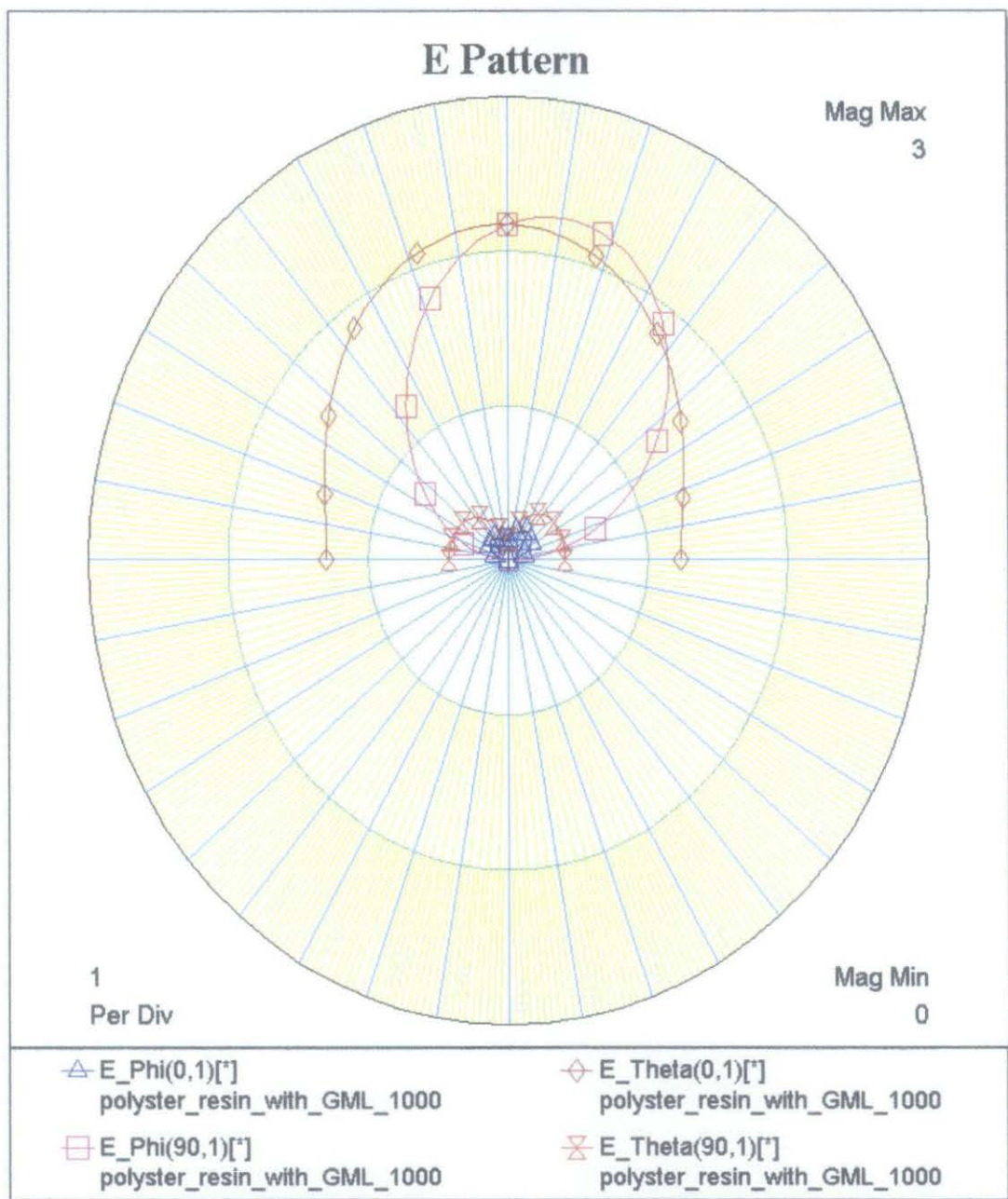


Figure 26 The antenna with Polyester/Resin laminated with GML 1000 dielectric substrate E\_PHI and E\_THETA

For this type of antenna, the E\_PHI is located at 12° and E\_THETA is at 0°.

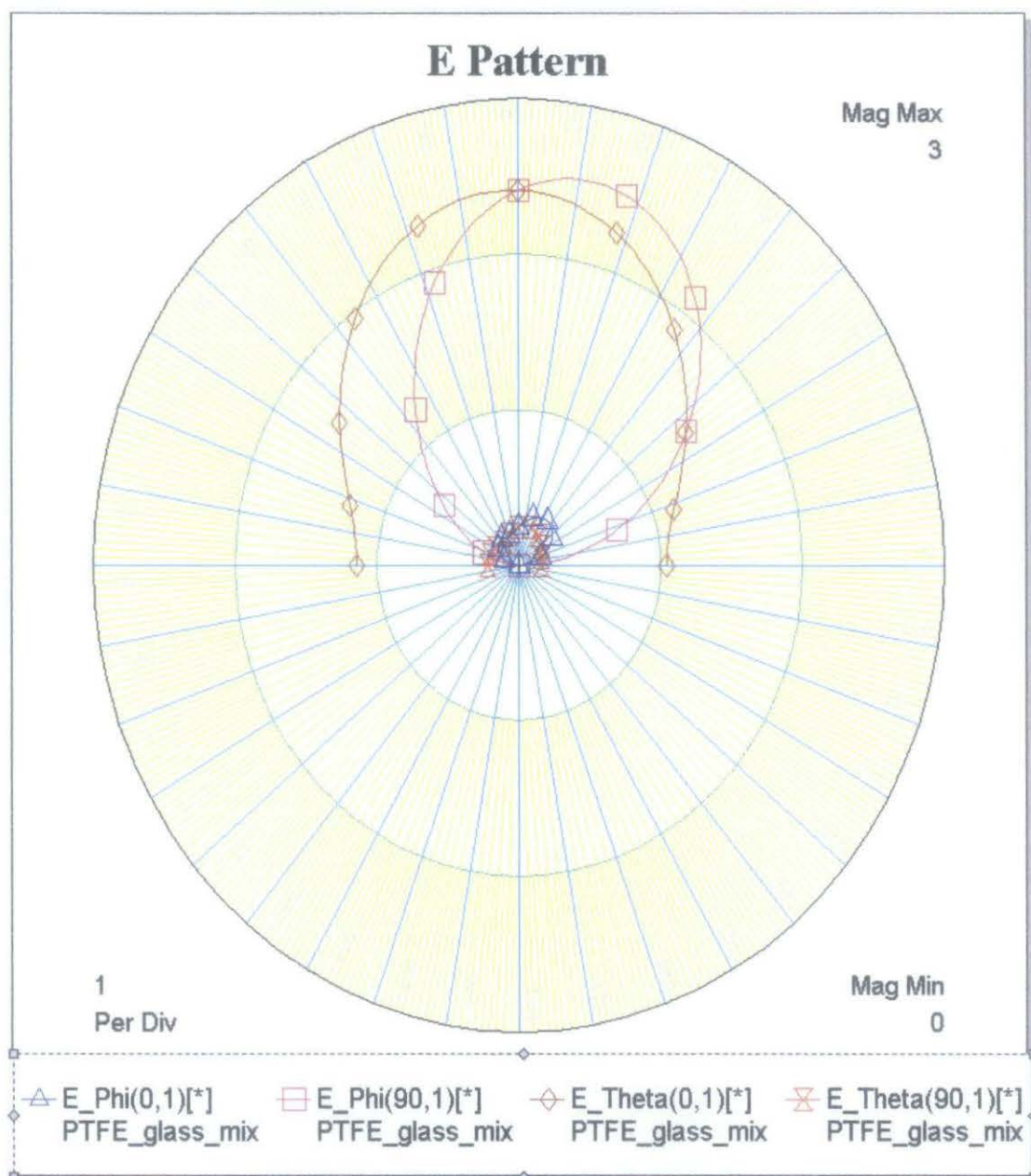


Figure 27 The antenna with PTFE/Glass mix dielectric substrate E\_PHI and E\_THETA

This antenna produced the E\_PHI at  $11.74^\circ$  and E\_THETA at  $-1.103^\circ$ .

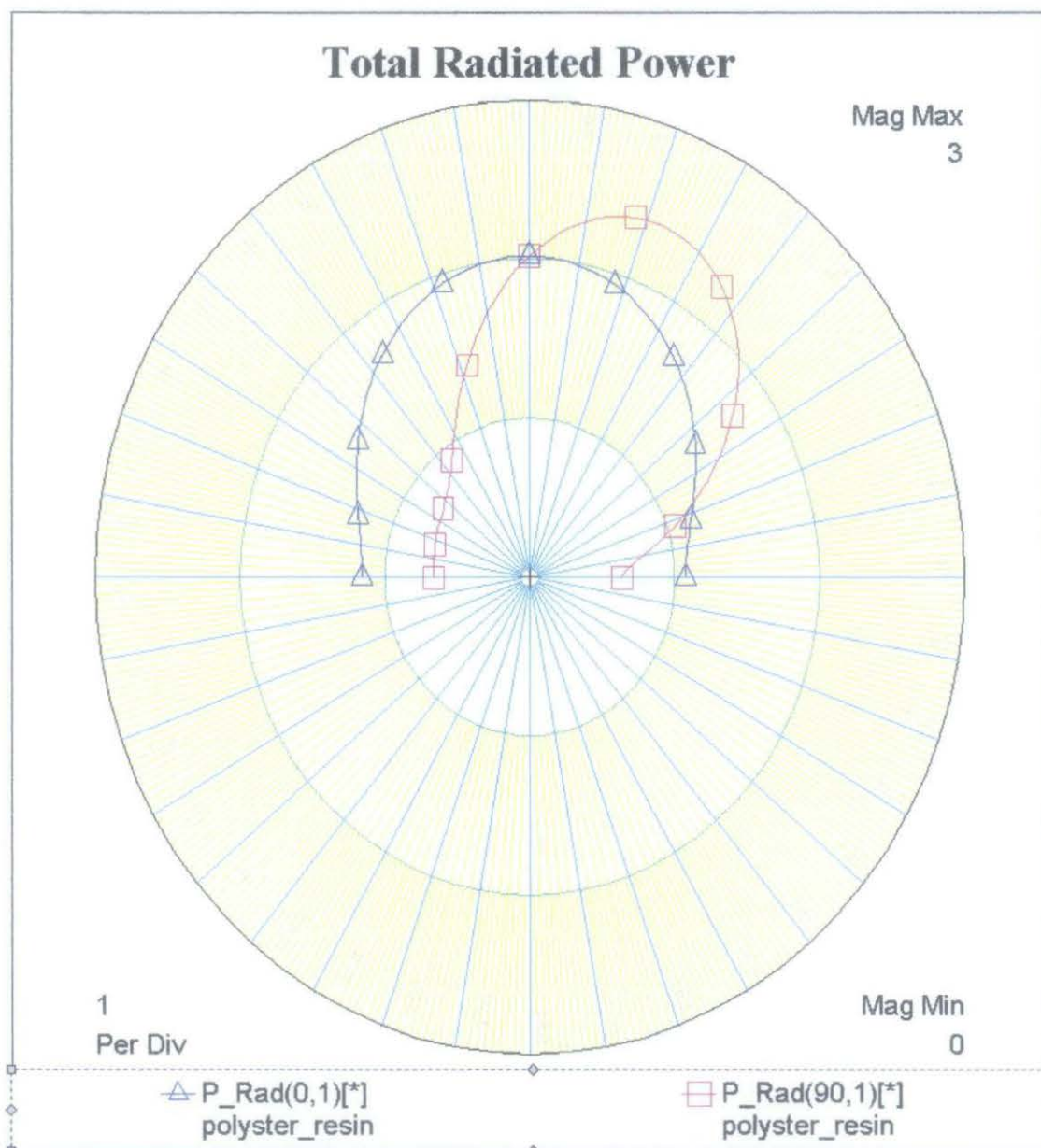


Figure 28 The antenna with Polyester/Resin dielectric substrate total radiated power

This figure shows the total radiated power of this type of antenna. It is also known as a Principal Plane Cut or Theta Sweep. This measurement captures the total power in all polarizations, and fixes the values of Frequency and Phi while sweeping Theta from 0 to 90 degrees or 0 to  $\pi/2$  radians. The total power is defined as the sum of the power contained in  $E_\phi$  and  $E_\theta$ . The maximum power radiated of the antenna with Polyester/Resin dielectric is  $0^\circ$  for  $\phi=0^\circ$  and  $22.04^\circ$  for  $\phi=90^\circ$ .

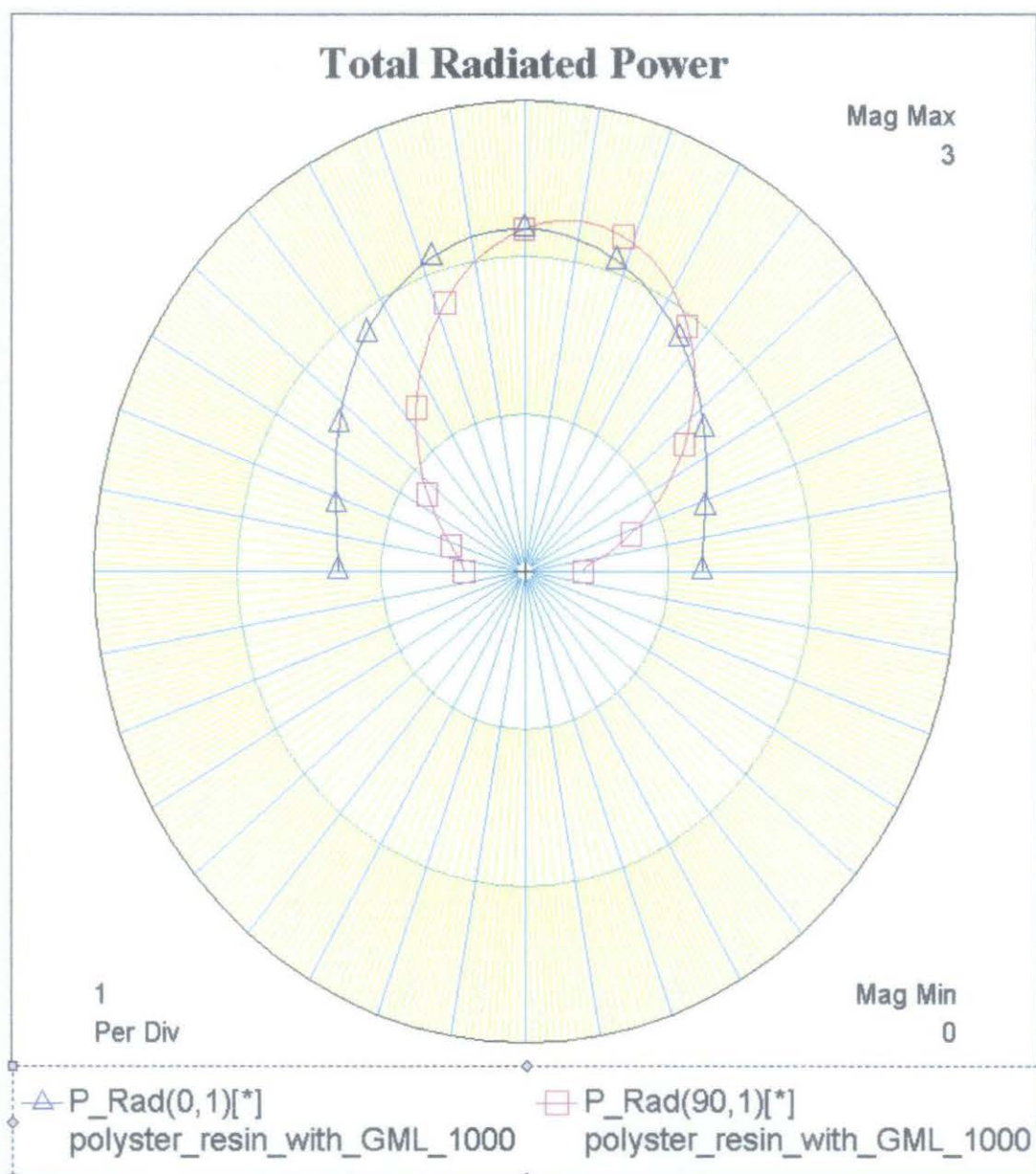


Figure 29 The antenna with Polyester/Resin laminated with GML 1000 dielectric substrate total radiated power

From this figure, this type of antenna produced the maximum power radiated at  $0^\circ$  for  $\phi=0^\circ$  and at  $11.89^\circ$  for  $\phi=90^\circ$ .

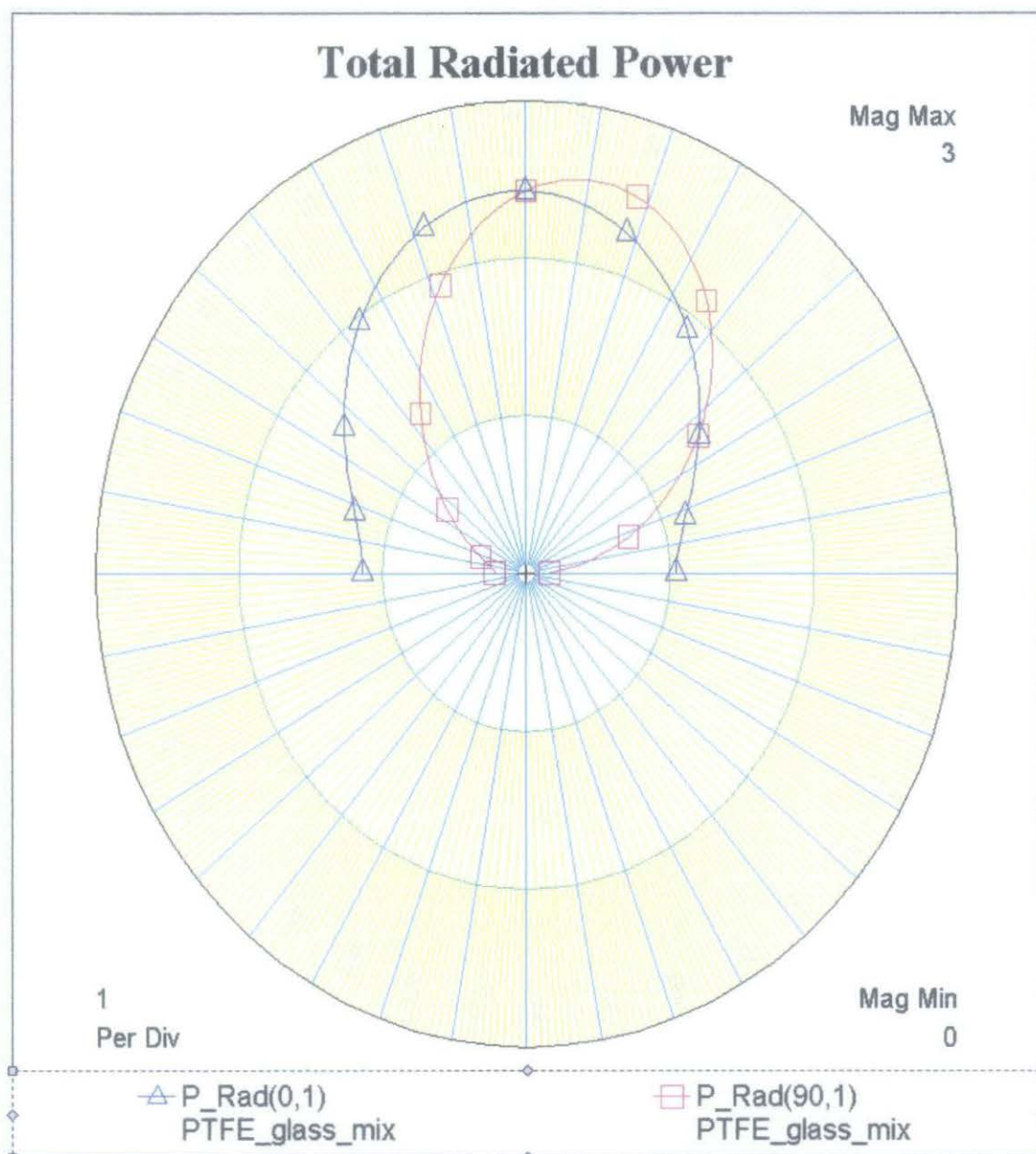


Figure 30 The antenna with PTFE/Glass mix dielectric substrate total radiated power

The total power radiated for the antenna using PTFE/Glass mix dielectric substrate as in Figure 30 is located at  $0^\circ$  for  $\phi=0^\circ$  and  $12.06^\circ$  for  $\phi=90^\circ$ .

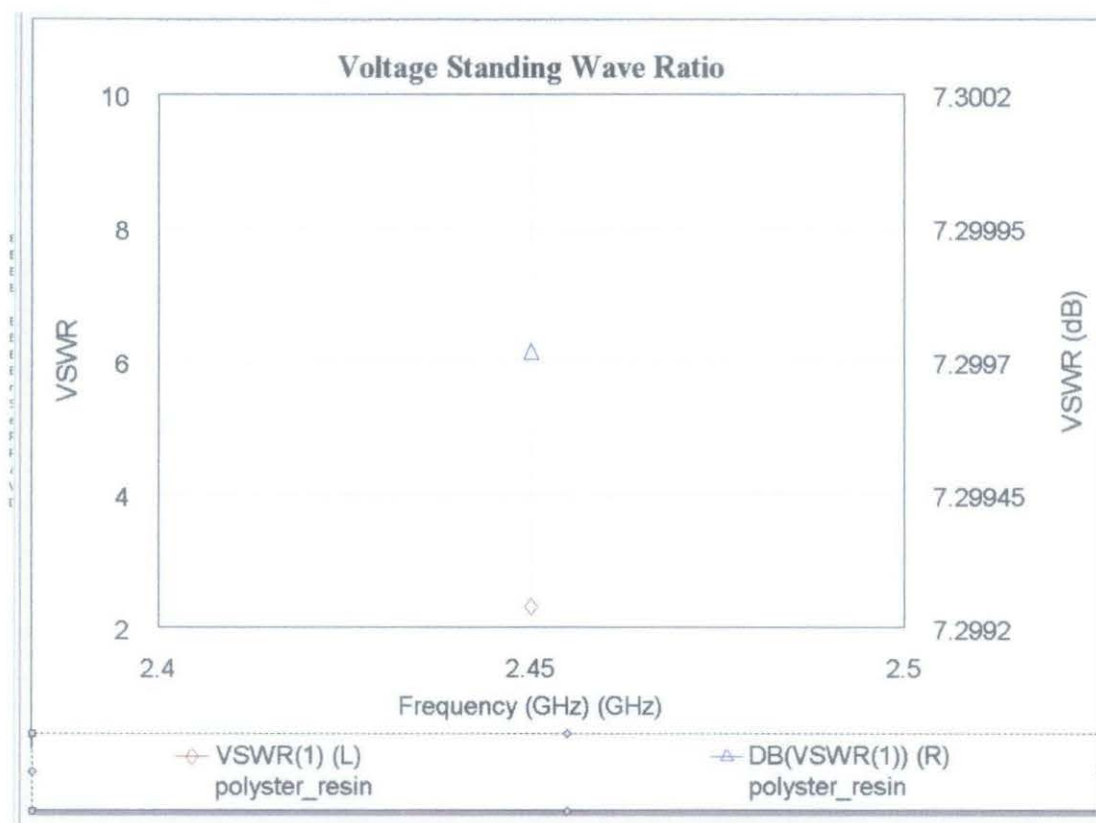


Figure 31 The antenna with Polyester/Resin dielectric substrate (single point simulation) Voltage Standing Wave Ratio (VSWR)

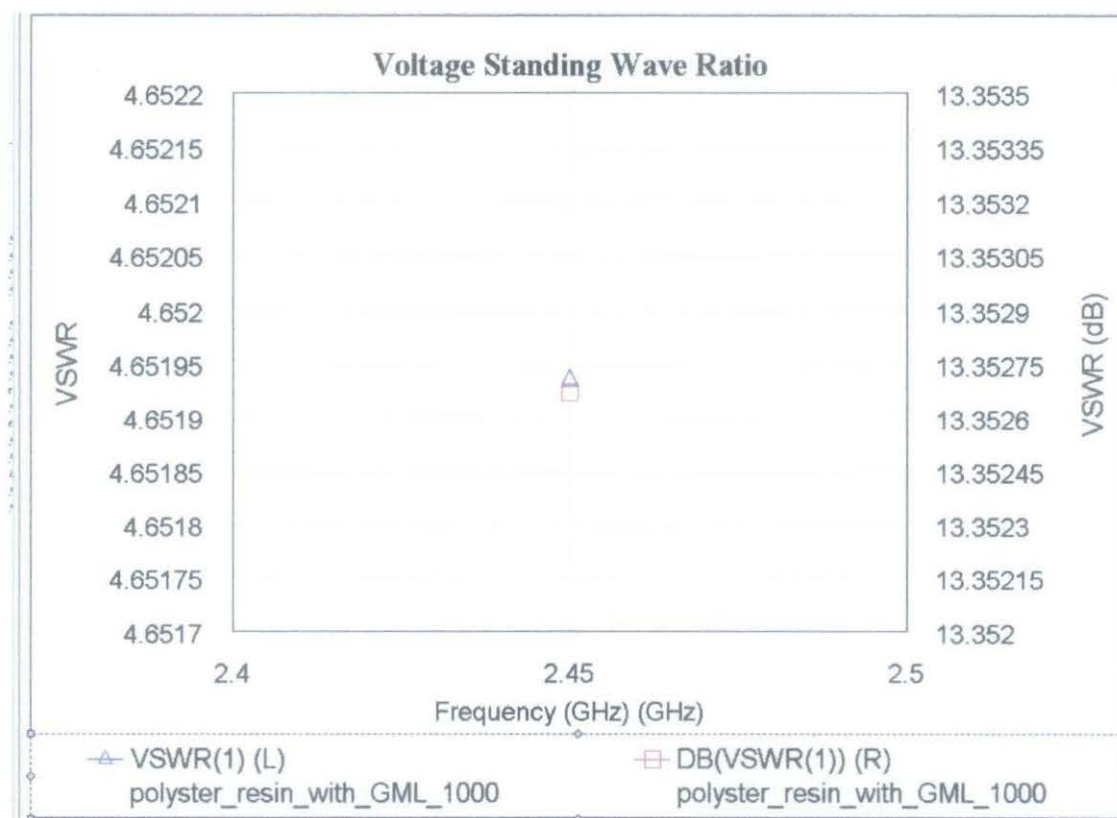


Figure 32 The antenna with Polyester/Resin laminated with GML 1000 dielectric substrate (single point simulation) Voltage Standing Wave Ratio (VSWR)

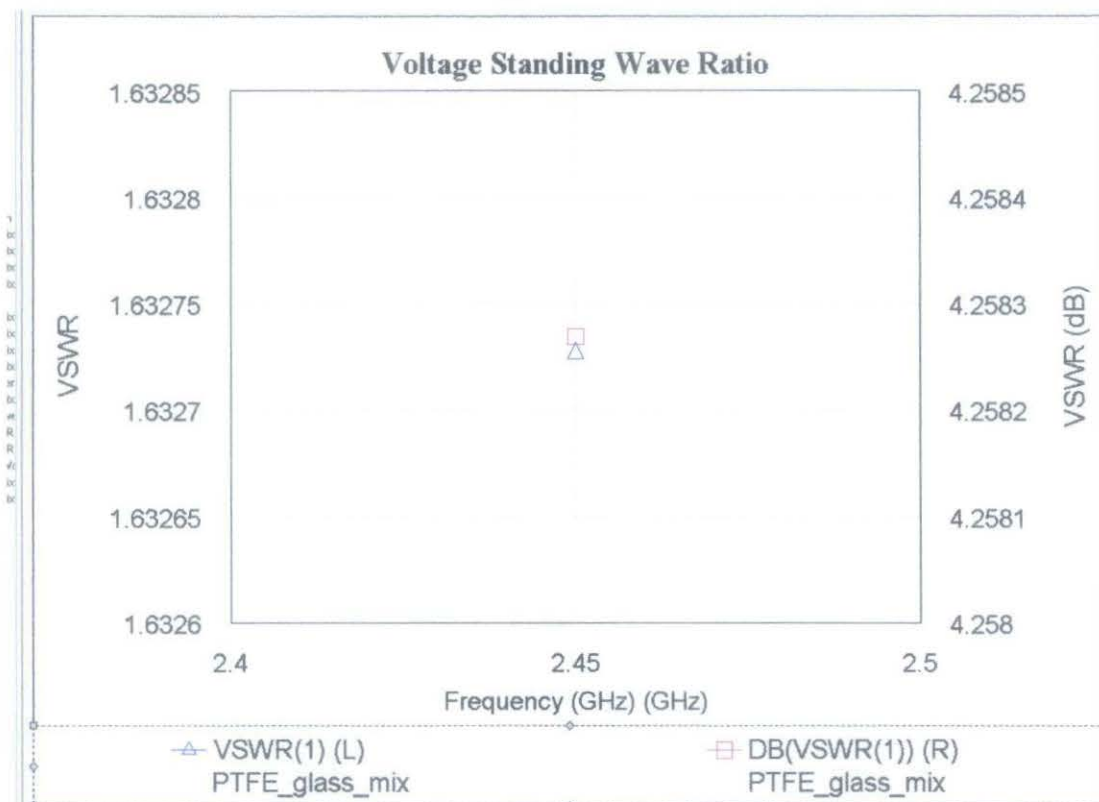


Figure 33 The antenna with PTFE/Glass mix dielectric substrate (single point simulation) Voltage Standing Wave Ratio (VSWR)

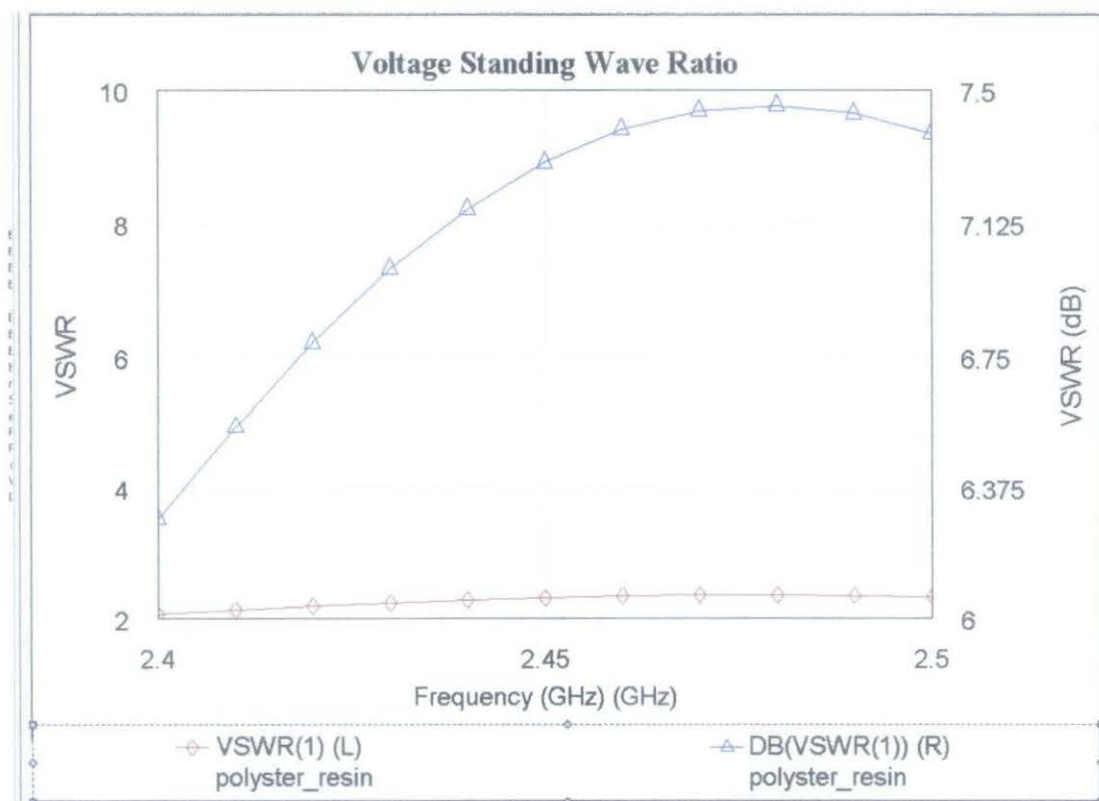


Figure 34 The antenna with Polyester/Resin dielectric substrate (simulation between 2.4 GHz and 2.5 GHz) Voltage Standing Wave Ratio (VSWR)

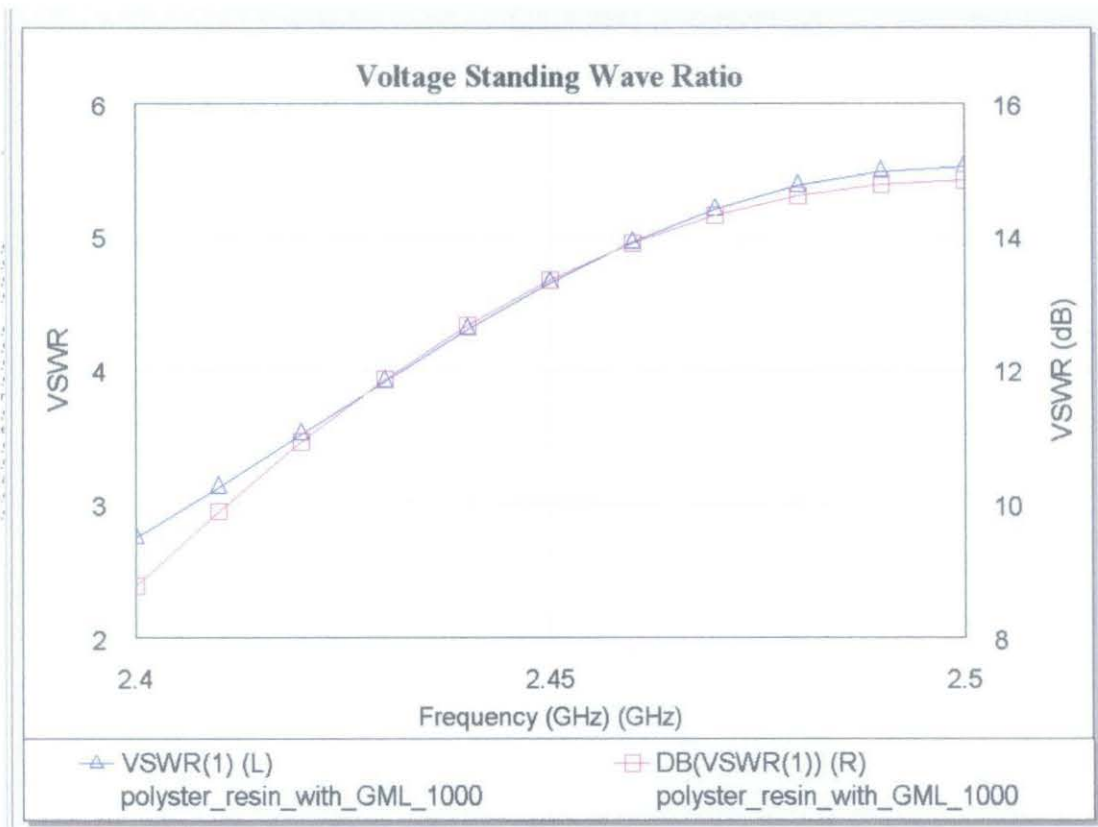


Figure 35 The antenna with Polyster/Resin laminated with GML 1000 dielectric substrate (simulation between 2.4 GHz and 2.5 GHz) Voltage Standing Wave Ratio (VSWR)

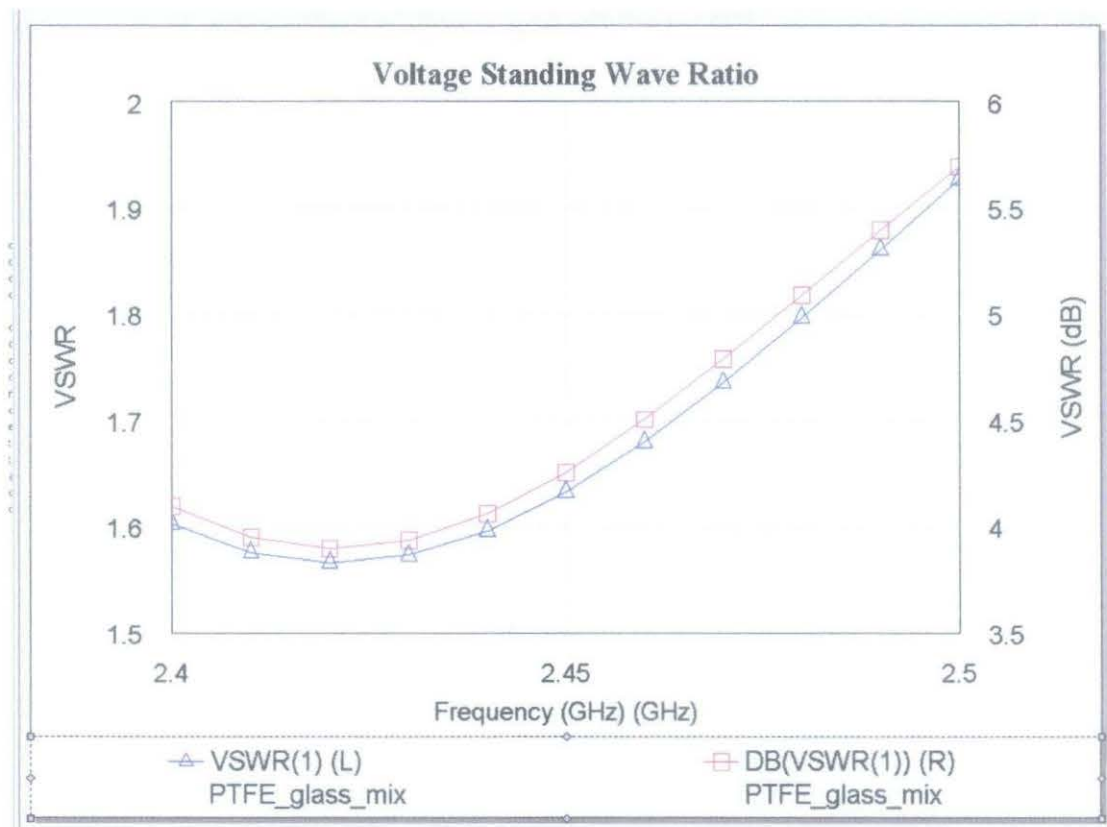


Figure 36 The antenna with PTFE/Glass mix dielectric substrate (simulation between 2.4 GHz and 2.5 GHz) Voltage Standing Wave Ratio (VSWR)

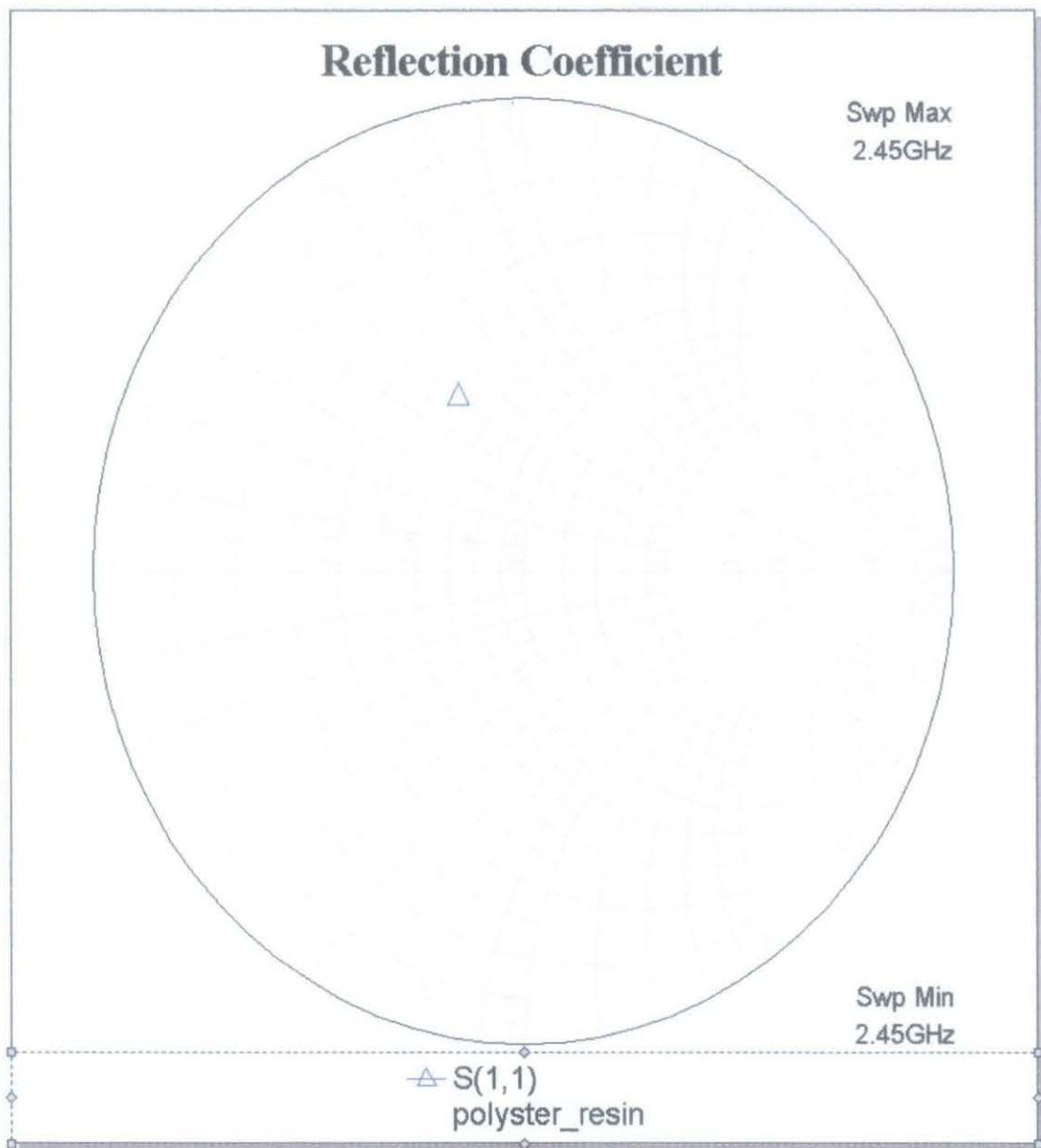


Figure 37 The antenna with Polyster/Resin dielectric substrate (single point simulation) Reflection Coefficient

The Smith Chart is a graphical aid or nomogram designed for electrical and electronics engineers specializing in radio frequency (RF) engineering to assist in solving problems with transmission lines and matching circuits. It can be used to represent many parameters including reflection coefficients. The higher is the magnitude of reflection coefficient, the higher is the value of VSWR. It showed that the value of VSWR is depends on the value of reflection coefficient. This chart is for single point simulation (2.45 GHz).

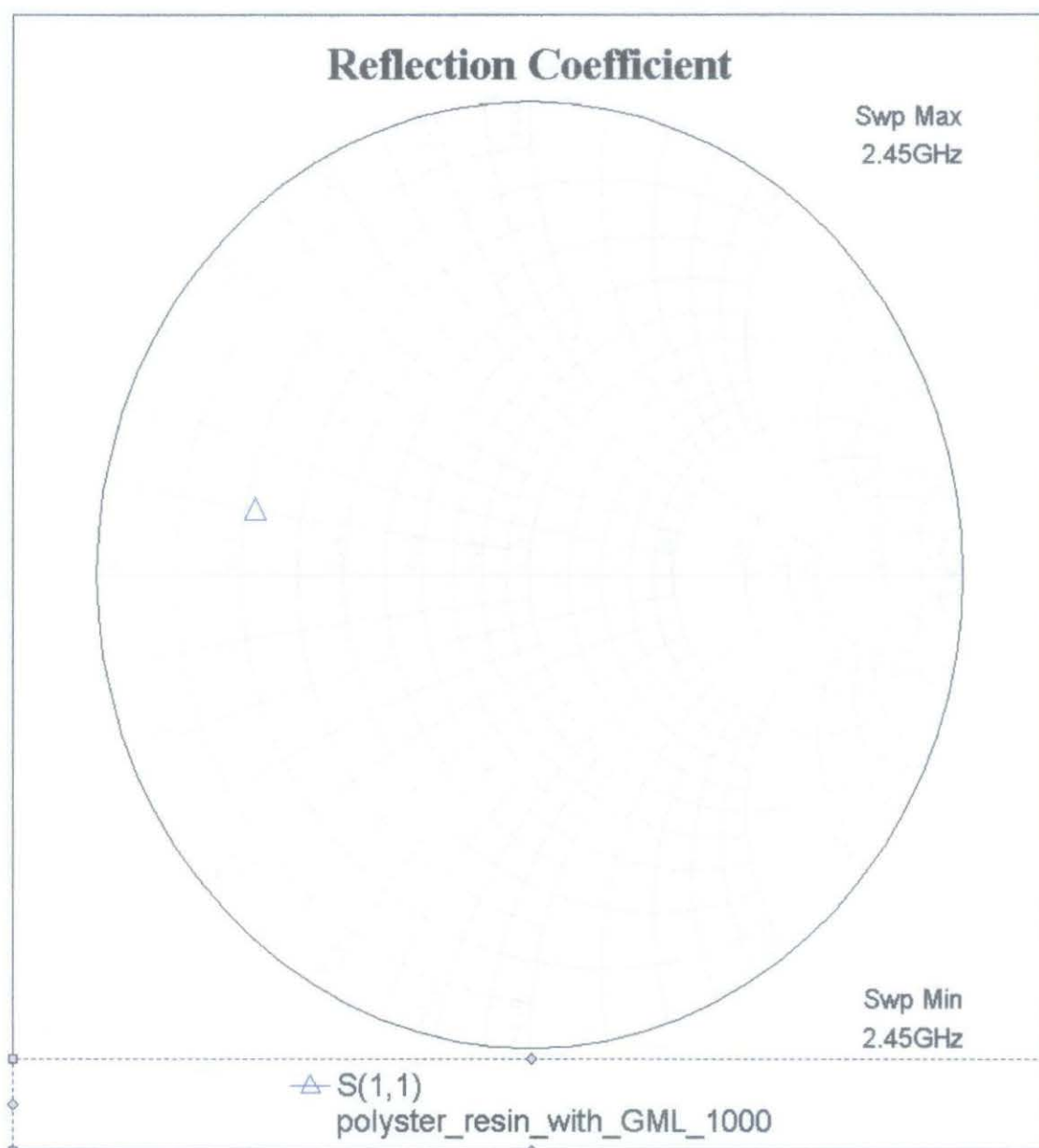


Figure 38 The antenna with Polyster/Resin laminated with GML 1000 dielectric substrate (single point simulation) Reflection Coefficient

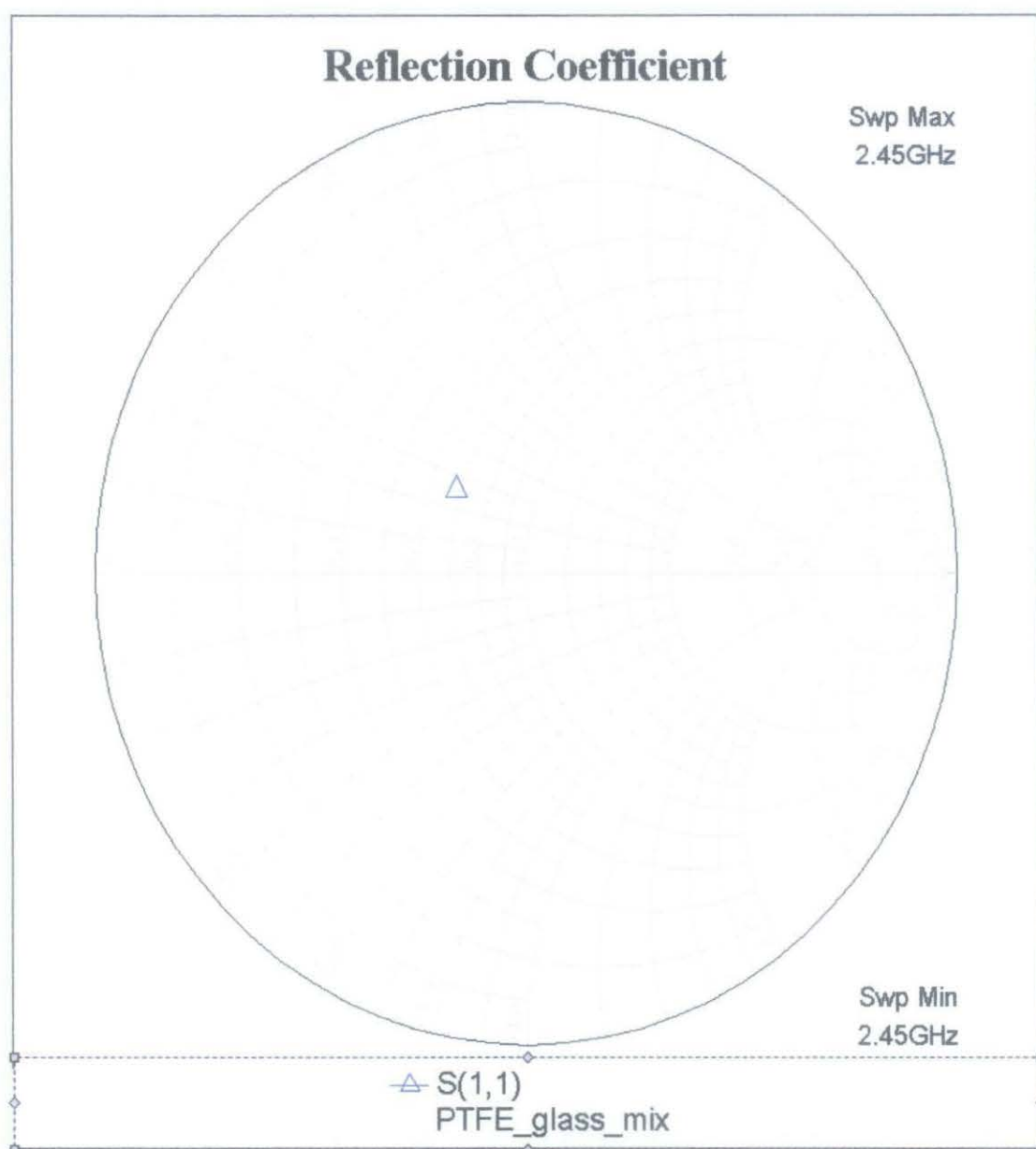


Figure 39 The antenna with PTFE/Glass mix dielectric substrate (single point simulation) Reflection Coefficient

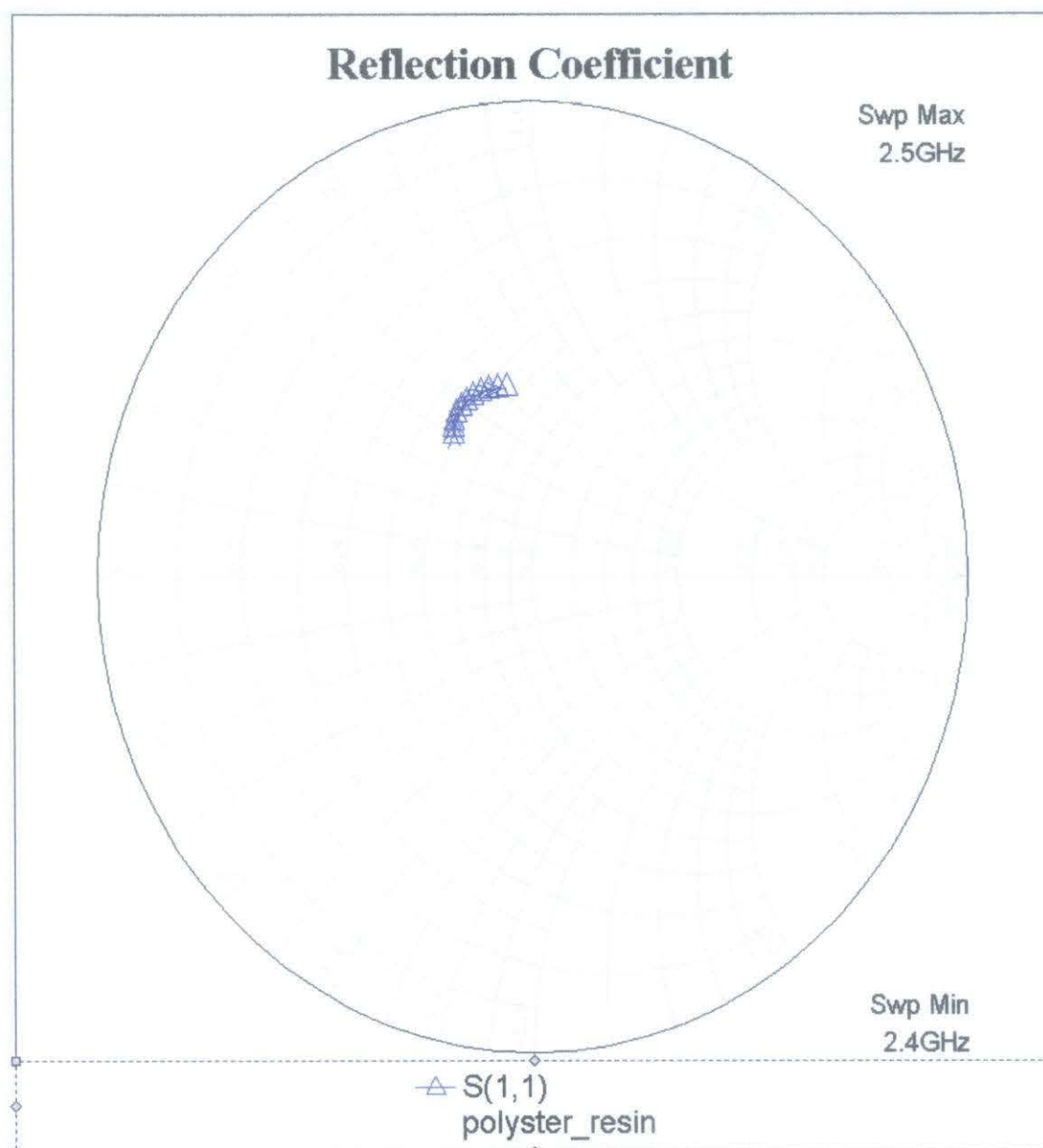


Figure 40 The antenna with Polyster/Resin dielectric substrate (simulation between 2.4 GHz and 2.5 GHz) Reflection Coefficient

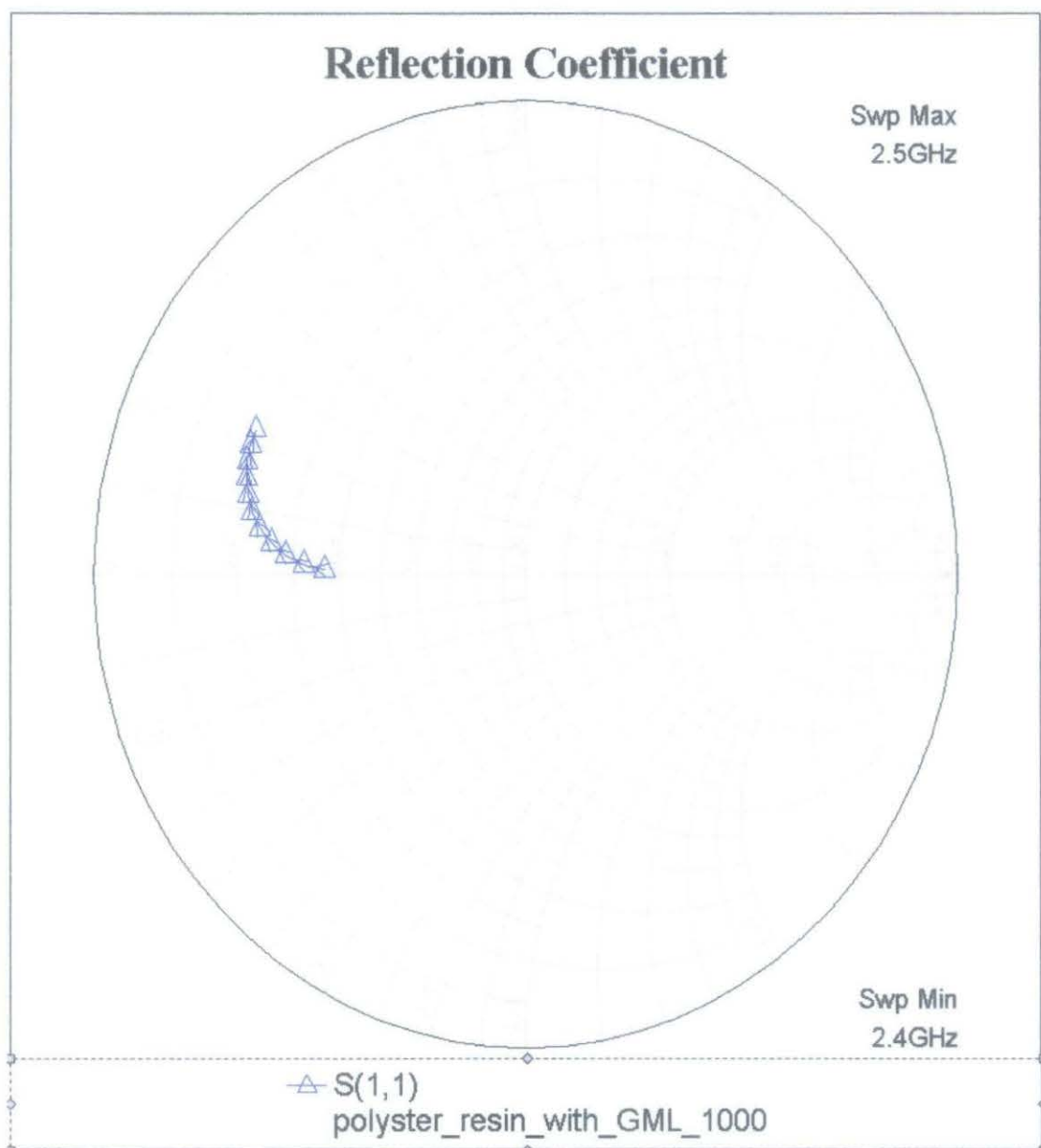


Figure 41 The antenna with Polyster/Resin laminated with GML 1000 dielectric substrate (simulation between 2.4 GHz and 2.5 GHz) Reflection Coefficient

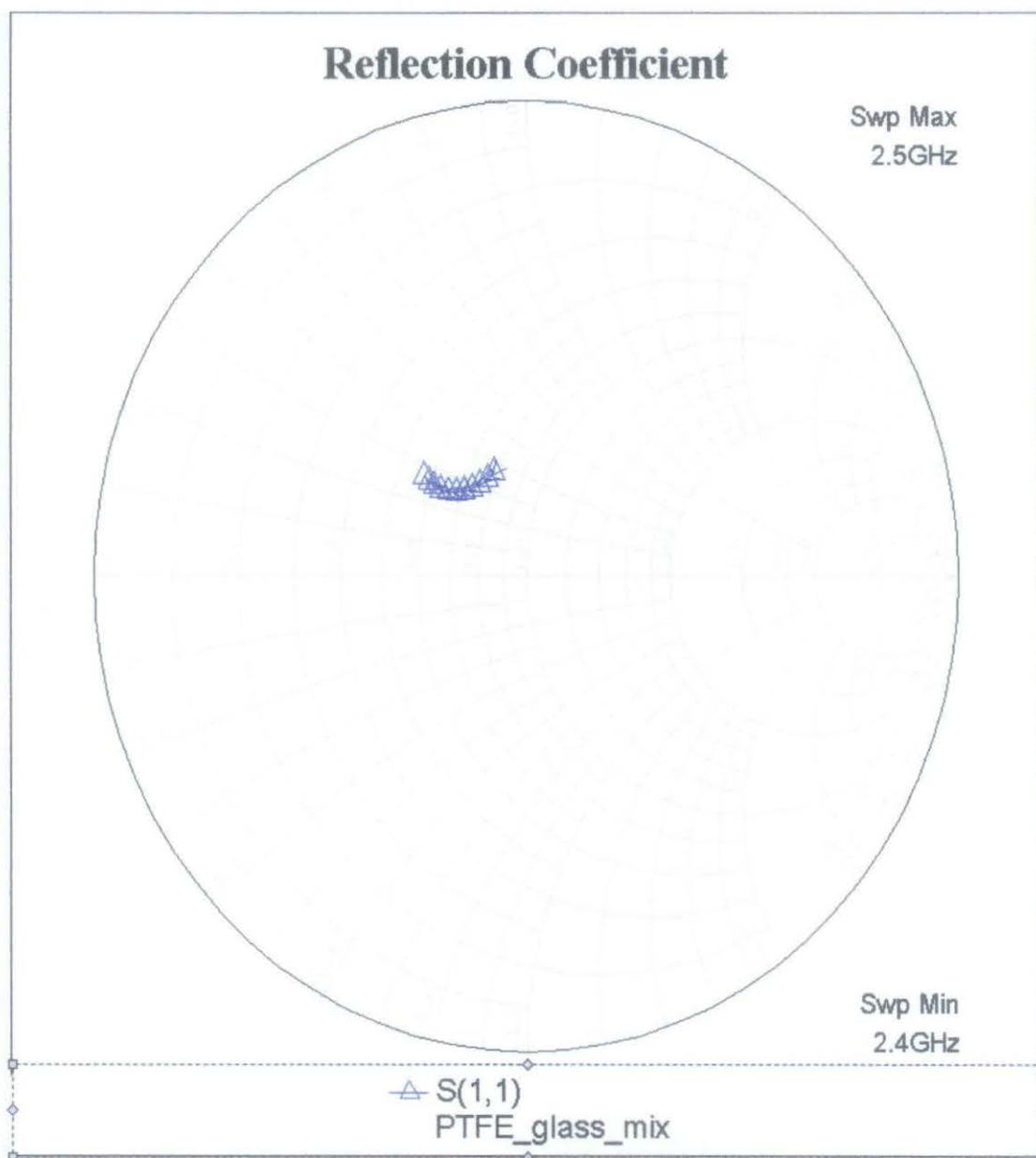


Figure 42 The antenna with PTFE/Glass mix dielectric substrate (simulation between 2.4 GHz and 2.5 GHz) Reflection Coefficient

4.2 Schottky Diode Results

By using nonlinear simulation, the simulations of Schottky diode can be done. To obtain the current, voltage and total power characteristic of the diode, the analysis was simulated.

During the positive cycles, the diode is off and during the negative cycles, the diode is on and the voltage is rectified at 106.5V as shown in Figure 43. In Figure 44, the current curve is then presented with the maximum value of 16619mA.

As in Figure 45, the total power that can be rectified by diode is recorded as 50199mW instead of 69054mW that have been supplied. Table 6 shows the maximum value of the voltage, current and total power that has been obtained.

Table 6 Voltage, current and total power of diode values

Component	Voltage (V)		Current (mA)		Total Power (mW)
	+ve	-ve	+ve	-ve	
Voltage Source	240	-240	16619	-16619	3988560
Schottky Diode	-106.5	106.5	16619	-16619	1769923.5

In Figure 46, 47 and 48 show the harmonics component of diode, and Table 7 is the values that have been observed and tabulated. To get a better system, the harmonics component must be reduced.

Table 7 Diode harmonics components

Frequency (GHz)	$V_{\text{harmonic}}$ (V)	$I_{\text{harmonic}}$ (mA)	$P_{\text{harmonic}}$ (mW)
2.45	240	16620	1994372

The diode conversion efficiency has been evaluated as 44.375%

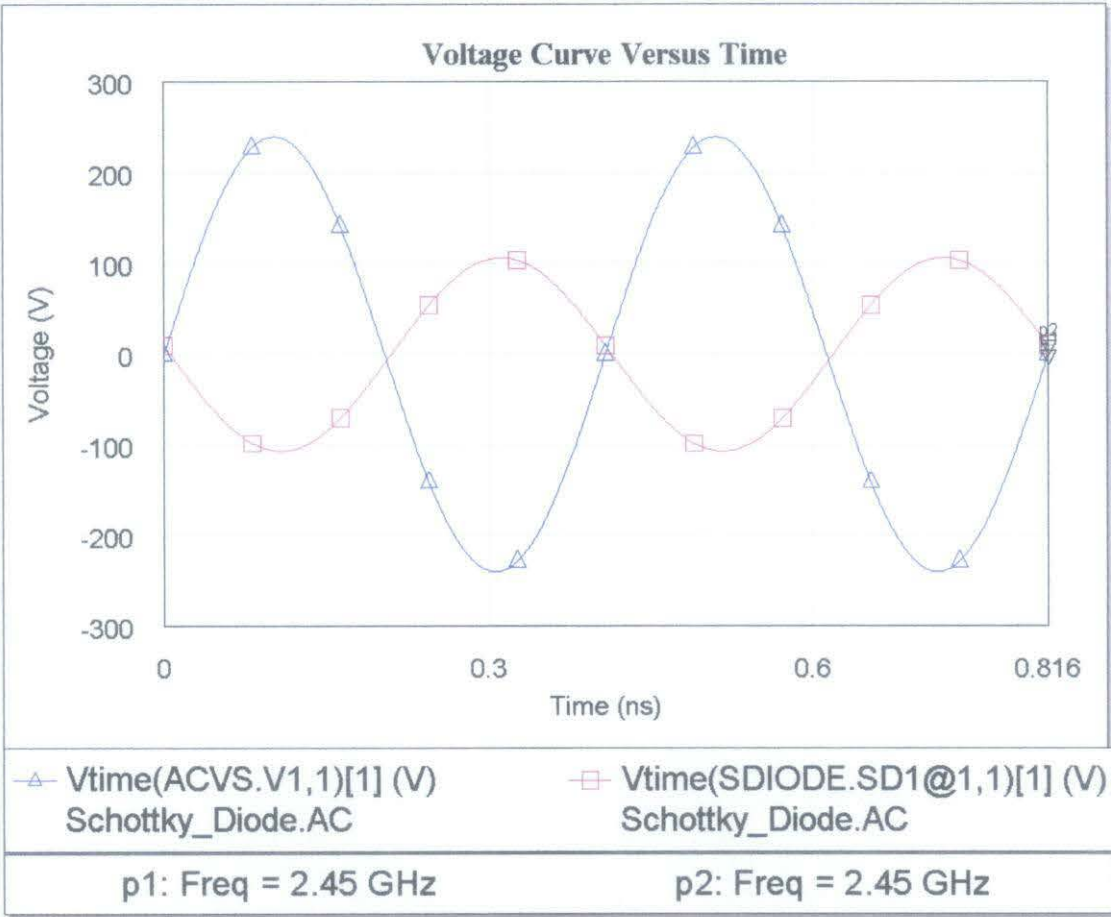


Figure 43 Voltage versus Time graph

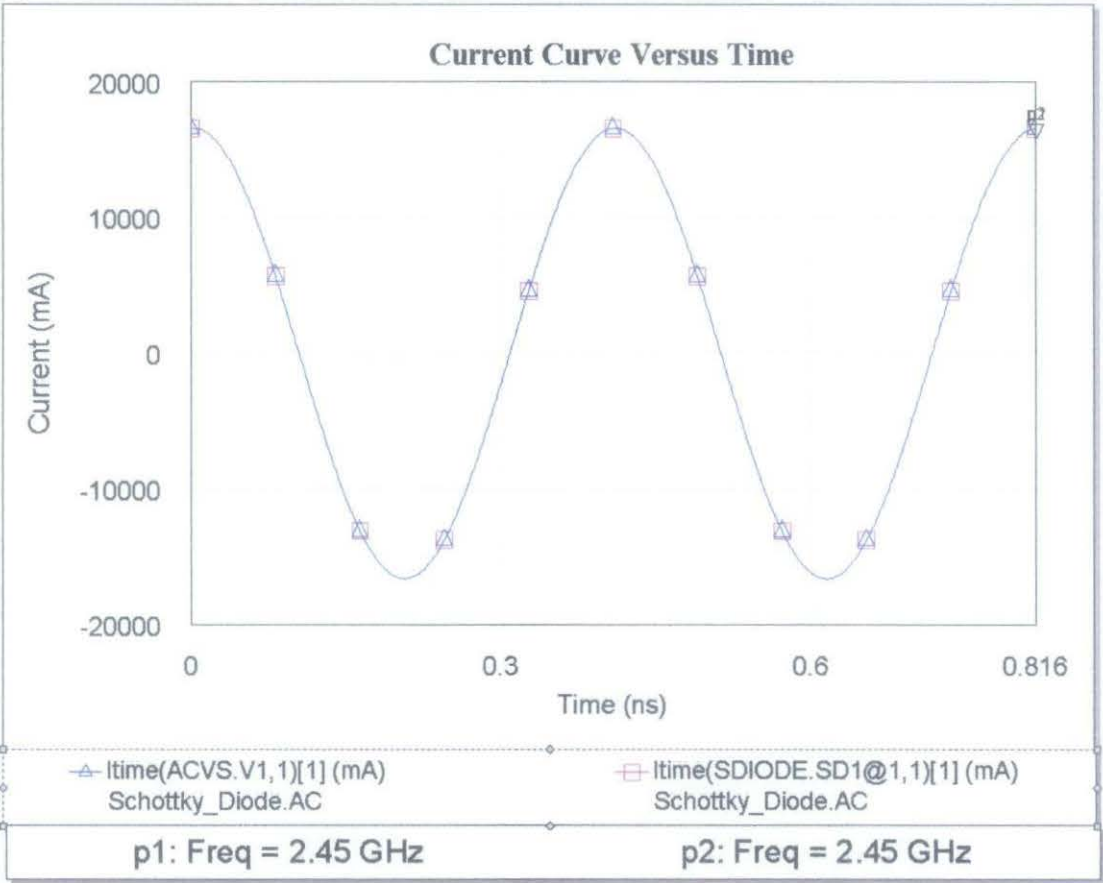


Figure 44 Current versus Time graph

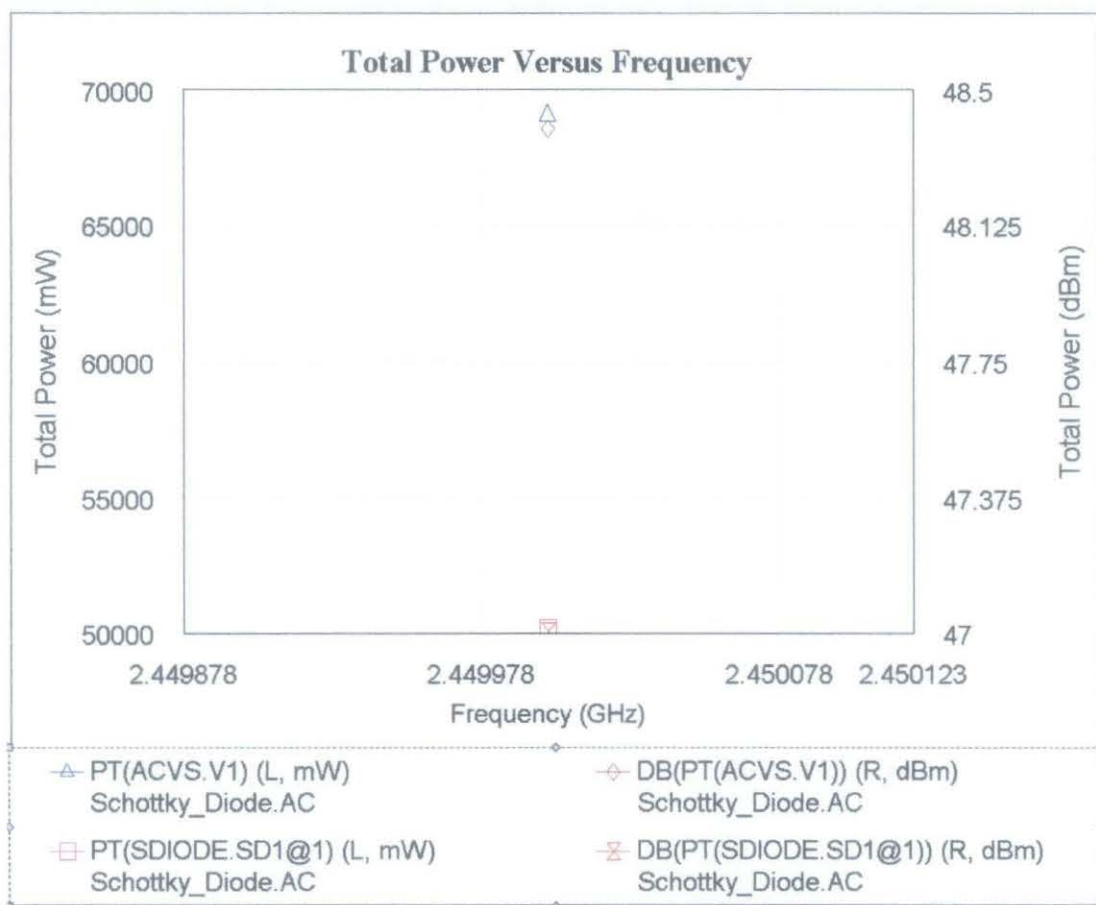


Figure 45 Total Power versus Frequency graph

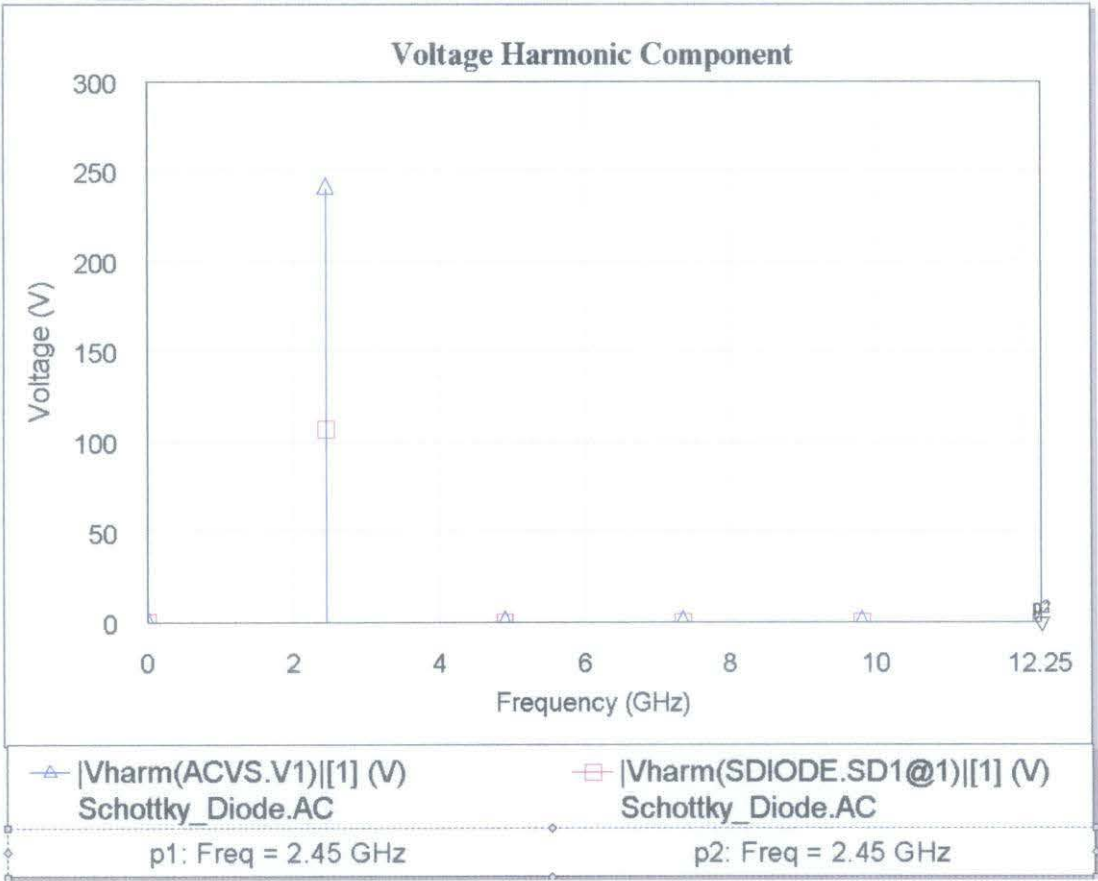


Figure 46 Harmonics Component of Voltage graph

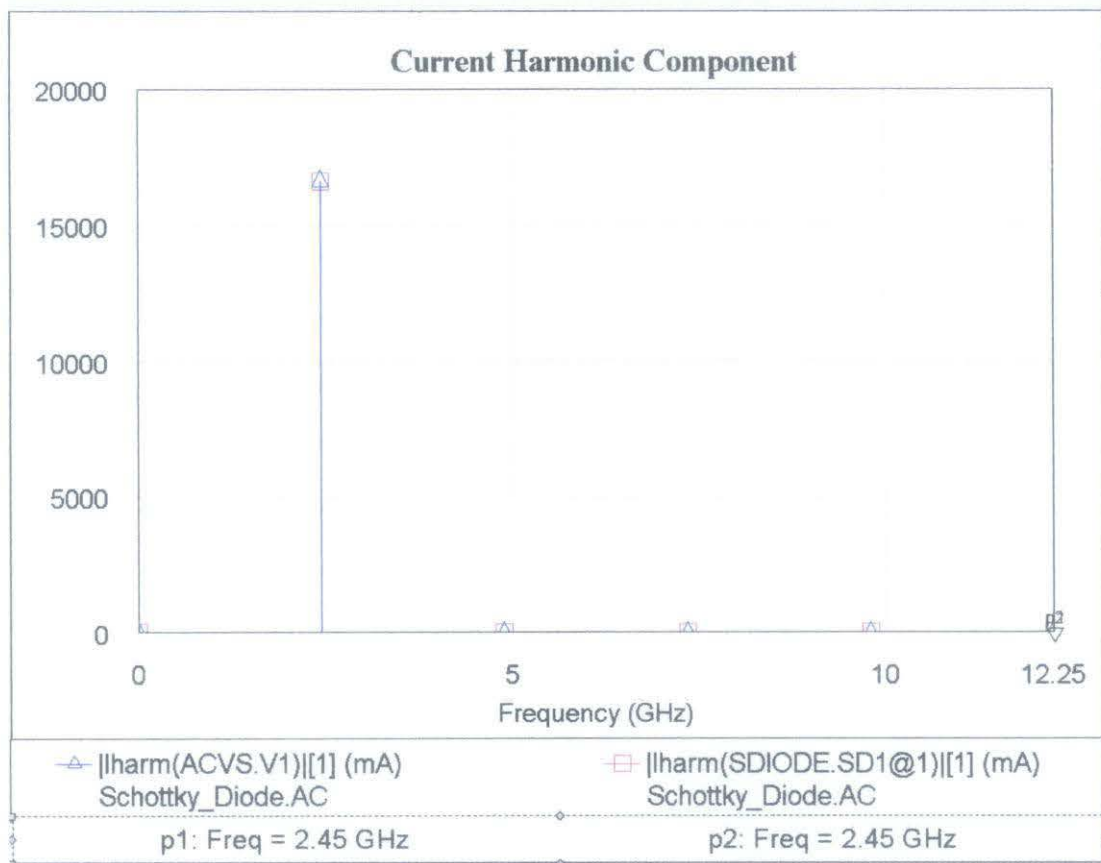


Figure 47 Harmonics Component of Current graph

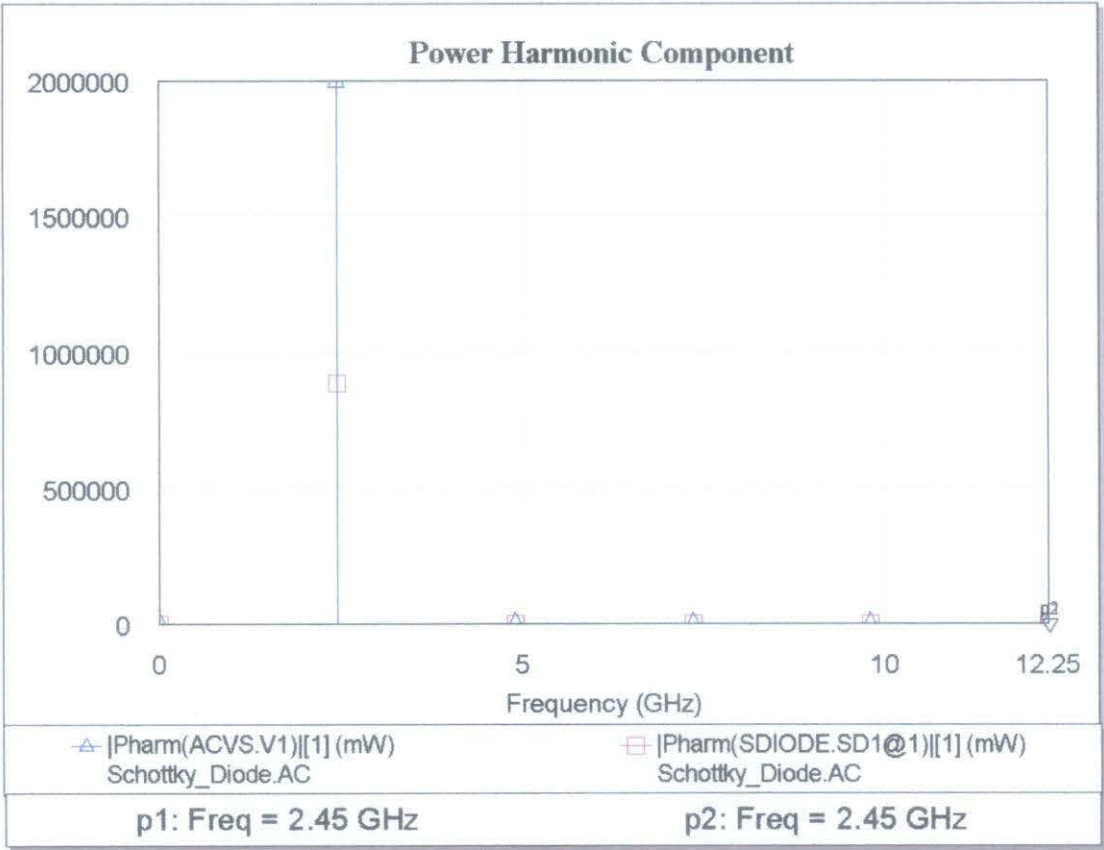


Figure 48 Harmonics Component of Power graph

## CHAPTER 5

### CONCLUSION AND RECOMMENDATION

#### 5.1 Conclusion

One of the alternative methods to transmit power is by using cableless and cordless method that known as Wireless Power Transmission. This technology uses microwave signal to transmit power. The main component in WPT is the transmitter and receiver element, known as rectenna. Reception antenna, rectifying circuit, impedance matching circuit and filtering circuit are the components of the rectenna.

Due to the rectangular microstrip patch antenna advantages, it is selected as a power reception antenna. By using the Microwave Office 2004, the simulations of the antenna evaluated and the performances of this antenna are recorded and analyzed. Based on the results that have been obtained, it is concluded that the rectangular microstrip antenna with PTFE/Glass mix gives the best performances with circular polarization and total radiated power located near to the centre of the graph. The bandwidth that this type of antenna can produce is 1.84%.

For the Schottky diode, the analysis has been simulated. The frequency that has been used is 2.45 GHz, and the material of the semiconductor is silicon, Si. In rectenna system, this diode acts as rectifying circuit. In Microwave 2004, by using nonlinear analysis method, the analysis of this diode also has been done. These diode performances are recorded and then analyzed. From the results, it is known that the total power rectified is 1769923.5 mW with 240 V power supply with the input power is 3988560 mW. Therefore, the efficiency of the diode is low, that is about 44.375%.

Based on all results, the simulation and analysis that have been done were quite successful. Hence, this WPT system, have the potential to be implemented to the exact system. However, to improve the performance of this antenna and diode, some modifications must be made.

## **5.2 Recommendation**

Single rectangular patch and single dielectric substrate have been used in the simulations for rectangular microstrip patch antenna and they give limited performances. The materials and the parameters for Schottky diode also have to be considered as well as improving the performances of the antenna. Therefore, some propositions have to be made for future development.

Firstly, safety zone have to be declared for human from the bad effects of microwave radiation. Then, the antenna has to be redesigned to increase the percentage power it received. Thirdly, the multilayer antenna technique has to be done in order to improve the bandwidth and efficiency of the antenna. Next, to reduce the harmonics that generated by the diode, frequency selective surface have to be done. And lastly, for higher power rectified and higher efficiency operation, the circuit design of Schottky diode has to be improved.

This kind of technology has to be researched thoroughly and extensive study on this system should be made since its ability as the alternative power energy resources that are renewable.

## REFERENCES

- [1] Dong, Gi Youn, Yang, Ha Park, Kwan, Ho Kim and Young, Chul Rhee (1999). "A Study on the Fundamental Transmission Experiment for Wireless Power Transmission System." *IEEE Tencon*. 1419-1422.
- [2] Dong, Gi Youn, Yang, Ha Park, Kwan, Ho Kim and Young, Chul Rhee (1999). "A Study on the Fundamental Transmission Experiment for Wireless Power Transmission System." *IEEE Tencon*. 1423-1426.
- [3] Naoki Shinohara and Hiroshi Matsumoto (1998). "Experiment Study of Large Rectenna Array for Microwave Energy Transmission." *IEEE Transaction on Microwave Theory and Techniques*. 46(3). 261-267.
- [4] Tae, Whan Yoo and Kai, Chang (1992). "Theoretical and Experimental Development of 10 and 35 GHz Rectennas." *IEEE Transaction on Microwave Theory and Techniques*. 40(6). 1259-1265.
- [5] McSpadden, J. O. Dickinson, R. M., Lu, Fan and Kai, Chang (1998). "A Novel Oscillating Rectenna for Wireless Microwave Power Transmission." *IEEE MTT-S Digest*. WE5E-5. 1161-1164.
- [6] McSpadden, J. O., Tae, Whan Yoo and Kai, Chang (1992). "35 GHz Rectenna Implemented with a Patch and a Microstrip Dipole Antenna." *IEEE MTT-S Digest*. IF1 M-3. 345-348.
- [7] Young, Ho Suh, Chunlei, Wang and Kai, Chang (2000). "Circularly Polarized Truncated – Corner Square Patch Microstrip Rectenna for Wireless Power Transmission." *Electronics Letters*. 36(7). 600-602.
- [8] McSpadden, J. O., Tae, Whan Yoo and Kai, Chang (1992). "Theoretical and Experimental Investigation of a Rectenna Element for Microwave Power Transmission." *IEEE Transaction on Microwave Theory and Techniques*. 40(12). 2359-2366.
- [9] McSpadden, J. O., Lu, Fan and Kai, Chang (1992). "Design and Experiments of a High Conversion Efficiency 5.8 GHz Rectenna." *IEEE Transaction on Microwave Theory and Techniques* 46(12). 2053-2060.
- [10] Maryniak, G. E. (1996). "Status of International Experimentation in Wireless Power Transmission." *Solar Energy*. 56(1). 87-91.

- [11] Strassner, B. and Kai, Chang (2000). "5.8 GHz Circular Polarized Rectenna for Microwave Power Transmission." *Iecec 35<sup>th</sup> Inter Society*. 2. 1458-1462.
- [12] Stutzman, W. L. and Thiele G.A (1998). "Antenna Theory and Design." 2<sup>nd</sup> ed. New York: John Wiley & Sons, Inc. 210-218.
- [13] Gradiol, F. (1994). "Microstrip Circuit." Switzerland: John Wiley & Sons, Inc
- [14] James, J. R, Hall, P. S. and Wood, C. (1981). "Microstrip Antenna Theory and Design." New York: Peter Peregrinus Ltd.
- [15] Puri, V. K. and Chand, P. (1995). "Dictionary of Electronics." Kuala Lumpur. Cresnet News (K.L.) Sdn. Bhd.
- [16] Ammann, M. J. (1998). "A Comparison of some Low Cost Laminates for Antennas Operating in the 2.45 GHz ISM Band." *The Institutes of Electrical Engineers*.
- [17] Hansen, R. C. (1998). "Phased Antennas." New York: John Wiley & Sons, Inc 150-265.
- [18] Lee, K. F., Chen, W. and Lee, R. Q. (1997). "Probe-Fed Microstrip Antenna." In Lee, K. F. and Chen, W. "Advanced in Microstrip and Printed Antenna." New York: John Wiley & Sons, Inc 1-70.
- [19] Johnson, R. C. (Ed) (1990). "Antenna Engineering Handbook." 3<sup>rd</sup>. ed. Georgia: McGraw-Hill Inc. 7-0 – 7-29.
- [20] Waterhouse, R. B. (1992). "Modelling of Schottky Barrier Diode Loaded Microstrip Array Elements." *Electronics Letters*. 28(19). 1799-1801.
- [21] Anand, Y. (1984). "Microwave Schottky Barrier Diodes." in Sharma, B. L. "Metal-Semiconductor Schottky Barrier Junction and Their Applications." New York: Plenum Publishing Corporation. 219-271.
- [22] Harsany, S. C. (1997). "Principle of Microwave Technology." New Jersey: Prentice Hall. 27-185.
- [23] Chang, C. Y. and Kai, F. (1994). „GaAs High-Speed Devices, Physics, Technology and Circuit Application.“ New York: John Wiley & Sons, Inc. 279-365.
- [24] Tyagi, M. S. (1984). "Physics of Schottky Barrier Junctions." in Sharma, B. L. "Metal-Semiconductor Schottky Barrier Junction and Their Applications." New York: Plenum Publishing Corporation. 1-57.

- [25] Theo G. Van de Roer (1994). "Microwave Electric Devices.: London: Chapman & Hall.
- [26] Ladbrooke, P. H. (1989). "MMIC Design: GaAs FETs and HEMTs." Boston Artech House. 136-141.
- [27] Seidel, L. K. And Crowe, T. W. (1988). "Novel GaAs Schottky Barrier Diode Structures." *IEEE Conference Proceeding*. 149-153.
- [28] Shurmer, H. V. (1971). "Microwave Semiconductor Device." New York: Pitman Publishing. 93-108.
- [29] Huang, J. and Pozar, D. M. (1997). "Microstrip Arrays: Analysis, Design and Applications." in Lee, K. F. and Chen, W. "Advanced in Microstrip and Printed Antenna." New York: John Wiley & Sons, Inc. 123-159.
- [30] Harsany, S. C. (1997). "Principle of Microwave Technology." New Jersey: Prentice Hall. 27-185.
- [31] Sharma, B. L. (1984). "Fabrication and Characteristic of Metal Semiconductor Schottky Barrier Junction." in Sharma, B. L. "Metal-Semiconductor Schottky Barrier Junction and Their Applications." New York: Plenum Publishing Corporation. 113-123.
- [32] [wikipedia.org](http://wikipedia.org)
- [33] [http://en.wikipedia.org/wiki/Microstrip\\_antenna](http://en.wikipedia.org/wiki/Microstrip_antenna)
- [34] [http://en.wikipedia.org/wiki/Patch\\_antenna](http://en.wikipedia.org/wiki/Patch_antenna)

## APPENDICES

- [A] List of some dielectric substrate with the dielectric constant and loss tangent.
- [B] Table of common dielectric materials and conductor types.
- [C] Table of Evaluation of the Selected Properties of GaAs, Ge, InP and Si
- [D] User Manual.
- [E] Gantt Charts

# **APPENDIX A** **LIST OF DIELECTRIC SUBSTRATE**

Table 8    List of some dielectric substrate with the electric constant and loss tangent.

Dielectric Substrate	$\epsilon_r$	$Tan\delta$	Thickness Tolerance (+mm)	Water Absorption (%)	Anisotropy
Thermoplastic polyphenylene oxide	2.55	0.0011 (3 GHz)	$1.52 \pm 0.08$	0.060	
Exposy/glass	4.2-4.5 $\pm 0.2$	0.02 (1MHz)	$1.5 \pm 0.15$	0.100	
Polyster/Resin	$3.05 \pm 0.04$	0.003 (2 GHz) 0.004 (10 GHz)	$1.52 \pm 0.08$	0.020	1.017
Ceramic/PTFE composite	$3.00 \pm 0.04$	0.0013 (10 GHz)	$1.52 \pm 0.08$	<0.100	$\approx 1.1$
PTFE/Glass mix	$2.33 \pm 0.02$	0.0012 (10 GHz)	$1.52 \pm 0.05$	0.015	1.04
Hydrocarbon/ Ceramic	$3.38 \pm 0.05$	0.0022	$1.52 \pm 0.10$	0.060	$\approx 1.1$

## APPENDIX B

### TABLE OF COMMON DIELECTRIC MATERIALS AND CONDUCTOR TYPES

Table 9 Table of common dielectric materials (This table is obtained from Microwave Office 2004)

Material	Loss Tangent	Relative Dielectric Constant ( $\epsilon_r$ )
RT/Duriod 5880	0.001	2.16-2.24
Silicon	0.001-0.003	11.7-12.9
RT/Duriod 5880	0.001	2.16-2.24
Alumina	0.0005-0.002	9.6-10.1
GaAs	0.0005-0.001	12.9
Beryllium Oxide	0.001-0.002	6.7
Air	0	1

Table 10 Table of common conductor types and its conductivities (This table is obtained from Microwave Office 2000)

Material	Conductivity (S/m)
Nickel	$1.47 \times 10^7$
Gold	$4.10 \times 10^7$
Silver	$6.14 \times 10^7$
Aluminum	$3.53 \times 10^7$
Copper	$5.88 \times 10^7$

## APPENDIX C

Table 11    Evaluation of the Selected Properties of GaAs, Ge, InP and Si

Properties	GaAs	Ge	InP	Si	Comments
Melting Point (°C)	1238	936	1058	936	The higher the melting point the better is the processing maneuverability
Energy Gap (eV)	1.43	0.67	1.35	1.11	The higher the energy gap, the higher is the power handling capacity, the lower is the saturation current and the better is the operating capability at higher operating temperature
Type of energy gap	Direct	Indirect	Direct	Indirect	Direct energy gap requirement essential for some special optoelectronic and microwave component
Maximum mobility of electrons (cm <sup>2</sup> /V sec)	8000	3950	4600	1900	The higher the mobility, the smaller are the transit time and parasitic resistance and the higher is the frequency operations
Maximum mobility of holes (cm <sup>2</sup> /V sec)	400	1900	150	450	

Properties	GaAs	Ge	InP	Si	Comments
Effective hole mass ( $m_o$ )	0.48	0.37	0.64	0.59	
Effective electron mass	0.067	0.55	0.077	1.1	The lower the effective mass the smaller are the transit time and parasitic resistance and the higher is the frequency operations
Intrinsic carrier concentration	$1.8 \times 10^6$	$1.7 \times 10^{13}$	$1.1 \times 10^6$	$1 \times 10^6$	The lower the intrinsic carrier concentration the better is doping maneuverability
Semi insulating material	Yes	No	Yes	No	Necessary for planar processing of components and ICs for high frequency applications. The higher the resistivity the better is the mutual insulation of elements in ICs and suppression on parasitic capacitances
i) doping	Cr	-	Fe	-	
ii) resistivity ( $\Omega cm$ )	$>10^8$	-	$\sim 10^8$	-	
Electron affinity (eV)	4.07	4.13	4.4	4.01	Important parameter required in the selection of materials for heterojunctions and Schottky barrier junctions

Properties	GaAs	Ge	InP	Si	Comments
Thermal expansion coefficient ( $10^{-6} / ^\circ\text{C}$ )	6	5.5	4.5	2.44	Thermal expansion coefficient helps in determining the suitability of the depositing materials as their different may possibly create destructive stresses on cooling
Thermal conductivity ( $\text{W}/\text{cm}^\circ\text{C}$ )	0.54	0.59	0.68	1.4	The higher the thermal conductivity the better is power handling capability
Dielectric	13.1	16	12.4	11.9	The lower the dielectric constant the lower are the junction capacitance and carrier storage effects and the better is high frequency performance
Lattice-matched heterostructure possible	Yes	Yes	Yes	No	Such heterostructure can be used to improve the device performance or ohmic contactability
Vapor pressure at melting point (Torr)	740	$8.4 \times 10^{-7}$	$1.5 \times 10^4$	$5.6 \times 10^{-4}$	The lower the vapor pressure, the better is high temperature process compatibility


Properties	GaAs	Ge	InP	Si	Comments
Maximum useful temperature of operation (°C)	400	100	250	150	This is the temperature at which thermally generated carrier concentration approaches uncompensated doping density

## APPENDIX D

### USER MANUAL

#### Simulation of Rectangular Microstrip Patch Antenna

The frequency point for the project has to be set first since it's specifying the frequency that will be used in the project. The frequency point of 2.45 GHz has been chosen for this project.

Then, by adding the new EM structure, an EM structure has been created. It can be done by choosing the File/New EM Structure from the main menu or from the tool bar. Next, edit the enclosure of the antenna. The dimension and resolution of the rectangular enclosure are described in the enclosure properties. It can be edited by selecting Structure/Enclosure from the main menu or by clicking this symbol  from the toolbar.

The information about the substrate must be filled to get the 2-D and 3-D view of the rectangular microstrip patch antenna from the enclosure. The value of x and y dimension must be filled at the first page of the substrate information dialog (refer Figure 49). The width and length of the enclosure are appointed as x and y dimension. These parameters can be determined by calculating the width ( $W$ ) and the length ( $L$ ) of the rectangular patch. Supposedly, the width of the rectangular patch is about  $\lambda_0/2$  (free space wavelength divided by two).

The height of the enclosure is determined by the thickness of the dielectric layers, therefore it is not set through this page, which is set by using the second page of the substrate information dialog.

In EM simulation, all shapes that are drawn should coincide with the drawing grid. By setting the number of divisions in the x and y direction, the grid is specified. The number of divisions and the division cell size do not need to be the same for x and y dimensions. As in Figure 50, the cell size in each direction is the dimension in each direction divided by the number of divisions in that direction. The smaller cell sizes will provide a more accurate simulation, but the cell size that are too small will increased the time required to analyze problems.

The enclosure must contain at least two dielectric substrate layers while designing the patch antenna. Choose the second page of the substrate information dialog as in Figure 51 to edit the substrate layers. Select the layers that are in the list of layers to edit the properties of the dielectric layer. Afterward, the properties of layer such as hatch pattern of the layer, the thickness of the layer, relative dielectric constant  $\epsilon_r$ , loss tangent factor, bulk conductivity of dielectric materials and the view scale can be edited by using the edit control below the list of the substrate layers (refer Figure 51) when desired layer is selected. The polyster/resin is used as a dielectric substrate for the first analysis, which is act as the second layer. Though, the free space characteristic layer has been used at the first layer for this microstrip antenna.

The structure inside of a rectangular enclosure has been analyzed by using the EM simulation. The top and the bottom of the enclosure can be perfect electric conductor or can be loss, while the enclosure sides are always assumed to be perfect electric conductor. The top of the enclosure always acts as an approximate open (377 ohm), which is the free space impedance on behalf of the analysis of the rectangular microstrip patch antenna. For the time being, the perfect conductor has been used at the bottom of the enclosure. It is similar as shown in Figure 52 below. Click at the third page of the substrate information dialog similar as the first two other page mentioned before to edit the boundaries information.

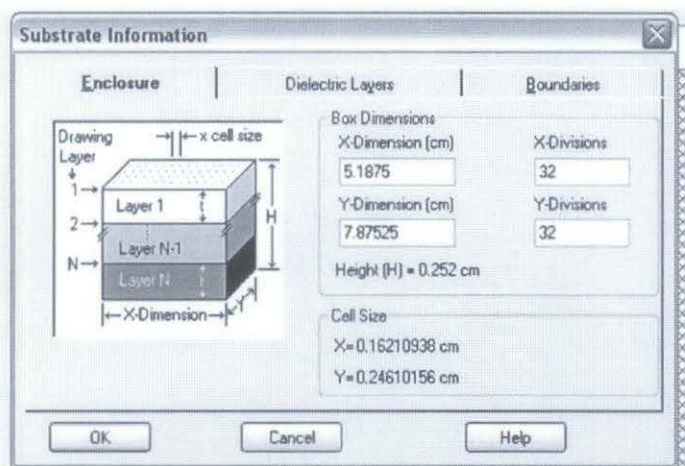


Figure 49 Enclosure information with polyster/resin as a substrate

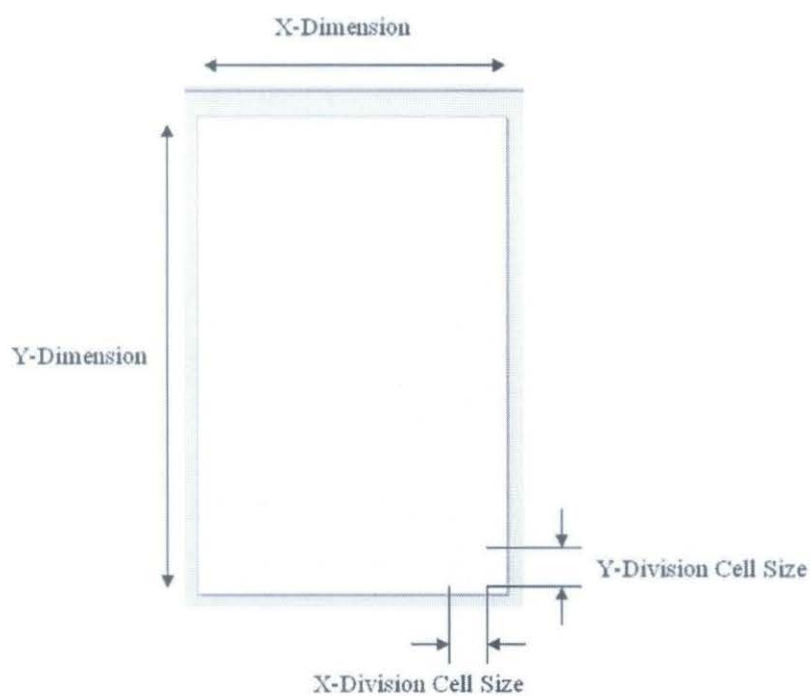


Figure 50 Division cell size and x and y dimension

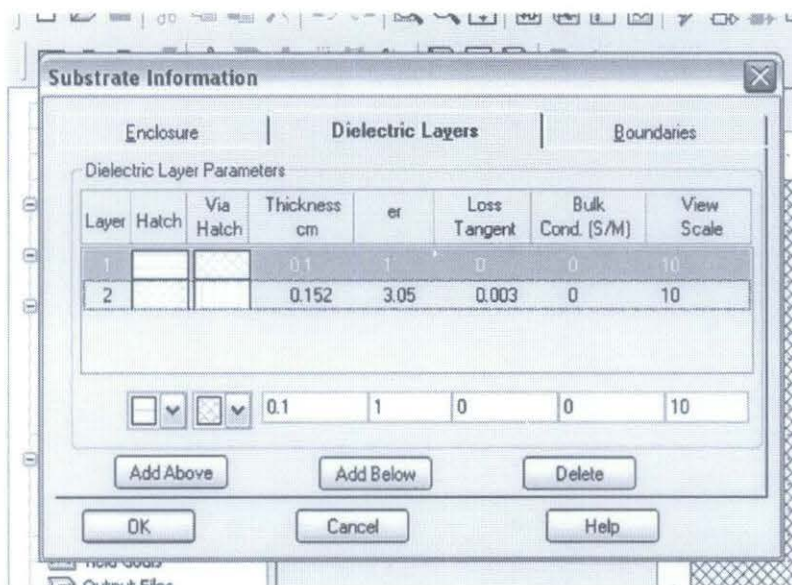


Figure 51 Dielectric layers information with polyster/resin as a dielectric substrate

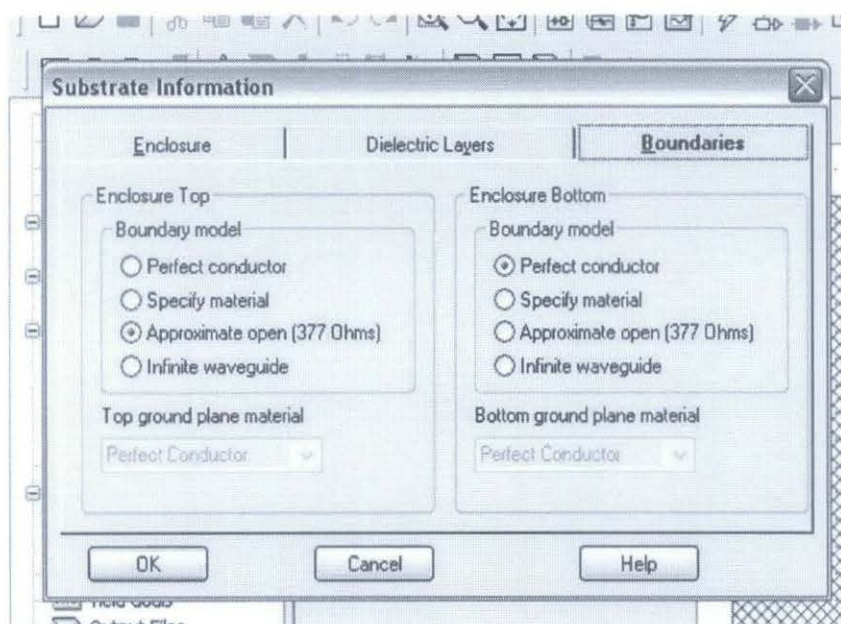


Figure 52 Boundaries information

On any layer, the planar conductor can be drawn but it should not be drawn on the layer 1 which coincides with the top of the enclosure. First of all, before draw the new conductor, select the active layer where the conductor will be drawn by clicking on the layer tab at the bottom of the 2-D view as shown at Figure 53, Choose Draw from the main menu or from the toolbar to draw the conductors. The active layer is

layer 2 and the conductor is act as the rectangular patch for the antenna as shown at the Figure 53.

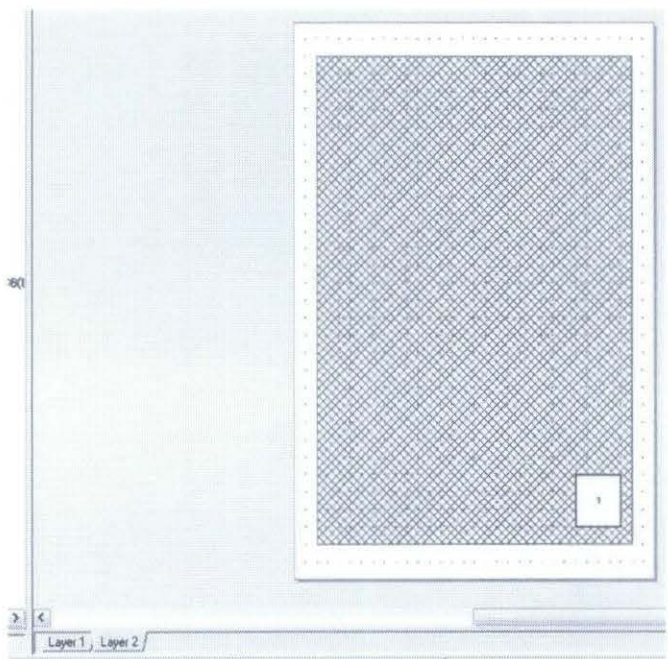


Figure 53 Rectangular patch

To add terminals between the bottom of the enclosure and the EM structure, via ports were used. To create probe feed for a rectangular patch antenna (as shown in Figure 53 and 54), via ports can be used. To add via port at the patch, select Draw/Add Via Port from the main menu. For this patch antenna, this port acts as a coaxial feed.

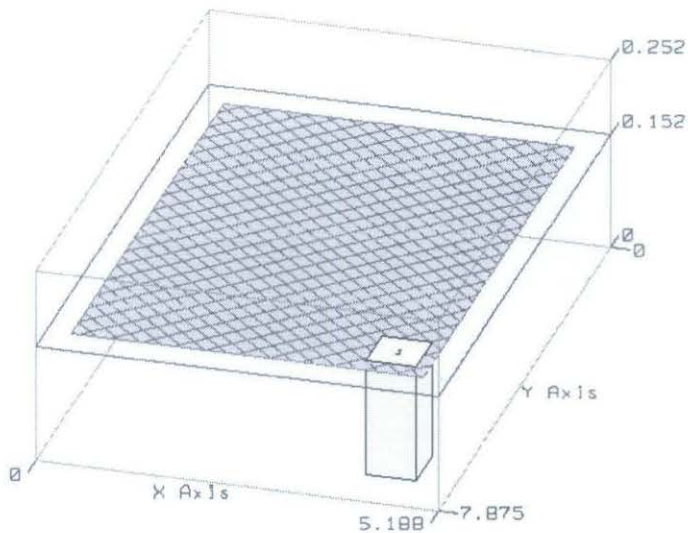


Figure 54 The position of Via Port

Smith Chart, antenna graph and rectangular graph can obtain the performance of the rectangular microstrip patch antenna. Click Project/Add Graph from the main menu or just click it from the toolbar to add the graphs for the project. Choose the type of graph that will be implemented from the Create Graph dialog as represented in Figure 55. Next, by clicking Project/Add Measurement from the main menu (refer Figure 56), the measurements for the analysis can be added. The antenna graph was chosen to perform the total radiated power of the antenna for this project. Other than that, to represent the reflection coefficient and the input impedance of the patch antenna, the Smith Chart was used. From the rectangular graph, analysis results for Voltage Standing Wave Ratio (VSWR) can be obtained.

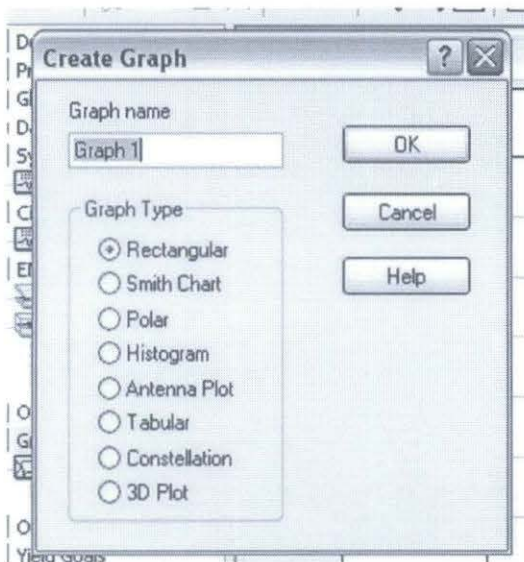


Figure 55 Type of graphs

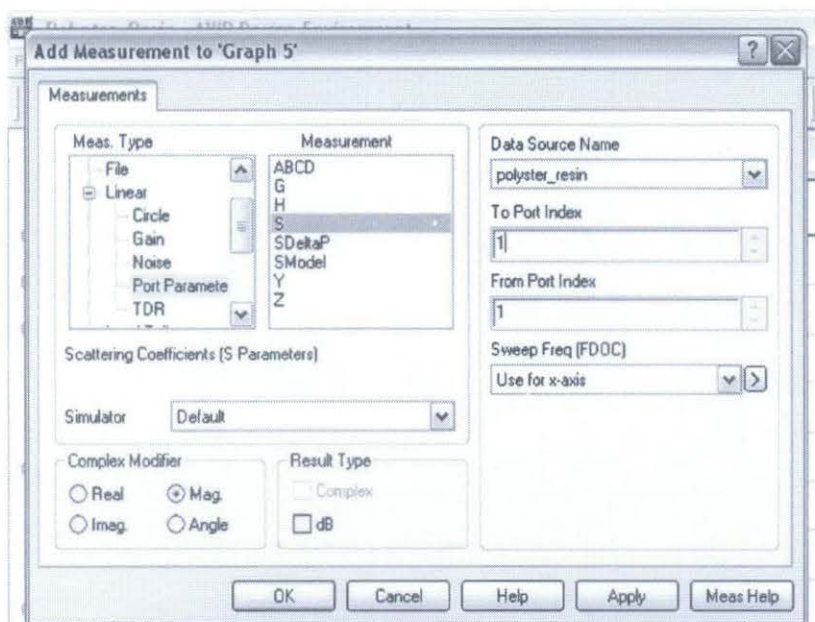


Figure 56 Add measurements for the graph

When all the setting of the antenna has been done, lastly, simulate or analyze the patch antenna by clicking Simulate/Analyze from the main menu or by clicking

this button  from the toolbar.

# Nonlinear Simulation of Schottky Diode

Initially, drag the sdiode element from the element browser into the schematic after created the new schematic. Next, ACVS (AC Voltage Source) element was chosen as the source and then, drags the symbol into the schematic like the previous step. Then, to connect the unconnected points on the source and the diode, the Wiring Tool is used. And lastly, the Ground (GND) element is put into the circuit. The designed full circuit will be look like in the Figure 57.

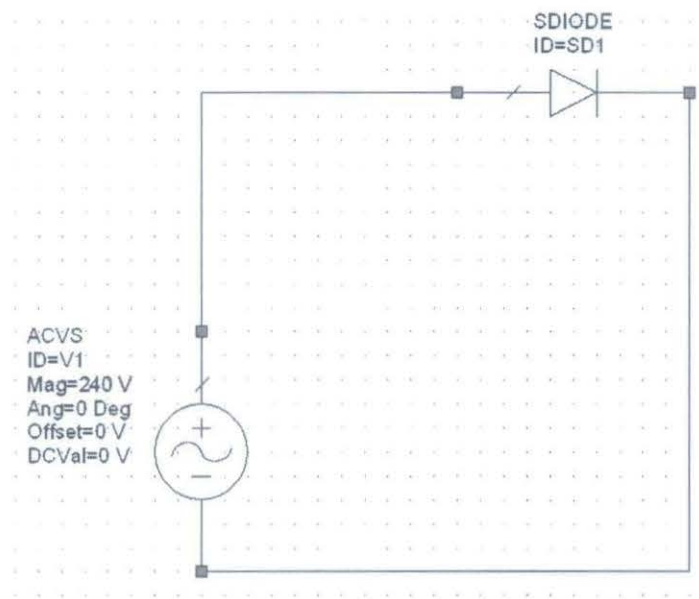


Figure 57    Circuit of Schottky diode

By double left clicking on any schematic symbols, parameters values can be edited. To edit the parameters, it is in the dialog box as shown in Figure 58. Zero-Voltage Junction Capacitance, Series Resistance and Breakdown Voltage are the important parameters that have to be entered.

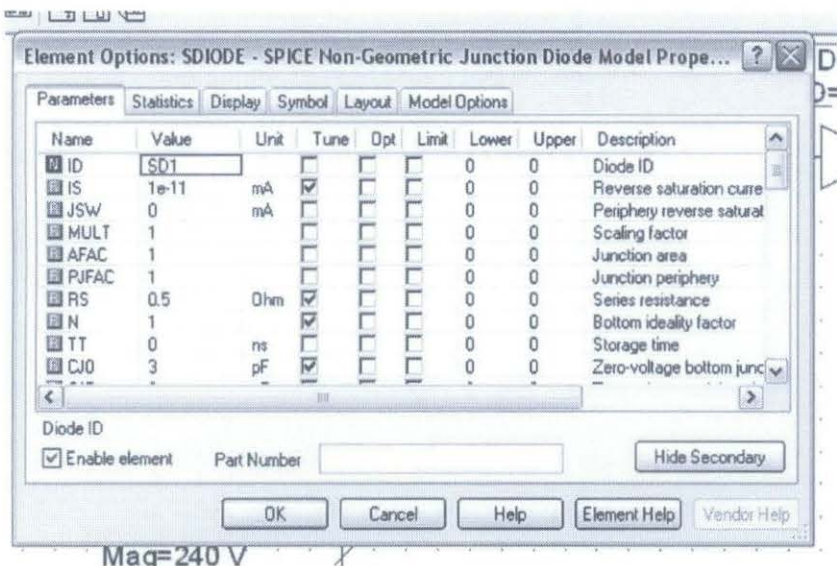


Figure 58 Dialog box to edit the parameter of Schottky diode

Likewise, by double clicking the magnitude of voltage source, the value of the component can be edited. 240V is the magnitude.

To show the performances of the diode, the rectangular graph is selected as a graph. Select Project/Add Graph from the main menu and select the rectangular graph to add graph. Next, choose Project/Add Measurement from the main menu. Choose the Nonlinear Voltage, Non Linear Current, Nonlinear Power and Nonlinear Parameter as the parameters to show the performance of the diode. The diode itself and also the voltage source are the measurement components that have been chosen to be measured.

APPENDIX E  
GANTT CHARTS

Table 12 Gantt Chart for FYP I July 2007

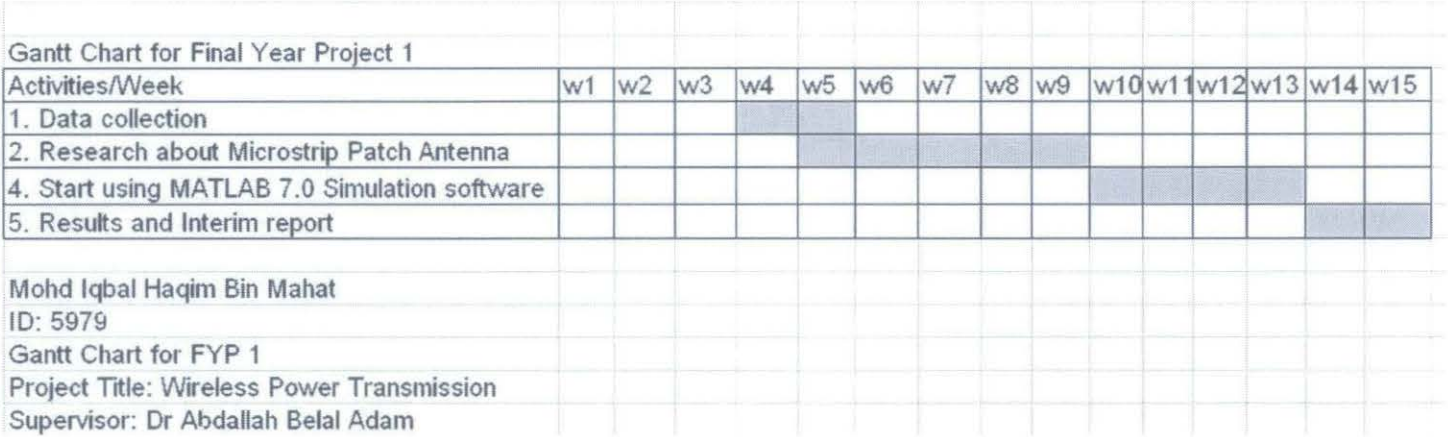


Table 13 Gantt Chart for FYP II January 2008

Gantt Chart for Final Year Project 2															
Activities/Week	w1	w2	w3	w4	w5	w6	w7	w8	w9	w10	w11	w12	w13	w14	w15
1. Designing RMPA and Schottky diode circuit															
2. Simulations using Microwave Office 2004															
4. Obtained results and doing reports															
5. Presentations															
Mohd Iqbal Haqim Bin Mahat															
ID: 5979															
Gantt Chart for FYP 2															
Project Title: Wireless Power Transmission															
Supervisor: Dr Abdallah Belal Adam															